

The influence of femoral component malalignment on the biomechanics of the knee after total knee arthroplasty

vorgelegt von
Dipl.-Ing. Christian König
geboren in Berlin

Von der Fakultät V – Verkehrs- und Maschinensysteme
der Technischen Universität Berlin
zur Erlangung des akademischen Grades

Doktor der Ingenieurwissenschaften
– Dr.-Ing. –

genehmigte Dissertation

Promotionsausschuss

Vorsitzender: Prof. Dr.-Ing. Christian O. Paschereit

Berichter: Prof. Dr.-Ing. Marc Kraft

Berichter: Prof. Dr.-Ing. Georg N. Duda

Betreuer: Dr. hum-biol. Markus O. Heller

Tag der wissenschaftlichen Aussprache: 10.11.2011

Berlin 2011

D 83

ABSTRACT

Total knee arthroplasty (TKA) is an established and successful procedure with increasing numbers performed each year. In the US alone, an increase from 611000 operations annually to as many as 3.5 million is estimated for the year 2030. However, the patients' high expectations of the functional and clinical outcome are not always met. Considering the current 10-year failure rates of as much as 12% and the projected number of cases in the future, a significant increase in revision TKA must be expected. One of the possible causes that lead to failure of the TKA is a sub-optimal placement of the femoral component, which can occur in six degrees of freedom (DOF) and is also referred to as a femoral component malalignment (FCM). While specific malalignment in a single DOF, such as frontal plane malalignment (varus-valgus malalignment), has been clinically associated with post-operative complications, knowledge of the effects of complex FCMs on the knee's biomechanics is limited. However, such knowledge is essential to identify and to avoid FCMs, which can cause unfavourable biomechanical conditions, possibly contributing to a negative post-operative result.

Therefore, the aim of this study was to analyse the biomechanical consequences of femoral component malalignment on the joint's biomechanics during the activities of daily living.

After basic investigations of the biomechanical conditions in the healthy knee, validated musculoskeletal models were adapted to simulate a post-TKA condition. A cranial-caudal malalignment of the femoral component, which has been associated with clinical complications, was then simulated, and its effect on the tibio- and patellofemoral contact forces and on the function of the collateral ligaments was characterized. While an elevated joint line was shown to lead to increased patellofemoral contact forces and thus, can contribute to failure-related complications such as pain and wear, a direct effect of joint line elevation on the function of the ligamentous stabilizers, specifically in mid-flexion, was not seen. Surprisingly, the data was indicative of increased loading in the ligaments, which has been previously associated with the development of arthrofibrosis, which can lead to a limited capacity in joint motion.

More complex FCM in all six DOFs was then simulated to represent situations more likely to occur in a clinical scenario. Calculating the contact forces for more than 160000 malalignment conditions revealed that the influence of a specific FCM is dependent on the joint analysed and the activity performed. The most influential parameters were found to be the internal-external rotation of the femoral component, the location of the joint line and the varus-valgus alignment. The analyses showed that, in 28% of the simulated malalignment conditions, FCM led to a 10% or greater increase in joint contact forces, relative to the optimally reconstructed joint. More incidences were found in the patello- than in the tibiofemoral joint. Such contact force increases can be caused by every type of malalignment. Even if an individual DOF was kept in its reference condition, malalignment in the remaining DOFs could lead to contact force increases of 10% or more, indicating that monitoring of a single DOF is not sufficient to detect a possible contact force increase.

In some DOFs, individual levels of malalignment were involved in more than 50% of all observed cases of increased contact forces, reaching a share of up to 92% (e.g. internal rotation $>5^\circ$, patellofemoral joint, stair climbing). In the clinic, this would give only few options to avoid a load increase by the targeted manipulation of the remaining DOFs. More significant load increases of 50% and more were found primarily when varus malalignment was combined with an internal rotation (each 5° or above). In the clinic this FCM should therefore be avoided.

The intra-operative identification of FCMs causing smaller load increases is almost impossible for the surgeon without assistance, especially since there is also a dependency on the activity and the analysed joint. Enhancing orthopaedic navigation systems with a database similar to the one presented in this study, which contains a matrix of malalignment in all DOFs and the resulting contact forces, would allow for the intra-operative detection of increased load conditions.

This study emphasises that it is not sufficient to analyse only individual DOFs of femoral component malalignment to draw a conclusion on its biomechanical effects, as the presence of malalignment in the remaining DOFs can have a significant impact on the joint's biomechanics. The approach presented in this study to biomechanically assess malalignment in all six DOFs is an essential step towards an intra-operative and patient-specific analysis of the femoral component placement. Ideally this can help to minimize the risk of creating overloading conditions, possibly also reducing the incidences of implant failure after TKA.

KURZFASSUNG

Der totale Ersatz des Kniegelenks ist ein etabliertes und erfolgreich angewandtes operatives Verfahren mit zunehmenden Fallzahlen. Allein in den USA wird ein Anstieg von derzeit jährlich etwa 611.000 auf 3,5 Millionen Operationen im Jahr 2030 prognostiziert. Schon jetzt können die hohen Erwartungen der Patienten an das postoperative klinische und funktionelle Ergebnis nicht immer erfüllt werden. Ausgehend von den aktuellen 10-Jahres Revisionsraten von bis zu 12% und den prognostizierten Fallzahlen ist ein erheblicher Anstieg von Revisionseingriffen zu erwarten. Eine der in klinischen Studien identifizierten möglichen Ursachen, die zum Versagen einer Knieendoprothese führen können, ist eine suboptimale Ausrichtung der femoralen Prothesenkomponente. Bisher wurde jedoch noch keine umfassende Studie durchgeführt, welche die Auswirkung der Fehlorientierungen der femoralen Komponente auf die Biomechanik des Kniegelenks untersucht und die beobachteten klinischen Probleme möglicherweise erklärt. Die Ergebnisse einer solchen Studie sind weiterhin eine wichtige Voraussetzung, um perioperativ unvorteilhafte biomechanische Bedingungen zu identifizieren und gegebenenfalls zu vermeiden.

Ziel dieser Arbeit war es daher, die Auswirkungen einer Fehlorientierung der femoralen Komponente auf die Biomechanik des Kniegelenks während der Ausübung von Aktivitäten des täglichen Lebens zu analysieren.

Nach der Durchführung von grundlegenden Untersuchungen zur Biomechanik des gesunden Kniegelenks wurden validierte muskuloskeletale Modelle modifiziert und eine klinisch oft mit Komplikationen assoziierte cranial-caudal Fehlpositionierung der femoralen Komponente simuliert. Die Auswirkung dieser Fehlpositionierung auf die Kontaktkräfte im patello- und tibiofemorale Gelenk sowie auf die Funktion der Seitenbänder wurde anschließend untersucht. Die Ergebnisse zeigten, dass eine erhöhte Gelenklinie zu erhöhten Kontaktkräften führt und somit versagensrelevanten Komplikationen wie Schmerz und verstärkter Abrasion zuträglich sein kann. Ein vermuteter Zusammenhang zwischen einer erhöhten Gelenklinie und Instabilität in mittleren Kniebeugewinkeln konnte hingegen nicht bestätigt werden.

Zur Untersuchung eines klinischeren Szenarios wurde angenommen, dass von den sechs möglichen Arten einer Fehlorientierung der femoralen Komponente mehrere gleichzeitig in einer klinisch repräsentativen Variationsbreite auftreten können. Die Berechnung der Gelenkkontaktkräfte für mehr als 160.000 simulierte Fehlorientierungen zeigte, dass der Einfluss eines Orientierungsparameters von der durchgeführten Aktivität und dem betrachteten Gelenk abhängig ist. Die einflussreichsten Parameter waren die interne-externe Rotation der femoralen Komponente, die Lage der Gelenklinie und eine varus-valgus Fehlorientierung.

In 28% aller untersuchten Fälle wurde eine Kontaktkrafterhöhung von 10% und mehr registriert, wobei die Häufigkeit im Patellofemoralgelenk höher war als die im Tibiofemoralgelenk. Diese Fälle erhöhter Kontaktkräfte traten bei allen Varianten von Fehlorientierung auf. Selbst bei optimaler Orientierung eines Parameters kann es zur Kontaktkrafterhöhung kommen. Es ist daher nicht ausreichend nur einen Parameter zu überwachen um Kontaktkrafterhöhung zu identifizieren.

Fehlorientierungen in bestimmten Ausprägungen können in bis zu 92% aller Fälle mit Kontaktkrafterhöhung vorherrschend sein (z.B. interne Rotation $>5^\circ$, Patellofemoralgelenk, Treppesteigen). Dies limitiert die Möglichkeiten, die Kontaktkräfte durch eine gezielte Manipulation der anderen Orientierungsparameter zu verringern. Erhebliche Belastungsanstiege von 50% und mehr wurden bei der Kombination von varus Fehlstellungen mit einer internen Rotation gefunden (bei beiden 5° und mehr). Diese Fehlstellung sollten daher in der Klinik vermieden werden.

Die intraoperative Identifizierung der häufiger auftretenden Fälle mit geringeren Kontaktkraftanstiegen ist für den Operateur kaum möglich, da ein komplexer Zusammenhang zwischen den einzelnen Orientierungsparametern, dem analysierten Gelenk und der Aktivität besteht, der ohne die Zuhilfenahme von computergestützten Assistenzsystemen schwer zu erfassen ist.

Die Ergebnisse dieser Arbeit unterstreichen, dass es nicht ausreicht, nur einzelne Orientierungsparameter zu betrachten, da zusätzlich auftretende Fehlorientierungen die Kontaktkräfte im Gelenk stark beeinflussen können. Der beschriebene Ansatz ermöglicht es patientenbezogen die postoperative Biomechanik abzuschätzen und die Implantation der femoralen Komponente hinsichtlich der Kontaktkräfte zu optimieren. Somit kann das Risiko von auftretenden Überlastungsbedingungen minimiert und postoperative Komplikationen möglicherweise verringert werden.

TABLE OF CONTENTS

ABSTRACT	II
KURZFASSUNG	IV
TABLE OF CONTENTS.....	VI
1 INTRODUCTION	1
1.1 The healthy knee	3
1.2 Loading conditions in the knee	5
1.3 Joint kinematics	7
1.4 Patellofemoral joint	9
1.5 Total knee arthroplasty (TKA)	10
1.6 Complications after TKA.....	12
1.7 Restoring joint geometry.....	13
1.8 Evaluating the impact of malalignment on the joint's biomechanics	14
Loading conditions	14
Function of collateral ligaments.....	15
1.9 Goals / Significance.....	16
2 BIOMECHANICAL ANALYSES OF THE INTACT KNEE.....	17
2.1 3D representation of active and passive soft tissue structures in the lower limb.....	18
Methods and results.....	19
3D models of muscles and ligaments	19
Muscle origin and insertion sites.....	22
Muscle centroid lines	22
Discussion	23
2.2 Kinematic models to describe tibiofemoral motion	25
Materials and methods.....	25
Acquisition of in vivo reference kinematics	25
Determining in vivo kinematics and ligament attachments.....	28
Kinematic model.....	29
Statistics	30
Results	31
In vivo kinematics	31

Subject-specific models 31

Ligament lengthening 33

Generic predictive models 35

Discussion 35

2.3 Contact mechanics in the patellofemoral joint..... 39

Materials and methods 40

 Specimen preparation 40

 Joint loading and muscle force model 40

 Mechanical test set-up 41

 Assessment of patellofemoral biomechanics 42

 Data analysis 43

Results 43

 Stair climbing vs. walking..... 43

 12° vs. 30° knee flexion..... 43

Discussion 46

2.4 In vivo assessment of collateral ligament function in the healthy knee 51

Materials and methods 51

Results 52

Discussion 53

3 THE EFFECT OF JOINT LINE ELEVATION ON JOINT CONTACT FORCES 55

3.1 Introduction..... 56

3.2 Methods 58

 Musculoskeletal model..... 58

 Kinematic adaptation 59

 Variation of the joint line..... 60

 Joint contact forces 61

3.3 Results..... 63

3.4 Discussion 65

4 THE EFFECT OF JOINT LINE ELEVATION ON COLLATERAL LIGAMENT FUNCTION IN MID-FLEXION AFTER TKA..... 69

4.1 Introduction..... 70

4.2 Methods 72

 Musculoskeletal model..... 72

 Variation of the joint line..... 73

 Kinematic adaptation 74

 Collateral ligament length change..... 74

4.3	Results.....	75
	Anatomical reconstruction.....	75
	Effect of JLE on DA relative to the anatomical reconstructed condition	76
	Effect of JLE on DA relative to the extended knee	76
4.4	Discussion	77
5	THE EFFECT OF COMBINED FEMORAL COMPONENT MALALIGNMENT ON JOINT CONTACT FORCES	83
5.1	Introduction.....	84
5.2	Methods.....	86
	Musculoskeletal model.....	86
	Simulation of femoral component malalignment.....	86
	Kinematic adaptation.....	88
	Joint contact forces	89
	Data analysis.....	89
5.3	Results.....	91
	The relative influence of individual malalignment parameters on total contact forces.....	91
	Patellofemoral joint.....	91
	Tibiofemoral joint.....	91
	Malalignment scenarios that caused contact force increases of 10% and more	92
	Patellofemoral joint.....	92
	Tibiofemoral joint.....	92
5.4	Discussion	96
6	SUMMARY AND CONCLUSIONS.....	101
7	REFERENCES	107
8	INDEX OF TABLES AND FIGURES.....	121
8.1	Index of Figures.....	121
8.2	Index of Tables	126
	CURRICULUM VITAE.....	127
	EIDESSTÄTTLICHE ERKLÄRUNG	133

1 INTRODUCTION

The knee joint is one of the most complex joints in the human body and its proper function is an integral part of human locomotion. But the knee is also more likely to be injured than any other human joint, resulting in functional loss. Besides injury, degenerative processes can also create conditions that significantly reduce the joint's functionality. Even in the ancient world, efforts had already been made to face this functional loss in the lower limb with prosthetic devices. The pioneer in the field of replacing the injured or degenerated joint with alloplastic implants was Themistocles Gluck (1853-1942) (Figure 1).

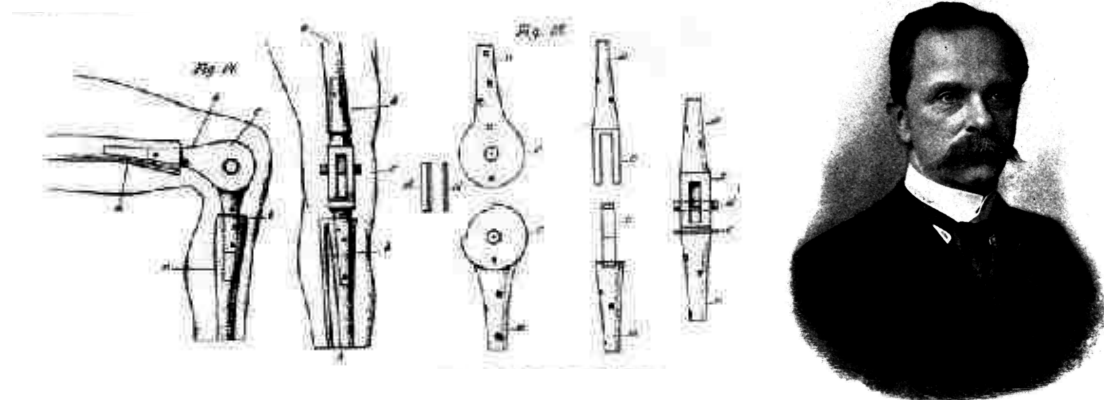


Figure 1: Sketches of first ivory implants to replace the knee joint. Themistocles Gluck (1853 – 1942) was a pioneer of modern total knee replacement (image source: (Eynon-Lewis et al. 1992) & Wikipedia).

In the year 1890 he implanted the first knee endoprosthesis made of ivory. Despite this revolutionary work, his implants were subjected to early failure, mostly caused by unmanageable infections and mechanical failure of the prosthesis' material. But even today, 120 years after Gluck's first attempts, the field of total knee arthroplasty (TKA) is still subject of extensive research. While today the share of implant failures due to infections is down to 20%, the sometimes suboptimal biomechanics of the replaced joint and its surrounding structures remain a principal reason to revise an implant (Robertsson 2009).

This study will present a detailed analysis of a specific aspect of this broad field of biomechanically related failures of the reconstructed joint. The effect of a variation in the positioning of the femoral part of the total knee prosthesis system on specific biomechanical parameters of the post-operative joint will be investigated. Conditions that are identified to be biomechanically unfavourable may then be avoided during TKA.

To approach this topic, the first chapter gives an introduction to anatomical and functional aspects of the knee joint, its motion, and methods to determine its loading conditions. Furthermore, the reasons why a replacement of this joint might be necessary are outlined. Total knee arthroplasty is introduced in more detail and the literature reviewed with respect to factors that can affect the success of the procedure and thus, may also lead to complications. Based on still unresolved issues, the goal of this study is derived and its significance presented.

1.1 The healthy knee

In order to analyse the loading conditions in the joint after TKA, it is necessary to understand the basic anatomy of the knee and the function of its individual structures. The knee joint is the largest joint in the human body. It is a synovial joint that connects the thigh (femur) and shank (tibia) in the lower limb and consists of three functional compartments: the femoropatellar articulation and the medial and lateral femorotibial articulations. Complex interactions of a number of active and passive stabilizers enable a large range of motion in the joint while also providing the stability needed throughout the large spectrum of human daily activities.

The passive stabilizers are the bony structures such as femur, tibia and patella along with soft tissues such as femoral, tibial and patellar cartilage, the menisci and the

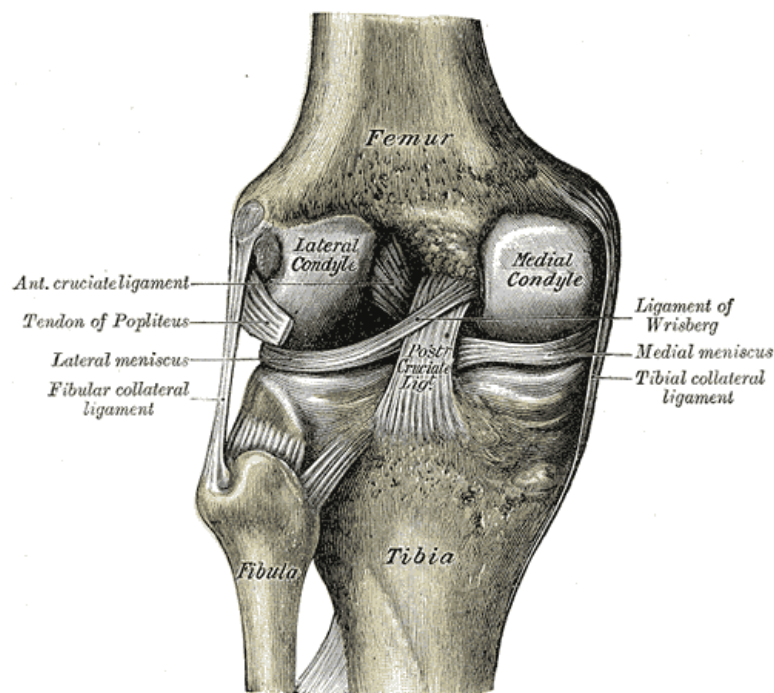


Figure 2: Posterior view of the knee showing the bony structures, the ligaments, menisci and the cartilages (Gray 1918).

ligaments (Figure 2). The main function of the passive stabilizers is to constrain the joint's motion and to absorb forces. The two cruciate ligaments are the knee's internal ligaments and mainly limit the anterior-posterior translation, but also resist rotation of the femur on the tibia. Passive stabilization of the extended knee is also provided by the medial and lateral collateral ligaments and the articular capsule. While the lateral collateral ligament primarily resists varus instability in extension, the medial collateral ligament is thought to resist valgus instability, external tibial rotation and anterior-posterior translations throughout flexion (Brantigan and Voshell 1941; Gardiner et al. 2001; Harfe et al. 1998).

Selected muscles of the lower limb control knee motion and also function as active stabilizers of the joint (Figure 3). These muscles can be subdivided into two main groups according to their function: joint extensors and flexors. The joint's extension is controlled by the musculus quadriceps femoris, consisting of four heads which are the musculus vastus lateralis, the musculus vastus intermedius, the musculus vastus medialis and the musculus rectus femoris. Distally these four heads combine in the quadriceps tendon and transmit their force via the patella and the ligamentum patellae into the anterior tibia.

The hamstring group controls knee flexion and is formed by the musculus semimembranosus, musculus biceps femoris caput longum, musculus biceps femoris caput breve and musculus semitendinosus. Together with the joint rotators – the musculus popliteus, musculus gracilis and musculus sartorius – the hamstrings insert circumferentially in the distal side of the joint, i.e. on the medial tibial condyle, the caput fibulae (lateral) and the pes anserinus (antero-medial), as well as the posterior tibia.

During activities of daily living, the structures of the knee are exposed to high loads (D'Lima et al. 2006; D'Lima et al. 2005b), mostly created by muscular activity (Pauwels 1951). Especially in reflex situations, significant peak loads can occur in joints (Bergmann et al. 1993), indicative of the stabilizing role of the muscles, achieved for example by co-activation (Baratta et al. 1988; Draganich et al. 1989; Li et al. 1999).

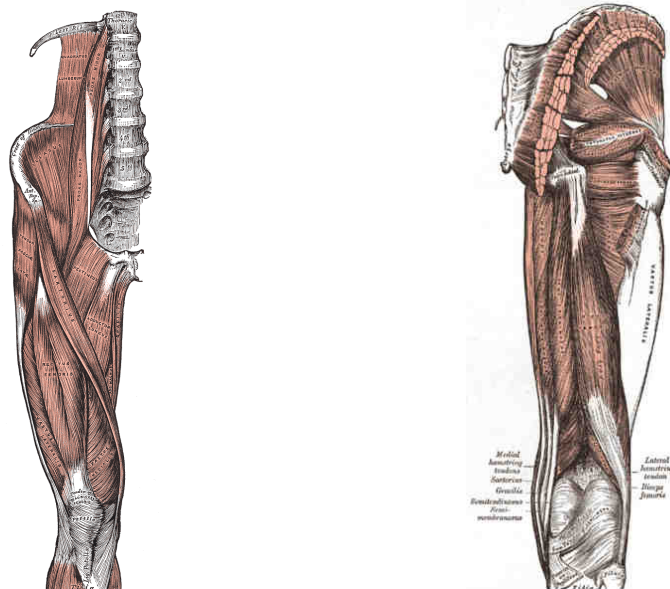


Figure 3: The muscles of the knee from an anterior (left) and a posterior view (right) (Gray 1918).

1.2 Loading conditions in the knee

Knowledge of the loading conditions in the healthy and also in the post-operative knee after TKA is essential to evaluate the impact of the joint replacement procedure on the knee's biomechanics. It is known that the mechanical boundary conditions in the joint are defined by the external loads on the body and their corresponding internal counterparts. In 1870, Julius Wolff described for the first time the interrelationship between loading, stress and strain in anatomical structures, which he later manifested in the so-called Wolff's Laws (Wolff 1892). Based on Wolff's investigations, Koch published the first analytical determination of the loading conditions in long bones (Koch 1917). The remarkable role that muscles play in the loading scenario of long bones was described later by Pauwels (Pauwels 1951). Using the abductors and the iliotibial tract, Pauwels illustrated the effect of the muscles in minimising the internal loading within the bone. In numerous examples, Pauwels described how muscles and tendons reduced the bending moments at the hip that were induced by the body weight, by examining areas of tensile and compressive strain within cross-sections of long bones (Pauwels 1973).

While it is now known that the contribution of the muscles is essential to describe the mechanical loading of bones, the actual loading conditions occurring *in vivo* are scarcely accessible. To date, direct measurement of the coordinated action of all muscle forces *in vivo* is still impossible. Ethical considerations discourage the use of invasive methods to determine muscle forces in humans. Therefore, the only opportunity to estimate the complex distribution of muscle forces is offered by computer analysis. A precondition to determining the muscle forces and the resulting loading conditions in the bones and the joints is the knowledge of the external loads, as well as the kinematics of the bony segments of the lower limb. Such data – the ground reaction forces in the foot, and the spatial positions of the pelvis, femur, tibia, fibula and of the foot – can be collected in a clinical gait analysis (Andriacchi et al. 1998; Brand et al. 1986; Heller et al. 2001b; Heller et al. 2007b). Based on these individually captured kinetics and kinematics, an inverse dynamics approach can be used to determine the joint forces and moments (Chao and Rim 1973).

To obtain a condition of equilibrium, the internal structures such as muscles and tendons must compensate these external moments. The capacity to compensate these moments is determined by the forces transmitted through the muscles and tendons, as well as by

their lever arms relative to the joint. Anatomical models which include the origins and insertions of muscles and ligaments can be used to approximate the lever arms during motion (Heller et al. 2007b).

However, there are a significant number of muscles and tendons that span the knee. On the femur, for example, more than 26 force-transmitting muscular or ligamentous insertions are present, which allow a specific motion to be achieved by several muscular activation patterns. Therefore no mathematically explicit solution for the calculation of muscle forces exists. Since the reduction of equations as a possible approach to this problem (Ghista et al. 1976; Pierrynowski 1982) will not allow conclusions to be drawn on the complex distribution of muscular activation, an alternative method is the identification of those solutions, from the infinite pool of solutions, which seem to be “reasonable” (Crowinshield 1978; Seireg and Arvikar 1973). The main challenge in such optimization processes is to define adequate optimization criteria.

An approach to validate the calculated muscle activation patterns obtained from such musculoskeletal models was to compare the simulation with measured muscle activities as determined by electromyography (EMG) (Winter 1991). Even though it was found that non-linear optimization strategies result in a better agreement with the EMG signals than a linear approach (Thunnissen et al. 1992), this validation method does not allow for a quantitative validation of the musculoskeletal loading conditions.

An additional method of validating the predicted musculoskeletal loading conditions is to compare the calculated joint contact force, which is the sum of all calculated joint and muscle forces acting in the joint, with forces measured in vivo. While instrumented implants, which give access to in vivo joint contact forces for the different activities of individual patients, were introduced several decades ago (Rydell 1966) and have been continuously enhanced (Bergmann et al. 1993; Bergmann et al. 1995; Bergmann et al. 1988; Brand et al. 1994; Davy et al. 1988; English and Kilvington 1979; Rydell 1966), in vivo measurements in the tibiofemoral joint have been only recently reported (D'Lima et al. 2006; D'Lima et al. 2005b; Heinlein et al. 2007; Heinlein et al. 2009).

In the first in vivo measurements of axial forces acting in the tibiofemoral joint, D'Lima and co-workers (D'Lima et al. 2006; D'Lima et al. 2005b) showed that in a 12 month follow-up, the contact forces increased during walking from magnitudes of 1.2 times the patient's bodyweight (BW) (after 3 months) to an average 2.8x BW with peak forces of more than 3x BW (D'Lima et al. 2006; D'Lima et al. 2005b). The instrumented prosthesis developed by Heinlein and colleagues additionally measured shear force components

and the three moments (Heinlein et al. 2009). In their preliminary study, they found the highest mean values of the peak load components during level walking of 2.8xBW in the axial, 0.2xBW in the medio-lateral and 0.3xBW in the antero-posterior directions. During other activities such as stair climbing and stair-descending, axial forces of as much as 3.5xBW were observed.

Despite these first promising results in determining the in vivo loading conditions in the tibiofemoral joint, further measurements in a larger patient cohort are required before general conclusion about the loading conditions in the knee can be drawn. So far, musculoskeletal loading conditions in the knee are determined with musculoskeletal models, which were validated against the hip joint contact forces measured in vivo (Heller et al. 2001a; Heller et al. 2001b; Heller et al. 2005; Heller et al. 2007b; Heller et al. 2003; Taylor et al. 2004).

Utilizing such musculoskeletal models, Taylor and co-workers (Taylor et al. 2004) reported average maximum axial contact forces of 3.3xBW in the tibiofemoral joint during normal walking. Here, the reported inter-individual contact force variation was larger than the intra-individual. In an averaged normal walking trial, peak loads of 2.8xBW occurred. During stair climbing, average peak loads as high as 5.9xBW were calculated. A first comparison to the in vivo data revealed reasonable agreement during walking, but also indicated that the calculated forces are higher during stair climbing. However, as a larger inter-individual variability was observed, more patients need to be measured before further conclusions on typical loads can be drawn (Kutzner et al. 2010).

1.3 Joint kinematics

Pathologies in tibiofemoral kinematics, caused for example by degenerative processes, trauma or even surgical interventions, can significantly disturb the complex interplay between the joint's active and passive stabilizers. This disturbed interplay can ultimately lead to functional deficits and pain. Besides its importance for implant design and assessing surgical procedures, the knowledge of tibiofemoral kinematics is also essential in the use of musculoskeletal models of the lower limb.

Fundamental research on tibiofemoral kinematics was published as early as 1836 by the Weber brothers (Weber and Weber 1836). For the first time, the kinematics of the knee

joint were described as a motion comprising rolling and gliding. To determine the knee kinematics in vivo, a number of more invasive techniques have been developed in recent decades, including Roentgen stereophotogrammetric analysis (Valstar et al. 2001), fluoroscopy (Banks and Hodge 1996; Dennis et al. 2005; Komistek et al. 2003; von Eisenhart-Rothe et al. 2007) and pin-based tracking of bone kinematics (Reinschmidt et al. 1997). To assess knee kinematics in a non-invasive manner, methods such as skin marker-based techniques (Andriacchi et al. 1998) and MRI-based procedures (Freeman and Pinskerova 2003) have been used. Even though MRI-based techniques provide a high degree of precision (von Eisenhart-Rothe et al. 2004), they are restricted by long acquisition times and spatial limitations. Skin marker techniques are limited by the accuracy of reproducing the positions of the underlying bones (Cappozzo et al. 1996; Heller et al. 2007b; Taylor et al. 2005), leading to inaccuracies in the estimation of the loading conditions at the tibiofemoral joint. However, there have been promising attempts to reduce the skin marker artefacts, allowing the determination of axes and centres of rotation in the knee with a sufficient precision (Ehrig et al. 2007). While thus far, tibiofemoral kinematics have been generally described as a combined rolling and gliding motion of the femur on the tibial plateau, recent in vivo studies give a more detailed insight into the motion of the knee joint.

During knee flexion, the medial femoral condyle does not 'roll back', at least from hyperextension to 90°, but the lateral condyle does (Dennis et al. 2005; P. Johal et al. 2005; von Eisenhart-Rothe et al. 2007). This results in an internal rotation of the tibia, which increases in higher knee flexion and reaches up to $24^{\circ} \pm 10^{\circ}$ in 120° flexion. The majority

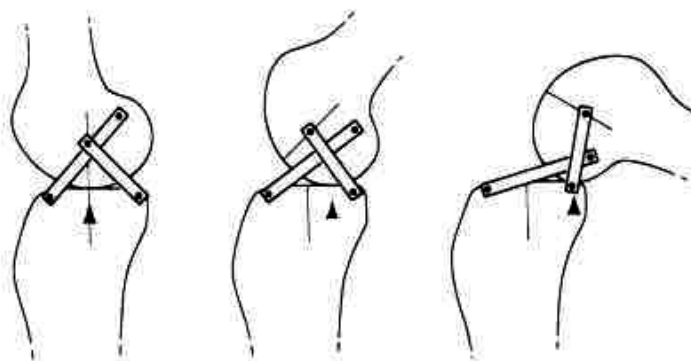


Figure 4: Schematic representation of knee kinematics as a four-bar linkage system, displaying the posterior displacement of tibiofemoral contact (Dye 1987).

of this internal tibial rotation is observed during the first 20-30° of flexion, with an average of 9° (Dennis et al. 2005). The main drawback in most of these studies that quantified tibiofemoral motion was that, due to limited space in the experimental setups such as MRI scanners and fluoroscopes, the range of

analysed activities was limited rather to quasistatic positions or squatting activities.

To describe the complex motion of the knee, as it is required to drive musculoskeletal models, a number of modelling concepts have been proposed in the literature (Blankevoort and Huiskes 1996; Caruntu and Hefzy 2004; Churchill et al. 1998; O'Connor et al. 1989). However, these have been limited to two-dimensional analysis (O'Connor et al. 1989), describe passive motion only (Blankevoort and Huiskes 1996), or lack validation against in vivo data from a larger population (Caruntu and Hefzy 2004). The concept of the four-bar linkage mechanism (Figure 4) has been used for several studies (Imran et al. 2000; Menschik 1974; O'Connor et al. 1989) and was developed from a planar 2D representation to a 2.5D model (Toutoungi et al. 1997; Zavatsky and O'Connor 1994), which considered the complete 3D shape of the ligaments in a simplified model. The description of the kinematics in this model was still based on the planar four-bar linkage system, however, which may not be capable of describing the complex three-dimensional in vivo knee kinematics (Smith et al. 2003; Zavatsky and O'Connor 1994). A validated kinematic model that is capable of reproducing the three-dimensional motion of the joint has not yet been developed.

1.4 Patellofemoral joint

The patellofemoral joint is the third joint compartment of the knee. The patella is a complex sesamoid bone within the quadriceps unit, where, similar to a pulley, the patella can change the quadriceps' direction of force (Figure 5). The patella also serves as a leverage system: the moment arm of the quadriceps is increased by the patella, especially in the earlier degrees of flexion. From 30% near extension to 15% at 30° flexion, it enhances the effects of the quadriceps muscles with respect to knee extension (Kaufer 1971). Besides this lever type, where increased moment arms reduce the required force, in certain activities and stages of the knee's flexion-extension cycle, the patella is also acting as the other side of the lever, where more displacement

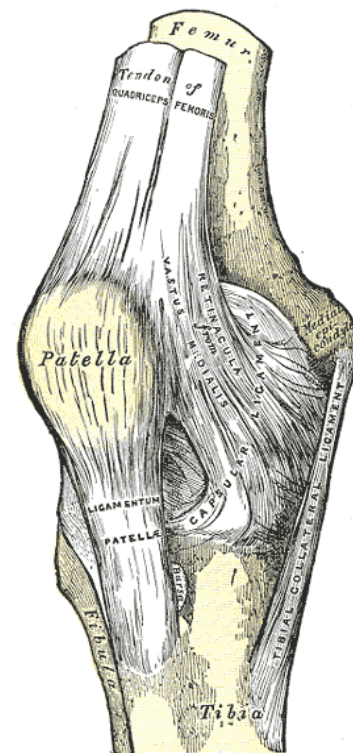


Figure 5: Anteromedial aspect of the knee with the patella, the patellar ligament and the tendon of the quadriceps muscle (Gray 1918).

is achieved by a high force on a shorter lever arm (Grelsamer and Weinstein 2001).

To date, the loading conditions within this biomechanically complex patellofemoral system are not fully understood. However, it has been observed that if this system is disturbed, patellofemoral pain can often occur, especially during challenging activities such as stair climbing (Doucette and Goble 1992; Dye 2005; Ficat et al. 1975). Analysing the patellofemoral loading conditions in the healthy knee may help to explain the observed phenomena and is important in understanding the loading conditions after TKA.

1.5 Total knee arthroplasty (TKA)

As a result of injury or progressive joint degeneration, the complex interplay and the balance between active and passive stabilizers in the knee becomes substantially disturbed, causing loss of function and pain, ultimately requiring a replacement of the joint.

Three main indications to replace the knee joint have been identified over recent decades, making up more than 98% of all such procedures: osteoarthritis, rheumatoid arthritis and trauma (Robertsson 2009). The most common indication for TKA is osteoarthritis (Mancuso et al. 1996; Quinet and Winters 1992), which is a chronic degenerative joint disease that leads to the degradation of the cartilage and the subchondral bone.

There are several factors that can contribute to the development of osteoarthritis. While age is the most important risk factor, genetic predisposition, obesity, female gender, greater bone density, joint laxity and mechanical loading beyond a level at which the joint can repair itself have also been identified (Buckwalter et al. 2004; Felson and Zhang 1998). Such mechanically challenging conditions can be created, for example, by joint injury, post-traumatic joint incongruity, instability or malalignment, joint dysplasia and the lifelong use of the joint (Buckwalter et al. 2004).

Rheumatoid arthritis accounts for far fewer knee replacements. Here, new types of medical treatment have advanced during the last few years, reducing the number of cases. Also the number of knee replacements performed due to post-traumatic situations is small in comparison to those necessitated by osteoarthritis (Robertsson 2009).

Whilst a partial, unicompartmental replacement of the knee is used in some cases of mainly younger patients, with local degeneration affecting only one side of the joint, the total replacement of the knee is becoming widely accepted by patients who have a pathologic knee, expecting pain reduction and a restoration of their normal knee function. The numbers of cases are constantly increasing and are expected to reach an estimated 3.5 million in 2030 in the US alone (Kurtz et al. 2007), where the annual number currently stands at about 611000 (HCUP-Databases 2007).

Several types of implants can be used for a total knee replacement (Figure 6). The main categorization criterion is the degree of mechanical stability offered by the implant. In non-constrained implants, the tibial and femoral components are not linked to each other. This type of implant requires sufficient stability provided by muscles and ligaments. The posterior cruciate ligament is not sacrificed when this implant type is used. Semi-constrained implants offer increased stability, chiefly by replacing the function of the sacrificed posterior cruciate ligament. This is usually achieved by a “cam / post” design where a post on the tibial insert engages in flexion with a cam on the femoral component, preventing anterior femoral translation. If a standard femoral component is chosen, an ultra-congruent (deep dish) tibial inlay can also be used to create a semi-constrained condition. The highest degree of mechanical stability is achieved by constrained or hinged implant types, which are used to compensate for severe insufficiencies of the patient’s collateral ligaments.

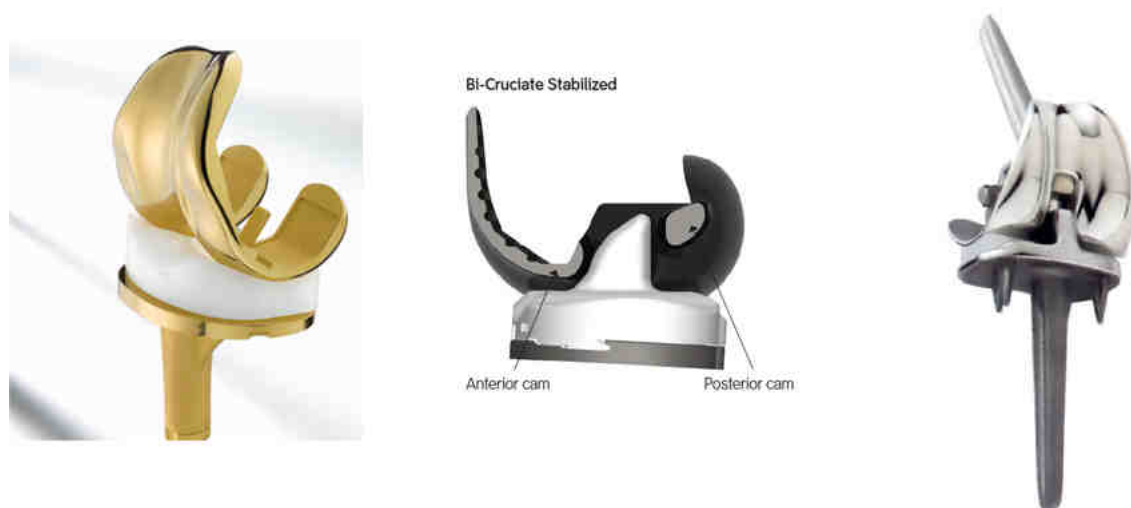


Figure 6: Implants can offer different degrees of mechanical stabilization: non-constrained (left, Aesculap Columbus), posterior stabilized (middle, Smith&Nephew JOURNEY™ BCS) and constrained or hinged (right, Aesculap Blauth Total Hinge Knee).

Several manufacturers offer a rotating platform / mobile bearing design of the interface between the tibial component and the polyethylene insert, which additionally allows internal–external rotation, possibly reducing the wear rate and the risk of implant loosening in younger and more active, as well as obese, patients. There is an ongoing discussion in the literature on the pros and cons of each design and the correct indication for their use (Breugem et al. 2008; Hasegawa et al. 2009; Kessler et al. 2008; Kim et al. 2009; Pietsch and Hofmann 2007), where the benefit of one over the others has not been demonstrated clinically.

In general, a replacement of the knee joint is, for the majority of patients, a successful intervention, not only leading to improved clinical results, but also creating a higher patient satisfaction and improved quality of life (Dorr and Chao 2007; Hawker et al. 1998; Noble et al. 2006).

1.6 Complications after TKA

Despite the undoubted success of the procedure in general, TKA is also subject to failure. The current 10-year failure rates have been reported to be as high as 12% (Burnett et al. 2004; Hardeman et al. 2006; Ishii et al. 2005; Mangaleshkar et al. 2002; Mayman et al. 2003). If related to the previously mentioned predicted growth in numbers of TKAs performed in the coming years, this will also lead to significant numbers of revision surgeries worldwide (Kurtz et al. 2007). To identify the reasons for an early prosthesis failure, the established Swedish Knee Arthroplasty Register (SKAR) and other institutions documented the main indications for revision surgery: aseptic loosening (>20%), infections (~20%), wear (~5%), fracture (~2%), patella problems (~20%, excluding loosening and wear), instability (~10%) and progression of femoro-patellar arthritis (~10%) (Robertsson 2009). Thus it seems that, with aseptic loosening, instability, wear, fracture, and patella-related problems, more than 50% of the revisions are related to non-optimal biomechanics in the reconstructed joint. This suggests that the complex interplay between the remaining soft-tissue stabilizers and the new artificial joint geometry is not optimally restored.

Clinical studies have indicated that an altered joint geometry can have a negative influence on the outcome of a TKA. Besides the circumstance that an individual joint is replaced by a rather generic implant, these geometrical alterations are also caused by a

surgical malalignment of the implant relative to the pre-operative condition. Such malalignment has been related to post-operative pain, instability, limited range of motion and additional functional deficits, which in severe conditions can all lead to revision (Akagi et al. 1999; Barrack et al. 2001; Berger et al. 1998; Catani et al. 2006; Choong et al. 2009; Dennis et al. 2001; Eckhoff et al. 1995; Hofmann et al. 2003; Insall et al. 2002; Jeffery et al. 1991; Lewis et al. 1994; Liao et al. 2002; Nagamine et al. 1995b; Romero et al. 2003; Sharkey et al. 2002; Takahashi et al. 1997; Wasielewski et al. 1994; Zihlmann et al. 2005).

While tibial malalignment was also clinically identified in the context of compromised post-operative results (Bellemans et al. 2005; Kansara and Markel 2006), a significant share of post-operative complications is related to malaligned femoral components. A malrotation of the femoral component in the axial plane, either isolated or in combination with a malrotated tibial component, can be linked to anterior knee pain, limited flexion capability, patellar maltracking and patellofemoral instability (Akagi et al. 1999; Barrack et al. 2001; Berger et al. 1998; Hofmann et al. 2003). A cranial malplacement of the femoral component, which leads to an elevation of the joint line, can be associated with patellofemoral problems (Laskin 1998), lower knee scores (Figgie et al. 1986; Partington et al. 1999; Porteous et al. 2008) and limited knee flexion capability (Chiu et al. 2002).

1.7 Restoring joint geometry

Even though the importance of restoring the joint's geometry – especially on the femoral side – is known, this aim is not always achieved in TKA. A fundamental limitation in achieving this aim is that an individually proportioned natural joint is replaced by a relatively limited variety of available prostheses. The non-symmetrical natural shape of the articulating joint surfaces is often replaced by symmetrical prosthesis designs, and the stabilizing function of either one or both cruciate ligaments, and sometimes also of the collateral ligaments, is replaced by alternative mechanisms.

In addition to the difficulties that might be involved with the prosthesis design, the acquisition of anatomical references for a correct alignment of the femoral component is difficult. Firstly, the field of view and available operating space is limited, as it is aimed to keep the soft tissue trauma and the number of required transfusions as small as possible. Furthermore, the clear identification and palpation of most of the anatomical references is difficult, as they are often covered by soft tissues, and their definition does

not always allow a highly reproducible acquisition (Jenny and Boeri 2004; Laskin 2002; Mason et al. 2006).

Malalignment can also be induced by certain situations in the surgical workflow, where a compromise between an optimal alignment and other factors is required. For example, to achieve a balanced interaction with the soft tissue stabilizers in flexion, the femoral component may be adapted in its internal-external rotation (Whiteside 2002). To achieve a stable joint in flexion in the case of distal femoral bone loss, a common compromise is the elevation of the joint line by using a higher inlay and a smaller femoral component (Bellemans 2004; Scuderi and Insall 1992).

In some cases, where the knee is severely diseased and exhibits bony deformities and adapted soft tissues, a restoration of the pre-operative joint condition is not always desired, as the native joint was exposed to unfavourable biomechanical conditions. These cases are not specifically analysed in this study, since they require an individual modelling approach, reflecting the native deformed condition of the joint in order to assess an optimal reconstruction.

1.8 Evaluating the impact of malalignment on the joint's biomechanics

Loading conditions

The possibilities to estimate the effects of a change in the joint's geometry on the biomechanics of the joint are limited and often do not allow us to understand and explain the clinical observations. While the in vivo measurement of moments and forces in the tibiofemoral joint has been achieved (Heinlein et al. 2007; Zhao et al. 2007), the number of patients that can be measured is very limited. Collecting data which cover a broad spectrum of femoral malalignment in this manner is therefore unlikely. While in vitro setups would generally allow the simulation of altered joint geometry, the adequate application of loading conditions remains challenging, especially in the tibiofemoral joint. The large number of possible variations in joint geometry that need to be simulated is another limiting factor in the use of an experimental in vitro setup.

Another established method to investigate musculoskeletal interactions is the use of analytical musculoskeletal models (Heller et al. 2001b). Besides the novel capability to determine a patient's loading conditions, such as internal loads, muscle forces and joint

contact forces, non-invasively and by external measurements only, such models also offer the possibility to study the effects of anatomical variation on loading conditions (Heller et al. 2001a; Heller et al. 2007a).

Adapting and utilizing such tools opens the possibility of answering clinical questions by systematically analysing the effects of femoral component malalignment, caused by either imprecise anatomical referencing or surgical compromises, on the joint's biomechanics. The knowledge gained can then help to identify and ultimately avoid overloading conditions that may compromise the performance and survival of the implant.

Function of collateral ligaments

Post-operative complications after TKA are often stability-related (Robertsson 2009), i.e. joint instability or joint stiffness. A possible reason for these stability-related problems is an imbalance in the system of the passive stabilizers, which could be caused by the implantation of the prosthesis. An approach to identify stability-related problems is the functional analysis of the collateral ligaments in the healthy knee, as well as in the knee after TKA. Assessing the function of the collateral ligaments after TKA in vivo is, however, difficult due to their restricted accessibility. Modern imaging systems now allow the visualization of the structures in the knee during even weight-bearing activities. A possible method to characterize ligament function is to analyse the distance between the ligaments' bony insertions (Park et al. 2005; Van de Velde et al. 2007).

Park (Park et al. 2005) used a combined MRI and fluoroscopy approach to investigate the distance between the proximal and distal collateral ligament insertion sites, and analysed the length-change patterns of the collateral ligaments during knee flexion. In a similar study, Van der Velde (Van de Velde et al. 2007) analysed the effect of an ACL insufficiency on the collateral ligaments during weight-bearing knee flexion. Applying this proposed technique to investigate post-TKA collateral ligament function might help to identify possible reasons for joint instability or stiffness.

1.9 Goals / Significance

The purpose of this study is to enhance the understanding of the effects of femoral component malalignment on the knee's biomechanics, specifically on the tibio- and patellofemoral contact forces, and the function of the collateral ligaments.

The specific aspects of this goal are to:

- Establish a 3D anatomical reference of the musculoskeletal structures of the knee
- Achieve a better understanding of the biomechanics of the intact joint in terms of tibio- and patellofemoral contact mechanics
- Investigate the impact of a cranial / caudal malalignment of the femoral component (joint line suppression or elevation) on the joint contact forces in the knee
- Investigate the effect of joint line elevation on the function of the collateral ligaments
- Analyse the effect of a complex malalignment in multiple orientations on the joint contact forces in the knee, to identify most influential aspects of malalignment

These investigations can help to provide a better understanding of how malalignment of the femoral component can affect the loading conditions and the ligament function after TKA. The knowledge gained can be beneficial in better assessing planned TKAs with the aim of avoiding such implantations as are likely to create increased loading conditions or may lead to stability-related complications. This study delivers a basis to ultimately make such biomechanical information available to the surgeon in the various steps of the surgical procedure: the pre-operative planning, the intraoperative alignment and the post-operative assessment.

2 BIOMECHANICAL ANALYSES OF THE INTACT KNEE

In this chapter, work is presented that aimed to extend the currently available data regarding the healthy knee's anatomy and contact mechanics. The knowledge gained from these studies of the healthy knee can then serve as a basis for analysing the knee after TKA.

As a first step, the currently available and quite simplified 3D representations of active and passive soft tissue structures in the lower limb were modelled at a higher precision level and integrated in the musculoskeletal model developed by Heller and co-workers (Heller et al. 2001b).

In the next step, the tibiofemoral kinematics of the healthy joint were analysed in passive as well as active knee flexion. Based on these investigations, a kinematic model of tibiofemoral motion was developed. Such a model may be used to augment the often imprecise gait analysis data that is currently used to simulate tibiofemoral kinematics in musculoskeletal models.

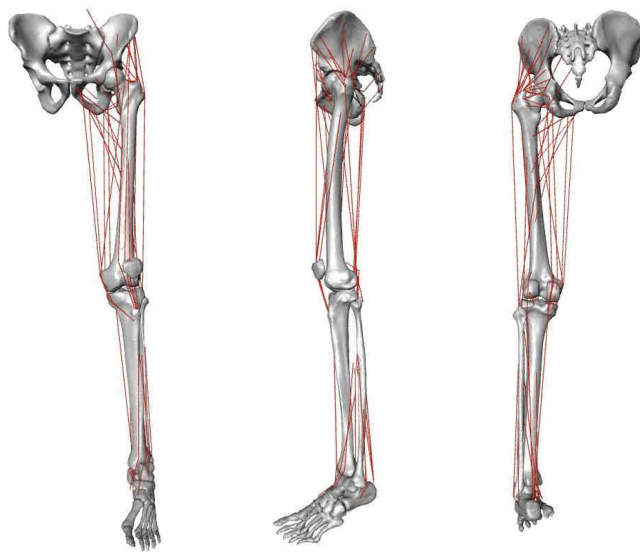
To gain more information about the contact mechanics of the patellofemoral joint, an in vitro setup was adapted to investigate the kinematics and loading in the patellofemoral joint under in vivo loading conditions.

The last section of this chapter presents a model to analyse the function of the collateral ligaments during the flexion of the healthy knee.

2.1 3D representation of active and passive soft tissue structures in the lower limb

To date, most musculoskeletal models use simplified straight line elements to approximate the 3D path of muscles and ligaments (Brand et al. 1982; Duda et al. 1997; Heller et al. 2001b; Scheys et al. 2006) (Figure 7). This simplification in the musculoskeletal model may lead to an over- or underestimation of the lever arm with which a muscle can act at the joint (Brand et al. 1982). Therefore the calculated muscle forces may in some conditions deviate from those acting in vivo.

While the calculations of the total joint contact forces using the musculoskeletal models with such simplified muscle representation are still of sufficient accuracy (Heller et al. 2001b), a more detailed modelling of the 3D muscle paths may allow the more reliable



estimation of the contribution of the individual muscles to these forces. Furthermore, a more detailed description of the collateral ligaments and their bony insertions is an essential precondition for analysing collateral ligament function during knee flexion.

Figure 7: anterior, lateral and posterior views (from left) of the musculoskeletal model developed by Heller and co-workers (Heller et al. 2001b).

Methods and results

3D models of muscles and ligaments

The basis for the 3D modelling of the muscles and ligaments was the Visible Human Male dataset (Spitzer et al. 1996), which was also used by Heller et al. to develop their musculoskeletal model (Heller et al. 2001b). While the model of Heller and co-workers was based on the CT data of the Visible Human dataset, the present 3D modelling of muscles and ligaments was performed using the high-resolution colour images of the same dataset (Figure 8). These images provided an in-plane resolution of 0.144x0.144mm and allowed a good differentiation of the various tissues.

For a better handling of this large dataset, which was about 6.1GB in size, the amount of data was reduced before further use. A direct comparison of the individual colour channels of the RGB image showed that the green channel alone provided sufficient contrast to reliably identify the individual structures.

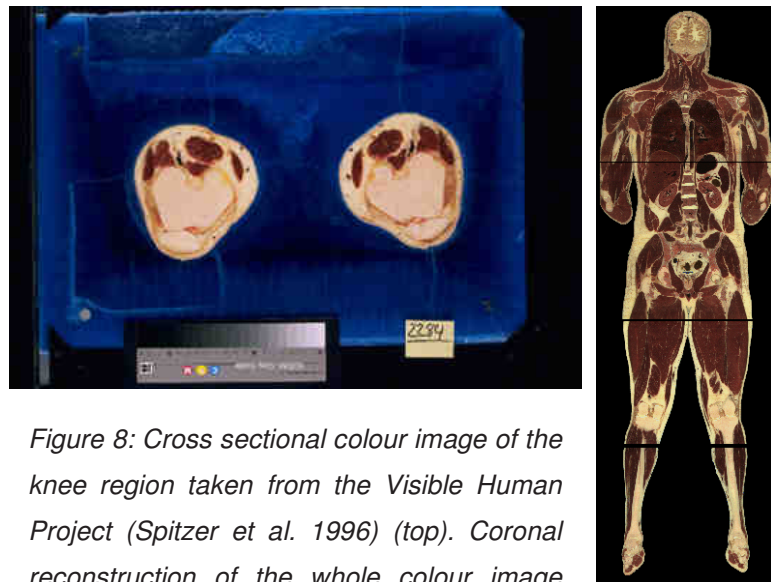


Figure 8: Cross sectional colour image of the knee region taken from the Visible Human Project (Spitzer et al. 1996) (top). Coronal reconstruction of the whole colour image data set (right)

The modelling process, which was performed on the greyscale images of the green colour channel, was conducted using the AMIRA visualization and volume modelling software (Mercury Computer Systems Inc., MA, USA). In the beginning, the images containing the origins and insertions of the analysed muscle or ligament were identified and located in the dataset, using anatomy textbooks as a reference (Frank. 1992; Rohen et al. 2002). To segment the individual structures within the images, the corresponding image voxels were marked and assigned to a material index (Figure 9). After the complete segmentation of a structure, a 3D surface model was generated from the set of marked voxels using a marching cube algorithm implemented in AMIRA (Figures 10, 11, 12).

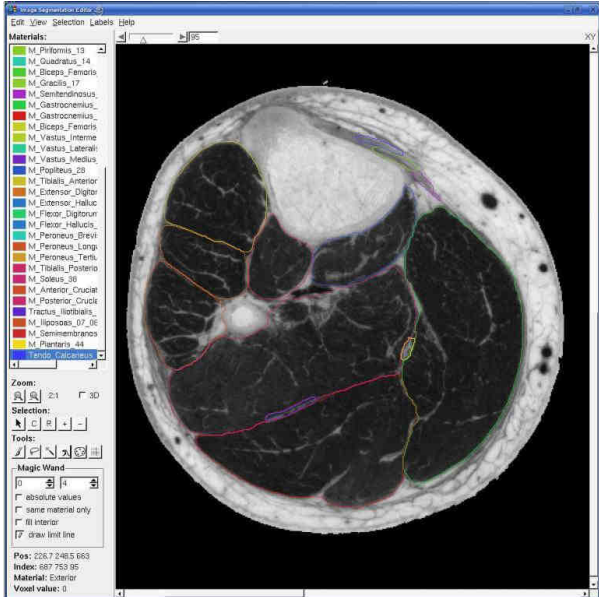


Figure 9: The soft tissue structures were segmented in the green channel, which was displayed as a greyscale image, using a segmentation editor. The specific structures were marked and assigned to a material ID (left). Three-dimensional surface models were then reconstructed from this data (top).

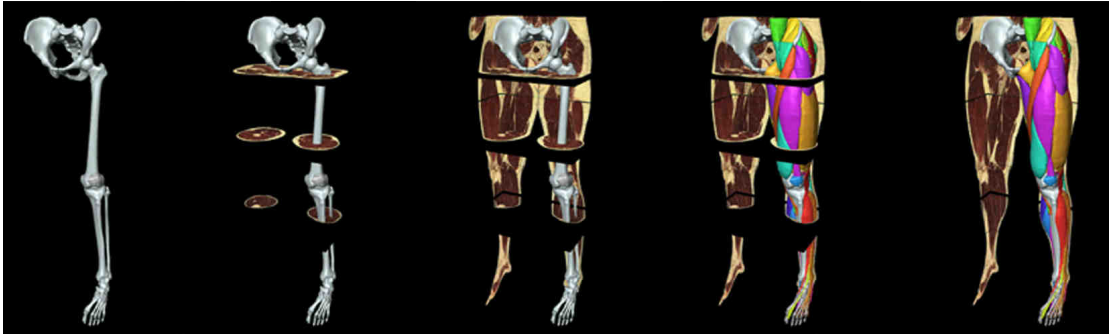


Figure 10: Process of combining the bony structures used by Heller and co-workers in their musculoskeletal model (Heller et al. 2001b) with a 3D representation using the high-resolution colour images of the Visible Human dataset (Spitzer et al. 1996).

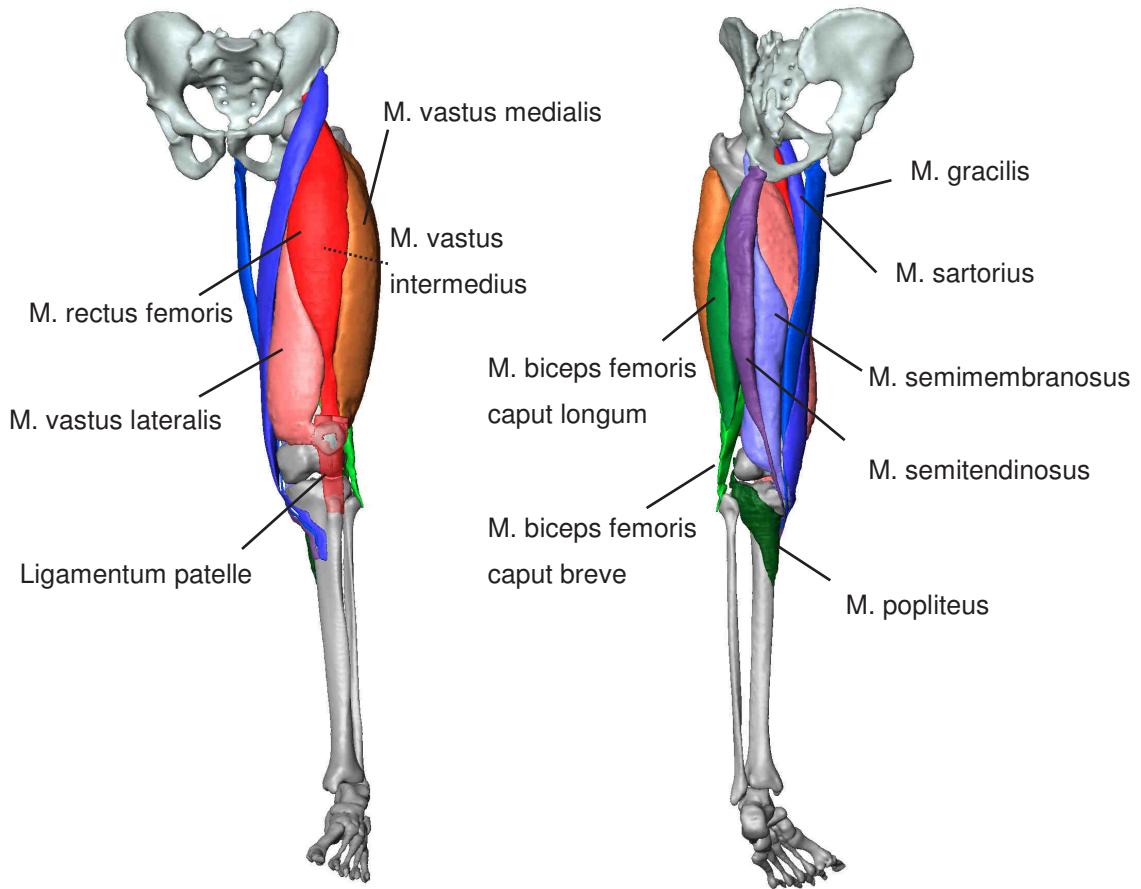


Figure 11: Three-dimensional representation of the muscles (including their tendons) that determine motion and stability in the knee joint (Moewis 2007). Muscles that are labelled in the anterior view (left image) are involved in joint extension, while muscles labelled in the posterior view (right image) mainly contribute to joint flexion.

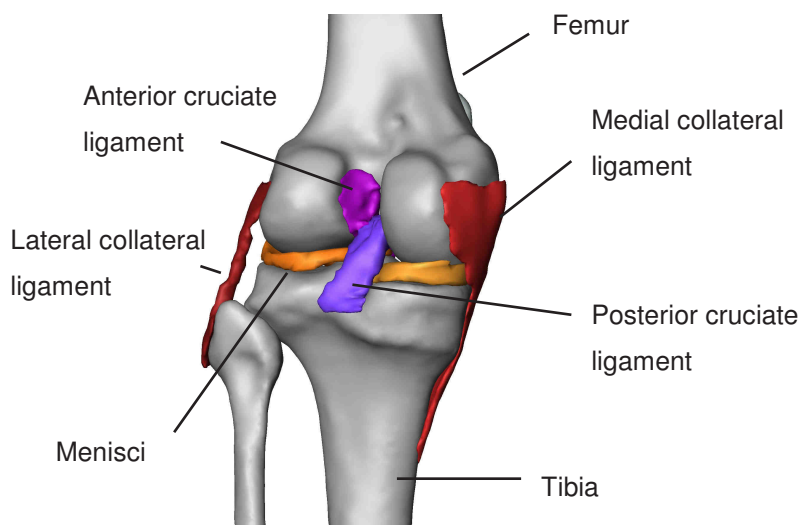


Figure 12: The main passive joint stabilizers: collateral and cruciate ligaments, both menisci, as well as femur and tibia. Not displayed are the tibial and femoral articular cartilage and the capsule.

Muscle origin and insertion sites

To define the bony muscle insertion sites, the areas of minimum distance between the 3D muscle surface and the surface of the bone were determined in the attachment region (Moewis 2007). To do so, the two surfaces were combined and the Hausdorff Distance calculated and mapped onto the bone as a colour field (Figure 13). The attachment areas were then defined as the areas of minimum distance.

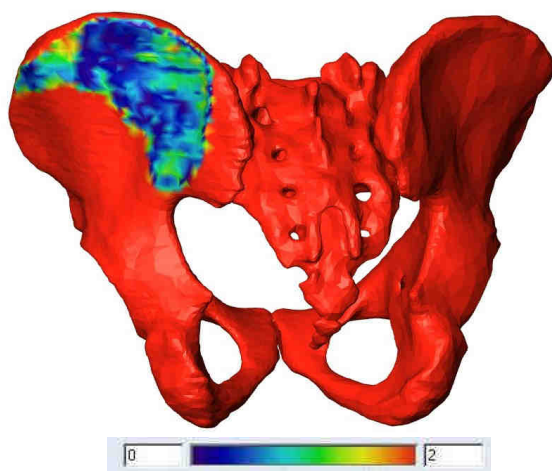


Figure 13: Hausdorff Distance between the surface of the muscle and the surface of the bone, projected as colour map onto the bone. The colour indicates the distance ranging from 0 mm (blue) to 2 mm and more (red).

Muscle centroid lines

For smaller muscle surfaces that did not show significant variation in their direction, the 3D surface model of the muscle was intersected with planes. The planes were oriented orthogonally to the line spanning between the muscle origin and insertion, and with intersections performed at equal spacing relative to the total distance between origin and insertion. The line that contained the geometric centres of all muscle intersection surfaces defined the centroid line of the muscle. In those cases where the muscles showed a large variation in direction, this method did not deliver adequate results. A manual procedure was then applied for these muscles (Figure 14). The planes that created the intersections were defined perpendicular to the muscle fibres that were identified and

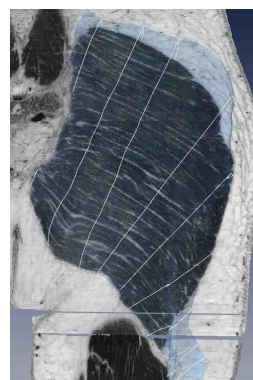


Figure 14: Example of a larger muscle with changing direction (Gluteus Maximus) in which the planes for the surface intersection were defined orthogonal to the direction of the muscle fibres.

marked in the colour images of the Visible Human dataset. Being directly derived from the 3D muscle anatomy, these centroid lines could be used to define the lines of action in the musculoskeletal model (Figure 15).

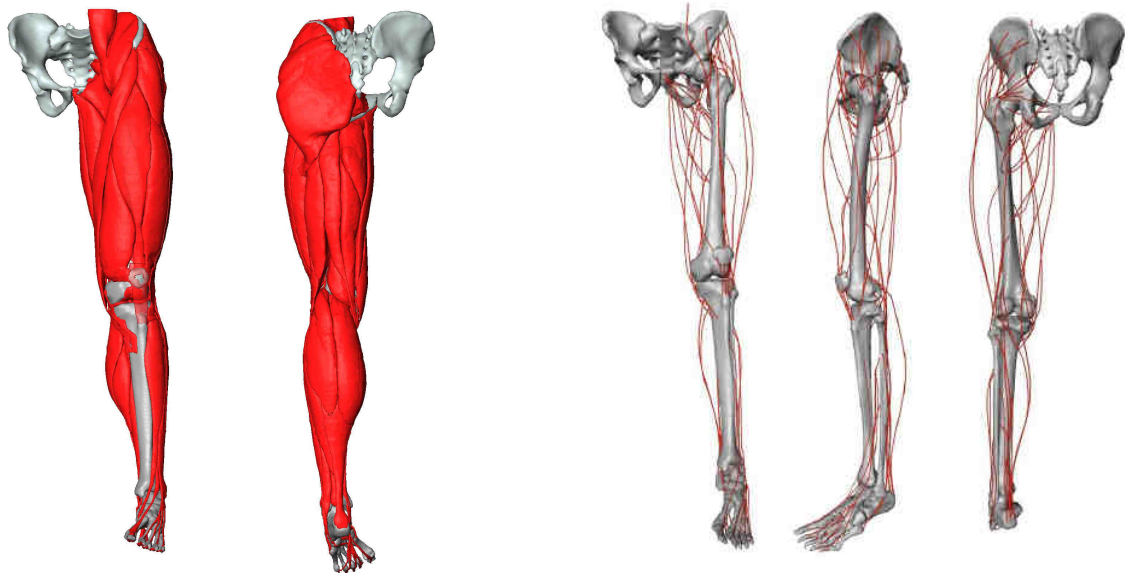


Figure 15: Musculoskeletal structures of the lower limb visualized as 3D surface models (left) and the muscular structures visualized as centroid lines (right).

Discussion

The modelling of the lower limb's muscular and ligamentous structures gave access to a more detailed and precise anatomical description than previously available. Specifically, the modelling of the collateral ligaments offers the possibility for a functional analysis of these structures. Deriving the muscular lines of action from a complex 3D representation of the muscles in the lower limb may contribute to

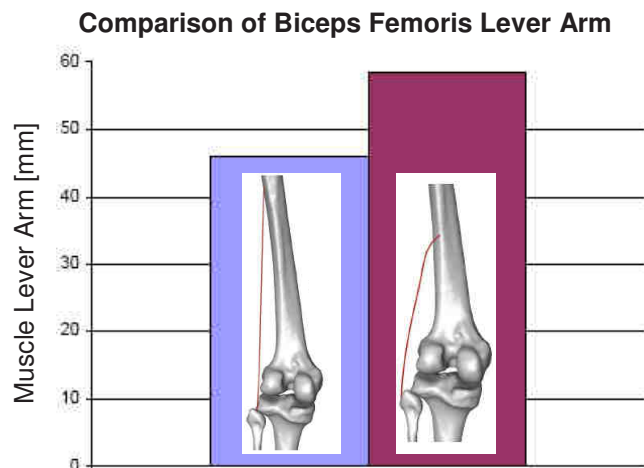


Figure 16: The lever arm length of the Biceps Femoris in the axial plane for the straight line (left bar) and the centroid line (right bar) muscle representation.

a further enhancement of the musculoskeletal model. A change in the lever arms of specific muscles as a result of the new muscle representation (Figures 16, 17) can affect the contribution of individual muscles to the total joint contact force. However, it remains a challenge to include a dynamic wrapping of these new muscle lines during knee flexion, as these muscle lines are derived from the straight knee only.

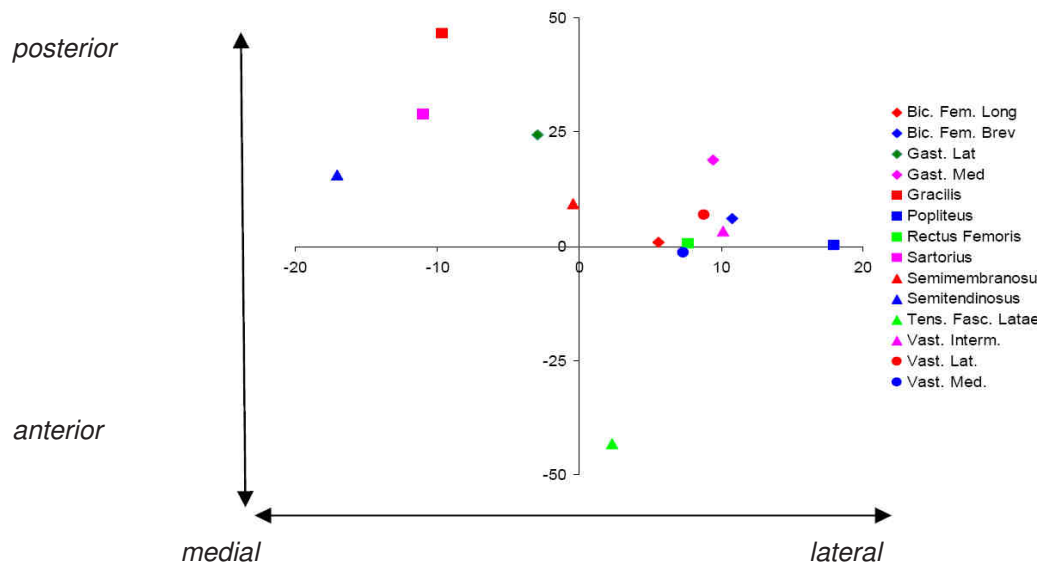


Figure 17: The diagram shows the relative difference (%) between the lever arms derived from the centroid line and the straight line models.

2.2 Kinematic models to describe tibiofemoral motion

Heller MO, König C, Graichen H, Hinterwimmer S, Ehrig RM, Duda GN, Taylor WR. 2007, *J Biomech*, 40 Suppl 1:S45-53

Kinematic models to simulate tibiofemoral kinematics on the basis of the four-bar linkage have been briefly described in the introduction. To date, these models are limited, as they do not consider internal/external rotation and ab/adduction. A further limitation of this four-bar linkage concept is that it so far relies on localizing an area within the ligament attachment zone where ligament fibres remain isometric throughout flexion. The existence of such isometric fibres has been brought into question due to an observed inter-patient variation in the location of the tibial ligament attachment zone relative to the bone, as well as variation in the knee's kinematics with different loading conditions (Amis and Zavras 1995).

It was therefore aimed to develop a new three-dimensional model of knee kinematics, based on a modified four-bar linkage that does not rely on isometric fibres, but considers the cruciate ligament lengthening characteristics, as well as reflecting tibiofemoral internal/external rotation. A further aim was to assess whether such a kinematic model is capable of simulating tibiofemoral kinematics during unloaded and loaded in vivo knee flexion. With parameter sets of the kinematic model that can reconstruct the known kinematics of a number of individuals, it may then be possible to create a predictive model for tibiofemoral kinematics that can be used to drive musculoskeletal models.

Materials and methods

Acquisition of in vivo reference kinematics

As reference data, MRI images from Bringmann and colleagues (Bringmann et al. 2000) were used and the knee joints of 12 healthy volunteers with no history of pain or injury were examined. Kinematic analysis was performed in an open MR system (0.2T; Magnetom-Open, Siemens, Erlangen, Germany) using a T1-weighted 3D gradient echo sequence (TR 16.1ms, TE 7.0ms, FA 30°)(Bringmann et al. 2000). Sagittal plane images (slice thickness: 1.875mm, in plane resolution: 0.86mm) were taken with an acquisition time of 4min 26s. The volunteers were placed on their side and the knee flexion angle (0°, 30°, 90°) was controlled by a special positioning device (Siemens,

Erlangen, Germany). Scans were taken with the knee either unloaded, or with the application of a weight of 3kg to the lower third of the shank to produce a torque of 10Nm at the knee joint. This torque was initiated in a flexing direction, leading to activation of the knee extensors. Isometric muscle activity over the entire acquisition period was verified by surface electromyography (Bringmann et al. 2000).

After image acquisition, semi-automated segmentation of the femur, tibia, ACL and PCL was performed, based on a grey-value oriented region-growing algorithm (Bringmann et al. 2000). Using a marching cube algorithm implemented in the visualization and volume modelling software, AMIRA (Mercury Computer Systems Inc., MA, USA), surface models of the bony structures and the cruciate ligaments were created (Figure 18) to derive in vivo joint kinematics and to determine attachment areas of the cruciate ligaments.

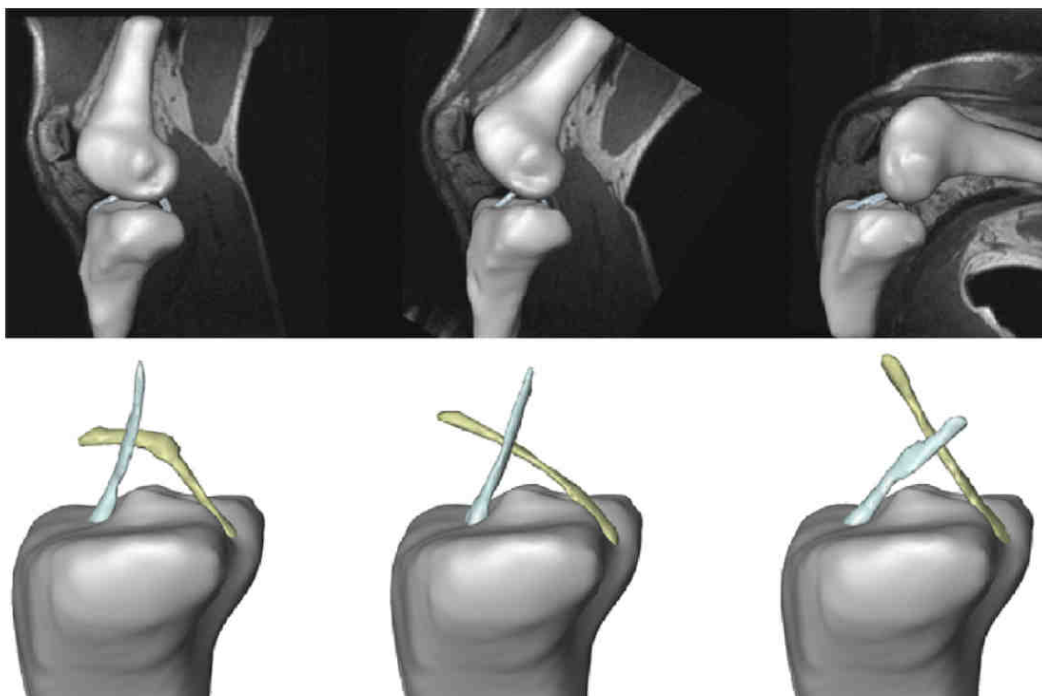


Figure 18: Reconstructed bone surfaces and cruciate ligaments from MRI images at 0°, 30° and 90° knee flexion. Top: The movement of the femur relative to the tibia was analysed by registering the surface models of the tibiae at 30° and 90° knee flexion onto the tibia at 0° flexion. Bottom: Sagittal view of the tibia and the PCL as reconstructed from the MRI data. A shift from a lax concave shape at 0° to a taut ligament at 30° and 90° can be seen, posing the question as to whether a linear four-bar linkage model is capable of simulating the kinematics of the knee.

Definition of local coordinate systems

The first axis (x) of the femoral coordinate system was defined by using a transepicondylar axis, as suggested by the International Society of Biomechanics (Wu et al. 2002). In order to establish this axis, cylinders were fitted to the medial and lateral posterior condylar surfaces using a comprehensive quasi-Newton (least squares fit) algorithm (NAG routine e04jbc, Numerical Algorithms Group Ltd, England).

The transepicondylar (TE) axis then passed through two landmarks, placed at the intersection of the centre line of the medial cylinder with the medial epicondylar surface and the intersection of the centre line of the lateral cylinder with the lateral epicondylar surface. The distance between these landmarks was defined as the femur width and the origin of the coordinate system was defined at the midpoint between these two landmarks. A plane was defined normal to the transepicondylar axis that passed through the origin. A contour describing the intersection of this plane and the femoral surface was then cut with a radius of 0.75 times the subject-specific femur width. The vector from the origin to the centroid of this contour then defined the second axis (y) of the coordinate system. The third axis (z) was calculated as the cross product of the x- and y-axes (Figure 19).

The proximal tibia was cut using a cylindrical clipping tool about the femoral TE-axis (radius of 0.75 times femur width). Using a least square optimization method, a plane was fitted to the sectioned proximal tibia that defined the axial plane. The x-axis of the femoral coordinate system was projected onto this plane, creating the x-axis of the tibial coordinate system. The y-axis was defined by a 90° rotation of the x-axis on this plane, describing the anterior-posterior direction. The z-axis was the cross product of x and y.

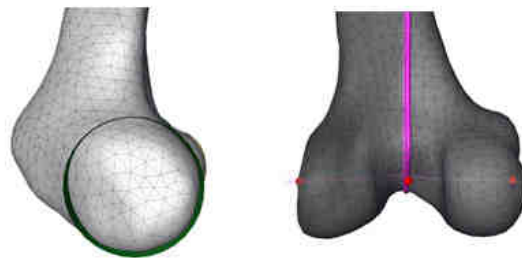


Figure 19: Definition of the femoral coordinate system. Left: A cylinder fitting technique was used to define the TE-axis. Right: A third proximal point was placed at the centre of the contour that was created by cutting the femoral surface orthogonal to the TE-axis through its centre.

Determining in vivo kinematics and ligament attachments

The reference for describing the kinematics during flexion was defined as the tibial position at 0° knee flexion (Patel et al. 2004). By registering the tibial surfaces using an iterative closest point transform (ICP) algorithm (Besl and McKay 1992) implemented within AMIRA, rigid transformation matrices were computed for the femur between each pair of poses (0° – 30° and 30° – 90°). The surface models of the femur at 30° and 90° flexion were then transformed into the reference system for registration of the ligament insertion sites.

In vivo internal/external rotation was calculated with reference to the transepicondylar axis of the femur (von Eisenhart-Rothe et al. 2004). Here, the axes were projected onto the tibial plateau represented by the x-y plane of the tibia coordinate system and the angle of their intersection was computed to define the internal/external rotation.

The cruciate ligament attachment sites at the femur and tibia were approximated by computing a proximity map between the reconstructed bone and the ligament surfaces at 0° knee flexion. Based on these maps, the bony attachment areas of the ACL and PCL were defined as elliptical grids containing a total of 37 grid points for each attachment site (Figure 20).

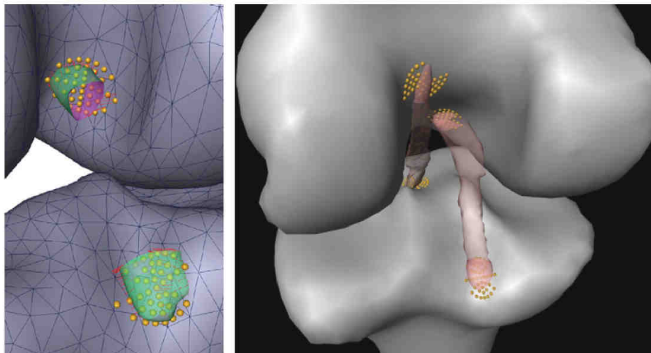


Figure 20: Surface models of the cruciate ligaments were used to create proximity maps on the bony surface. Left: Elliptical attachment regions were defined by 37 landmarks, here demonstrated for the PCL's AM bundle. Right: Attachment regions (landmarks) for the ACL and PCL, shown as transparent structures, as reconstructed in one subject.

Appropriate proportions of the overall attachment areas were assigned to the antero-medial (AM) and postero-lateral (PL) bundles of the ACL, as well as the antero-lateral (AL) bundle of the PCL (Amis et al. 2005; Giron et al. 2005). Identification of the relatively small PM bundle of the PCL in the T1-weighted MR image was difficult, due to the low intensity of the signal of the PCL (Servant et al. 2004). As a result, information regarding the insertion site was augmented using high-resolution colour images of the visible human (VH) (Spitzer et al. 1996), by determining the vector from the centre of the AL bundle to the centre of the PM bundle. In the subject's knees, this vector was

transferred into the local femoral coordinate system, normalized to the width of the VH femur (length of the TE-axis) and then scaled to the femoral width of the subject.

To characterize the laxity / extension of the cruciate ligaments during knee flexion, the relative change in the distances between the grid points representing the tibial and femoral attachment zones of the cruciate ligaments were calculated (Friederich et al. 1992; Li et al. 2004; Nakagawa et al. 2004) throughout the 30° and 90° positions in each subject.

Kinematic model

The original four-bar linkage models required that the tibial and femoral insertion points of the cruciate ligaments were projected on the sagittal plane as a model input (Imran et al. 2000; Lu and O'Connor 1996; Menschik 1974; Muller 1993; O'Connor et al. 1989; Zavatsky and O'Connor 1994) and remained isometric, i.e. constant in length (O'Connor et al. 1989). The proposed kinematic model deviates from these archetypal models in that all possible three-dimensional ligament attachments served as an input to the model, as well as each subject's internal/external (i/e) rotation, which was superimposed onto the planar movement described by the four-bar linkage. Between the measured values at 0°, 30° and 90° flexion angle, the i/e rotation was interpolated linearly. Furthermore, to allow for possible laxity of the ligaments, the fibre lengths were not isometrically constrained, but were allowed to vary within values determined by Friederich and co-workers (1992). Thus, a range of fibre lengths were covered, from 0% to -25% for the ACL and 0% to 31% for the PCL from the reference 0° position, applied linearly between flexion angles of 0° and 30°, but remaining isometric from 30° to 90°. This was justified, as the gradient in the ACL strain, and thus its length change, is reportedly highest in this range of flexion angles (Beynon et al. 1992). The slack-taut transition of the PCL is also reported to occur in this region of flexion angles (Makris et al. 2000).

The accuracy of the four-bar linkage mechanism was assessed for every possible combination of points in each cruciate ligament attachment grid, along with every possible ligament lengthening configuration, that modelled the correct i/e rotation for each subject (Figure 21).

In this manner, the model set out to determine the specific set of parameters that minimized the deviation between the pose of the femur predicted by the kinematic model and the pose derived directly from the in vivo MR data at 30° and 90° knee flexion, as described by the three femoral landmarks.

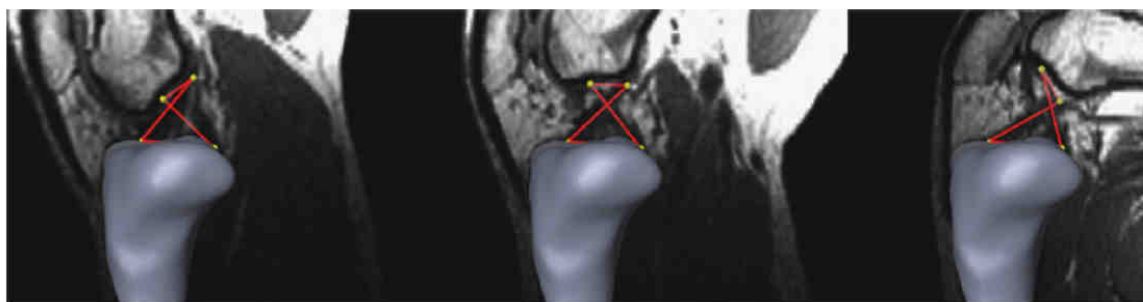


Figure 21: The four-bar linkage model (solid bars) for describing the movement of the femur relative to the tibia. Here, the reconstructed surface of the tibia is overlaid on the in vivo MR images at 0°, 30° and 90° flexion angle.

Once this optimal parameter set was determined for each subject, it was aimed to then use these parameters to create a predictive model for joint kinematics and assess its efficacy against the known in vivo positions. By averaging the five best parameter sets (combinations of i/e rotation and the ligament extension / laxity characteristics) for each subject, a generic four-bar linkage model was constructed for general prediction of knee joint motion. The efficacy of this new model was then assessed by predicting the motion of the tibiofemoral joint for each subject and comparing against the known positions at 30° and 90°.

Statistics

Statistical analysis was performed to investigate the effect of including i/e rotation in the model, by comparing the distances between the femoral reference points (Student's *t*-test, level of significance 0.05). Whether the remaining distance between the reference points was influenced by muscle activity was investigated with the Wilcoxon test using the same level of significance. Whether the kinematic model was capable of reproducing the differences in ligament lengthening throughout knee flexion caused by muscle activity was investigated with an ANOVA for repeated measures (Brunner et al. 2002).

Results

In vivo kinematics

The in vivo kinematics of the tibiofemoral joint were derived from open MRI for 12 healthy subjects for knee flexion under both passive and active neuromuscular patterns. An average tibial internal rotation of $1.8^{\circ} \pm 0.9^{\circ}$ was observed for the unloaded knee at 30° and $7.1^{\circ} \pm 4.6^{\circ}$ at 90° knee flexion. When loaded, an average tibial internal rotation of $4.0^{\circ} \pm 2.5^{\circ}$ occurred at 30° and $5.6^{\circ} \pm 3.6^{\circ}$ at 90° .

Subject-specific models

In passive knee flexion, the average distances between the predicted and the in vivo femoral TE-axis reference points, using the archetypal planar four-bar linkage mechanism (i.e. with no internal/external rotation), were medial: 1.8 ± 0.9 mm and 5.5 ± 2.6 mm, and lateral: 1.8 ± 0.8 mm and 5.6 ± 3.0 mm (Figure 22) at 30° and 90° flexion respectively. When the kinematics were determined using the new model that includes i/e rotation, the average distances were 1.8 ± 1.2 mm and 2.5 ± 1.4 mm on the medial side and 1.7 ± 1.2 mm and 2.4 ± 1.2 mm on the lateral side. The consideration of subject-specific i/e rotation in the new model therefore resulted in a greatly improved positional correlation at 30° , as well as a significant decrease in the error at 90° flexion (Student's *t*-test, $p < 0.004$).

When active knee flexion was considered, deviations between the predictions and the known poses were 3.5 ± 2.1 mm and 2.9 ± 1.2 mm on the medial side and 3.2 ± 1.6 mm and 2.8 ± 1.1 mm on the lateral side at 30° and 90° flexion respectively. As with passive flexion, the inclusion of i/e rotation led to a significant improvement at 90° (Student's *t*-test, $p < 0.05$) and improved the calculated positions at 30° , compared to the archetypal model (medial: 3.3 ± 1.4 mm and 4.7 ± 2.5 mm lateral: 3.4 ± 1.8 mm and 4.8 ± 2.6 mm).

When the influence of neuromuscular activity on the reconstructed positions was considered, a higher accuracy was observed in reconstructing knee kinematics for passive knee flexion at 30° (Wilcoxon, $p < 0.05$). At higher flexion angles (90°), however, the model was able to predict passive and active kinematics equally (Wilcoxon, $p > 0.05$). These conditions were not influenced by i/e rotation.

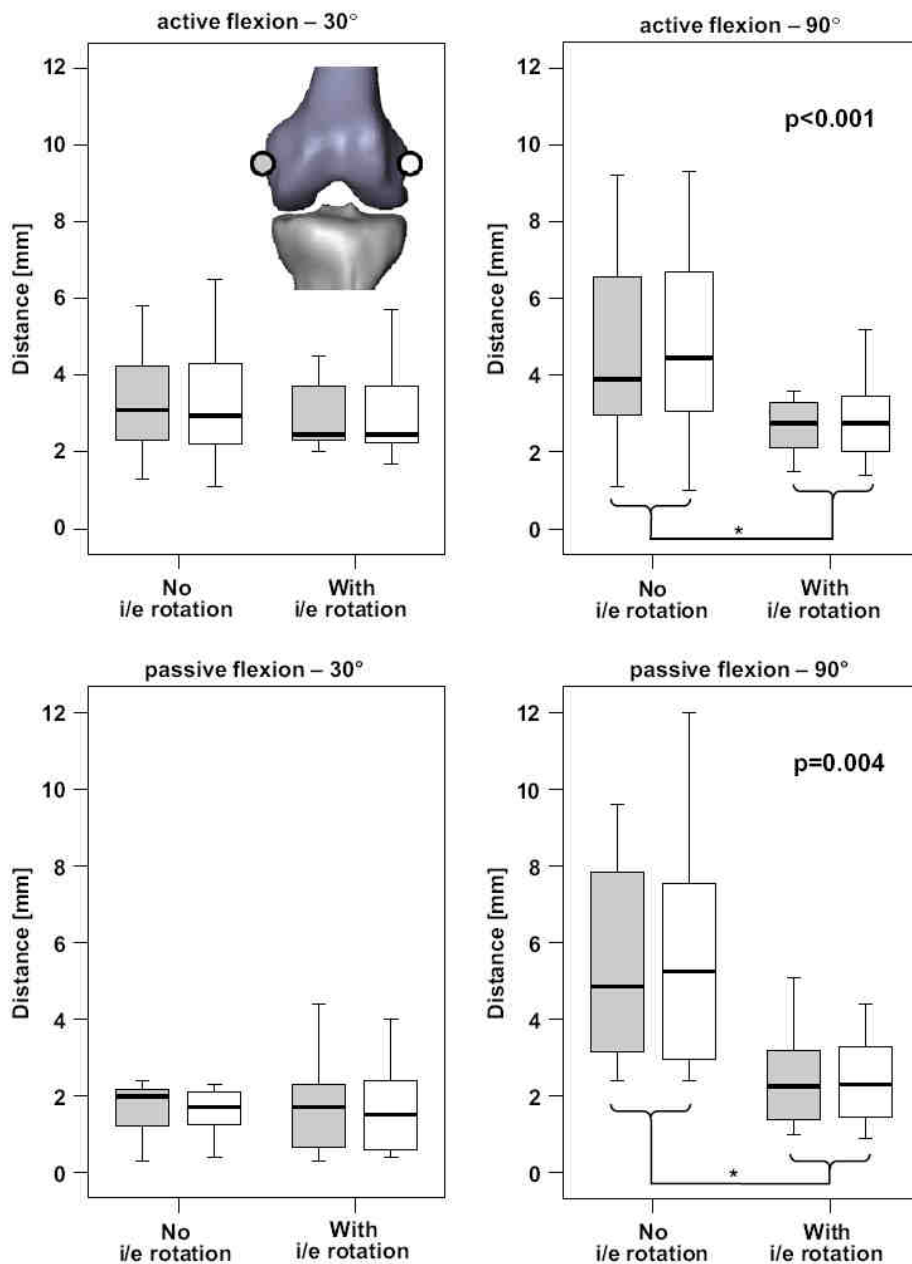


Figure 22: Effect of the considering internal / external rotation in the four-bar linkage model on the deviation between the predicted and the in vivo pose of the femur at 30° & 90° during passive (top) and active (bottom) knee flexion. The box plots show the median (bold line), the 25% quartiles (box dimensions) and the extreme (vertical lines) deviations of the predicted positions against the in vivo measured positions of the medial (grey) and the lateral (white) femoral reference TE-axis points.

Ligament lengthening

Whilst the new kinematic model predicted a relative shortening of the ACL, the PCL was predicted to lengthen with flexion (Figure 23). The unloaded kinematics were best reconstructed using almost isometric behaviour of the AM bundle of the ACL. Shortening of the PL bundle of the ACL was more pronounced, however, under both loaded and unloaded conditions, with changes in length of approximately 20% required. In the PCL, little change in length was required in the PM bundle. The largest lengthening was observed in the loaded AM bundle (26%) during loaded flexion, with the majority of the change in length occurring within the first 30° of flexion.

Loading led to significantly different lengthening patterns in both the ACL and the PCL (ANOVA, $p < 0.02$) over the whole flexion cycle, compared to the unloaded knees. When the functional bundles of the ligaments were considered, the AM and PL bundles of the ACL, as well as the AL bundle of the PCL, showed a significant difference when applying muscle forces (ANOVA, $p < 0.03$). Muscle activity, however, led to no significant difference in lengthening the PM bundle (ANOVA, $p > 0.05$).

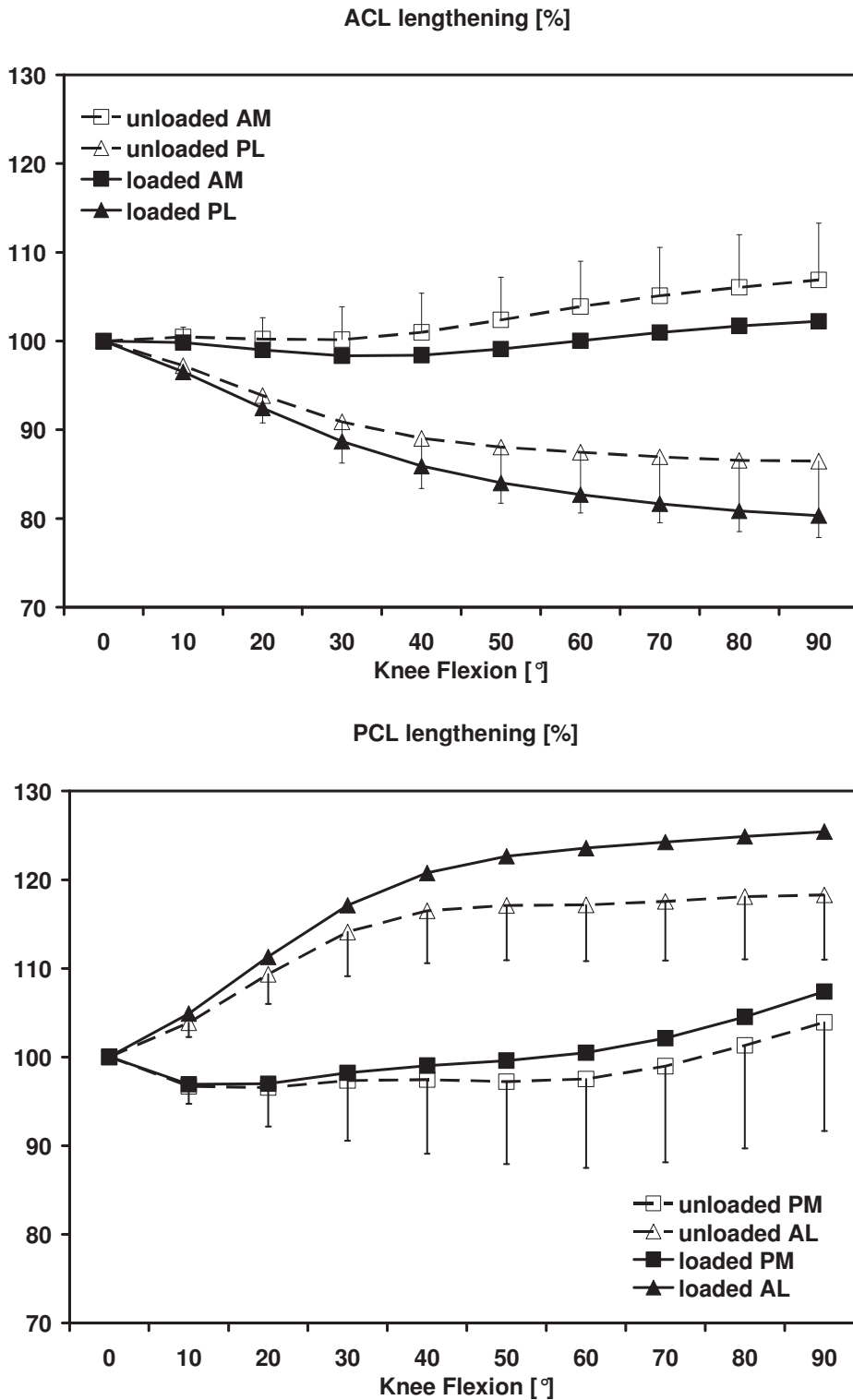


Figure 23: Extension characteristics of the AM and PL bundles of the ACL (top) and AL and PM bundles of the PCL (bottom) under loaded (solid lines) and unloaded (broken lines) conditions throughout a full flexion cycle, as determined by the kinematic model. Standard deviations are indicated for the unloaded conditions.

Generic predictive models

Generic four-bar linkage models were constructed for passive and active neuromuscular activity using the average lengthening and i/e characteristics. When applied to predicting each subject's kinematics, the model determined similar errors in both the axial and coronal planes for the unloaded knees (Table 1). The maximum average error of 4.9mm was found at the lateral reference points at 90° flexion. When these models were applied to the active knee kinematics, the errors were greater, reaching an average of 6.7mm in the axial plane, also at the lateral reference point at 90° flexion. In nearly all cases, the predictions were better at 30° than 90°.

Table 1: Deviation of the predicted and in vivo locations of the femoral reference points in the axial plane and in the coronal plane at both 30° and 90°. The deviation is shown for the model using the average i/e rotation of all subjects as an input. The deviations for passive and active knee motion are shown.

		30°		90°	
		medial point	lateral point	medial point	lateral point
Passive knee flexion	axial plane	2.3±1.4mm	1.9±0.9mm	4.4±2.4mm	4.9±3.1mm
	coronal plane	2.4±0.9mm	1.8±1.1mm	3.2±1.8mm	3.4±1.8mm
Active knee flexion	axial plane	3.7±2.1mm	3.8±1.6mm	6.4±3.6mm	6.7±3.3mm
	coronal plane	2.4±0.9mm	1.7±0.6mm	3.5±2.0mm	4.1±1.9mm

Discussion

The aim of this study was to analyse whether a new kinematic model, based on a modified version of the four-bar linkage that accounted for laxity or lengthening characteristics of the ligaments and internal/external rotation of the tibiofemoral joint, could predict the tibiofemoral kinematics of healthy subjects for passive and active neuromuscular activity during knee flexion. Although the efficacy of this model could only be assessed at certain positions throughout the flexion cycle, validation of these

subject-specific models at known positions enables confidence in the movement patterns for the remainder of the flexion-extension cycle, for use in e.g. musculoskeletal models. Furthermore, the augmentation of these data into generic models for prediction of kinematics has been demonstrated.

Even though knee kinematics have long been a research focus, there is still no commonly accepted standard for describing and modelling knee kinematics (Smith et al. 2003). A number of approaches have been proposed, ranging from computationally demanding models based on the complex description of the anatomy and mechanics of the knee (Caruntu and Hefzy 2004), to more simple models that describe knee kinematics as a series of rotations about fixed axes (Blankevoort et al. 1990; Churchill et al. 1998; Hollister et al. 1993; Shaw and Murray 1974) or instantaneous centres of rotation (Menschik 1974; O'Connor et al. 1989; Strasser 1917). Until now, none of these proposed models have been validated against in vivo data in a larger subject cohort.

The kinematic model of the four-bar linkage is an established model and has often been used to describe the movement of the tibiofemoral joint (Imran et al. 2000; Menschik 1974; Muller 1993; O'Connor et al. 1989). However, this model is also criticised for oversimplifying the complex in vivo kinematics (Smith et al. 2003). It is argued that the concept, based on instant centres of rotation, assumes planar knee joint movement and therefore neglects the offset of the flexion axis to the sagittal plane (Hollister et al. 1993), as well as assuming isometry of the cruciate ligaments (Butler et al. 1980). By including subject-specific *i/e* rotation and by allowing non-isometric ligament fibre lengths, this study has, for the first time, been able to validate a four-bar linkage model of the human knee against in vivo data. The model was validated for passive motion, but more importantly, also for joint motion caused by physiological like neuromuscular-like activation patterns in a larger group of 12 healthy subjects (Bringmann et al. 2000).

The introduction of *i/e* rotation to the model had a significant effect on the accuracy of reproducing subject-specific kinematics, with the largest differences at 90° knee flexion for passive motion (Figure 22) – the conditions for which maximum tibial internal rotation was observed. The translation into a predictive model produced an average error between 4.4mm and 6.7mm in the anterior-posterior direction at 90° flexion – a great improvement on the error expected, e.g. due to measurements that are subject to soft-tissue artefacts (Stagni et al. 2005). A flexion angle-dependent model that does not assume *i/e* rotation about a fixed axis (Matsumoto et al. 2000) might therefore be able to further improve the overall performance of the kinematic model, particularly in respect to the *i/e* rotation.

The laxity and lengthening characteristics of the ligaments seem to play an important role in not only the functioning of the knee, but also in the kinematics predicted by the proposed models. It has been suggested that the AL bundle of the PCL straightens from its concave shape to become active at flexion angles above 40° (Amis et al. 2003), very much in agreement with the findings of this study (Figures 18, 23). This presupposition is also supported by the study of in Friederich and co-workers (Friederich et al. 1992), in which the length of the PCL is described as increasing with flexion as well as decreasing within the ligament itself from the AL to the PM region, a behaviour also reproduced by the kinematic model in this study. Furthermore, for flexion angles from 40° to 90°, the kinematic model predicted an increase in strain of 1.8% for the AL bundle, which concurs with the maximum strain of 2% reported by Nakagawa et al. (Nakagawa et al. 2004). The PM bundle has been reported to be tense throughout the whole flexion cycle, unfolding its load-bearing capacity in higher flexion angles (Amis et al. 2003). Our findings of a 3.9% increase in the bundle's length are in agreement with the 5% found by Ahmad et al. (Ahmad et al. 2003). In a similar manner, the isometric behaviour of the AL bundle of the ACL seen in this study has been reported at angles of up to 30° flexion (Li et al. 2004). For the PM bundle, a shortening of 14% was reported, compared to the 13% derived in this study. Again, the majority of the shortening characteristics for this bundle occur within the first 30 – 40° flexion, consistent with the functioning of the model.

The development of the existing models has assumed localisation of the ligament attachment sites. Small differences in the location of the chosen point within the attachment areas may, however, lead to a considerable change in ligament's strain behaviour (Amis and Zavras 1995). The method introduced in this study has directly linked the ligaments' attachment sites to each subject's anatomy and therefore allowed an inter-individual comparison of the ligament length change.

The four-bar linkage models presented here were able to reproduce individual knee kinematics, not only for passive, but also for active neuromuscular flexion, and were validated against a group of 12 subjects. The levels of accuracy achieved have shown that kinematics may be accurately reconstructed and integrated into e.g. subject-specific musculoskeletal models (Heller et al. 2001b; Taylor et al. 2004), allowing a better understanding of the load distribution within the structures of the knee. The generic predictive models, created by taking the average parameters from all the subject-specific models, further provide a predictive capacity for augmenting models used in, for example, clinical gait analysis, where artefacts associated with skin movement etc. can

limit the accuracy of reconstructing individual models. As such these models may be a valuable tool for pre-operative planning, by intra-operatively providing information on the expected biomechanical loading conditions in the joint after reconstruction surgery.

2.3 Contact mechanics in the patellofemoral joint

Goudakos IG, König C, Schöttle PB, Taylor WR, Singh NB, Roberts I, Streitparth F, Duda GN, Heller MO. 2009, J Biomech, 42: 2590

In vitro testing allows simultaneous measurement of kinematics and forces and has often been used to quantitatively assess the biomechanics of the patellofemoral joint (Beck et al. 2007; Lee et al. 1997; Ostermeier et al. 2007; Ramappa et al. 2006; Wilkens et al. 2007; Zavatsky et al. 2004). In vitro testing of this joint, however, has typically been performed under simplified uniaxial quadriceps muscle loading (Powers et al. 1998) and/or has been criticized for using arbitrarily chosen force magnitudes (Mason et al. 2008), considerably lower than those occurring during the demanding activities of daily living, which can reach multiples of body weight (Sakai et al. 2000; Taylor et al. 2004). This has made extrapolation and transfer of the findings to the in vivo condition questionable (Heino Brechter and Powers 2002). The analysis of patellofemoral biomechanics under demanding physical activities (Besier et al. 2005) and the determination of the pressure distribution in vivo (Zhao et al. 2007) remain, however, challenging. Whilst it seems likely that the contribution of the muscles to the mechanics and stability of the joint is most critical at early knee flexion, when the bony geometry provides only limited stability (Powers 2000), whether and how the muscle forces that occur during demanding activities influence patellofemoral biomechanics remain to be established.

Validated musculoskeletal models can provide the muscle forces that occur during activities of daily living (Heller et al. 2001b; Taylor et al. 2004). Furthermore, a recently developed muscle fixation technique was shown to be competent in transmitting loads of a physiological magnitude to the muscle-tendon complex (Schöttle et al. 2009), without tearing the muscles at the fixation interface – a common problem in cadaveric studies (Farahmand et al. 1998; Huberti and Hayes 1984; Sakai et al. 1996; Sakai et al. 2000). The use of these recently developed techniques would therefore offer the opportunity to investigate the effect of more demanding physical activities on patellofemoral biomechanics in an in vitro set-up.

Demanding physical activities, such as stair climbing, have also been identified as a risk factor for both patellofemoral pain (Dye 2005) and the onset of osteoarthritis (Felson 2004). Besides investigating the patellofemoral contact mechanics during normal walking, it was therefore also hypothesized that loading conditions of stair climbing

induce a higher patellofemoral pressure, a more lateral force distribution on the trochlea and a more lateral shift and tilt of the patella compared to walking. The aim was to investigate the interaction between musculoskeletal loading and patellofemoral contact mechanics and kinematics in the healthy joint at early knee flexion.

Materials and methods

Specimen preparation

Eight fresh-frozen, non-arthritic, left cadaveric knees, with non-dysplastic trochleae and no signs of previous surgery, were sectioned, ensuring preservation of the joint capsule and the surrounding retinaculum. The distal 8 cm of the tendinous attachments of four muscle groups – a) the rectus femoris with the vastus intermedius, b) the vastus medialis c) the vastus lateralis and d) the two hamstrings (semimembranosus and semitendinosus) – were instrumented with a specially developed fixation technique (Schöttle et al. 2009). The trans-epicondylar axis (TEA), a standardized anatomical reference (Blaha et al. 2002; Churchill et al. 1998; Yau et al. 2005; Yoshino et al. 2001), was drilled with a tibial drill guide for ACL reconstruction (KARL STORZ GmbH & Co. KG, Tuttlingen, Germany) and both femur and tibia were sectioned transversely, 14.8 cm distant from the TEA. The proximal end of the femur and the distal end of the tibia were then potted into cylindrical casts using polymethylmethacrylate (Beracryl, Bauers Handels GmbH, Adetswil, Switzerland).

Joint loading and muscle force model

Based on a validated musculoskeletal model (Heller et al. 2001b; Taylor et al. 2004), muscle forces for four subjects (median body weight 839 N, median height 167.5 cm) were determined for gait cycles of both walking and stair climbing. Models were created for each subject by scaling a reference model of bony and muscular anatomy (represented by 95 individual muscle lines of action) to fit the individual segment lengths. Although the contribution of the inertial forces to the overall loading conditions was small, owing to the moderate speed of the activities, the model still accounted for their contribution within the inverse dynamics approach (Deuretzbacher and Rehder 1995) to further improve the overall accuracy of the model's predictions (Heller et al. 2001b). Quasi-static optimization procedures, which minimized the sum of the squared muscle stresses (Taylor et al. 2004), used the intersegmental resultant forces and

moments to determine the muscle and bone-on-bone joint contact forces. The results from two representative instances of the gait cycles for each activity, averaged over the four subjects, were selected and used to realize a load profile that represented the in vivo conditions. The selection was based upon the knee flexion angle and the magnitudes and directions of the forces of the quadriceps components, as well as of the forces of the hamstrings (Table 2). To apply the numerical data from the musculoskeletal model to the in vitro set-up, the TEA was used as a location and orientation reference.

Table 2: Load profiles for each load case

Load profiles for the different load cases						
Knee Flexion (°)	Load case	Muscle loads (N)				Total Load
		rectus femoris / vastus intermedius	vastus lateralis	vastus medialis	semimembranosus / semitendinosus	
12	Walking	630	122	0	0	752
	Stair climbing	507	380	51	51	989
30	Walking	670	302	184	8	1164
	Stair climbing	1499	981	555	474	3509

Mechanical test set-up

Mechanical testing was performed using a previously described set-up (Kassi et al. 2005), which was modified to apply the different load cases to the knee joint (Figure 24). Four servo-electric actuators (PowerCube Drive Unit 70-100, AMTEC GmbH, Berlin, Germany) generated the muscle forces that were transmitted to the muscles through synthetic fibre ropes (LIROS-Hiload, Rosenberger Tauwerk GmbH, Lichtenberg, Germany). The ropes were passed through pulleys attached to a custom-made traverse platform, to allow precise configuration of the three-dimensional directions of the muscle forces, the magnitudes of which were measured with force sensors (OCDZ-3kN, Wazau GmbH, Berlin, Germany). By controlling the size and position of the pulleys relative to the TEA, the moment arms of the muscles were also replicated in the set-up, facilitated by a 3D CAD model. The actuator, rope and sensor for each muscle force were configured in an independent closed-loop control unit. The lax muscle attachments were symmetrically loaded until the patellar tendon showed no apparent slack, so as to

provide a pre-loading tension. Regulated by the control unit, the actuators synchronously increased the muscle forces up to the target levels in a linear fashion, sustained them for a period of 5 s and then returned them back to initial levels.

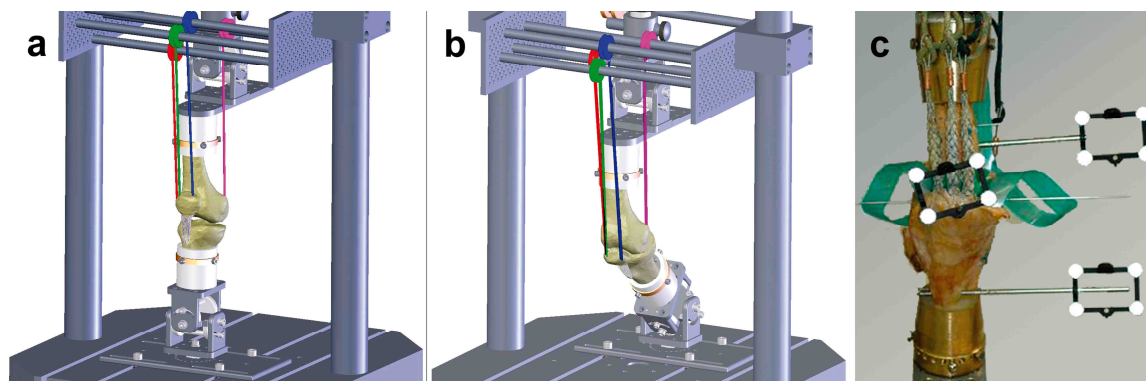


Figure 24: Experimental set-up: a) at 12°; b) at 30° knee flexion in a CAD environment, and c) the cadaver knee with attached optical markers, pressure sensor and muscle loading devices.

Assessment of patellofemoral biomechanics

Patellofemoral contact mechanics were assessed using an electronic pressure measuring sensor (K-Scan #4000, TekScan Inc., South Boston, MA). A new sensor foil was used for each knee. The sensors were conditioned and calibrated in a material testing machine (Zwick 1455; Zwick GmbH, Ulm, Germany) according to a published protocol (Wilson et al. 2003). The two pads of the sensor – one each for the medial and lateral facets of the trochlea – were then inserted into the joint and positioned onto the trochlea. The proximal and distal flaps of the pads were reinforced with transparent adhesive tape and then firmly pinned onto the femur. Care was taken to ensure optimal coverage of the joint surface, avoiding wrinkling and overlapping. The acquired raw data were processed with MATLAB (The MathWorks Inc, Natwick, MA) to calculate patellofemoral peak and mean pressure, contact area and the medial-lateral position of the centre of the force on the trochlea (CoF).

The femur, tibia and patella were all instrumented with markers (Taylor et al. 2006) to measure joint kinematics with a motion capture system (Vicon, Oxford Metrics, UK) using three infrared cameras. After testing, CT scans of the samples were performed and surface reconstructions of the bones and markers were obtained, with the help of 3D visualization software (AMIRA, Mercury Computer Systems Inc., MA, USA). After coordinate systems were defined for the femur and patella, patellar kinematics were

evaluated with the help of in-house software. Patellar motion was defined in terms of femoral and patellar body fixed axes, as previously suggested (Bull et al. 2002). Patellar shift was defined as the change in position of the patellar origin along the TEA. Consistent with radiographic evaluation (skyline view), patellar tilt was defined as the angle between the patellar medial-lateral axis and the projection of the TEA onto the transverse plane of the patella.

Data analysis

A Wilcoxon signed-rank test ($p < 0.05$) was used to detect statistical differences between walking and stair climbing loads at 12° and 30° knee flexion (SPSS 14.0, SPSS Inc., Chicago, IL).

Results

Stair climbing vs. walking

At 12° knee flexion, stair climbing loading resulted in no significant differences in mean pressure ($p = 0.069$), contact area ($p = 0.123$) and shift ($p = 0.093$) compared to walking loads (Figure 25, Table 3). At this flexion angle, however, a significantly higher peak pressure ($p = 0.012$) and a more lateral tilt ($p = 0.012$) and CoF ($p = 0.012$) were recorded for stair climbing loads compared to walking. At 30° knee flexion, stair climbing loads resulted in a significantly higher peak ($p = 0.012$) and mean ($p = 0.012$) pressure, a higher contact area ($p = 0.025$) as well as a higher tilt ($p = 0.017$). However, the medial-lateral CoF ($p = 0.674$) and shift ($p = 0.575$) did not differ significantly (Figure 26).

12° vs. 30° knee flexion

At 30° knee flexion, a significant increase of contact area ($p = 0.012$) and a more medial CoF ($p = 0.012$) and tilt ($p = 0.012$) were observed for the walking loads compared to 12° knee flexion. Neither the peak ($p = 0.093$) nor mean ($p = 0.575$) pressure, however, nor the shift ($p = 0.123$), differed significantly. For the stair climbing loads, both increased peak ($p = 0.012$) and mean ($p = 0.012$) pressures, as well as increased contact area ($p = 0.012$), were found for the higher knee flexion angle. Furthermore, a more medial CoF ($p = 0.012$) and tilt ($p = 0.012$) were observed for stair climbing in higher flexion, while the values for shift ($p = 0.093$) did not differ significantly between 12° and 30° knee flexion.

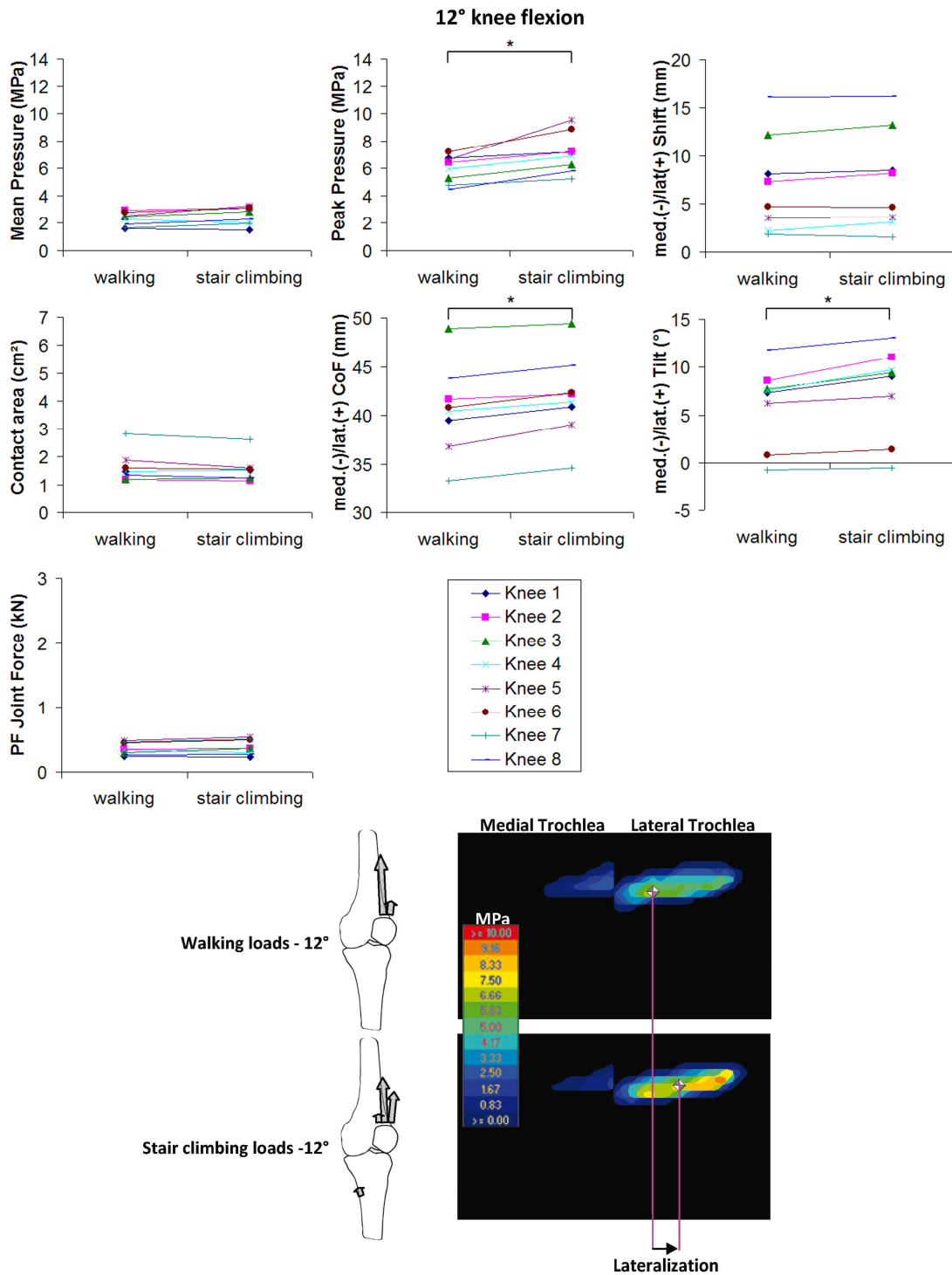


Figure 25: Comparison of patellofemoral mean and peak pressures, contact area, joint force, medial-lateral position of the centre of force on the trochlea (CoF), patellar shift and tilt between a walking and a stair climbing load case at 12° knee flexion. Representative data of pressure distribution, contact area and medial-lateral CoF on the trochlea are presented graphically for each load case.

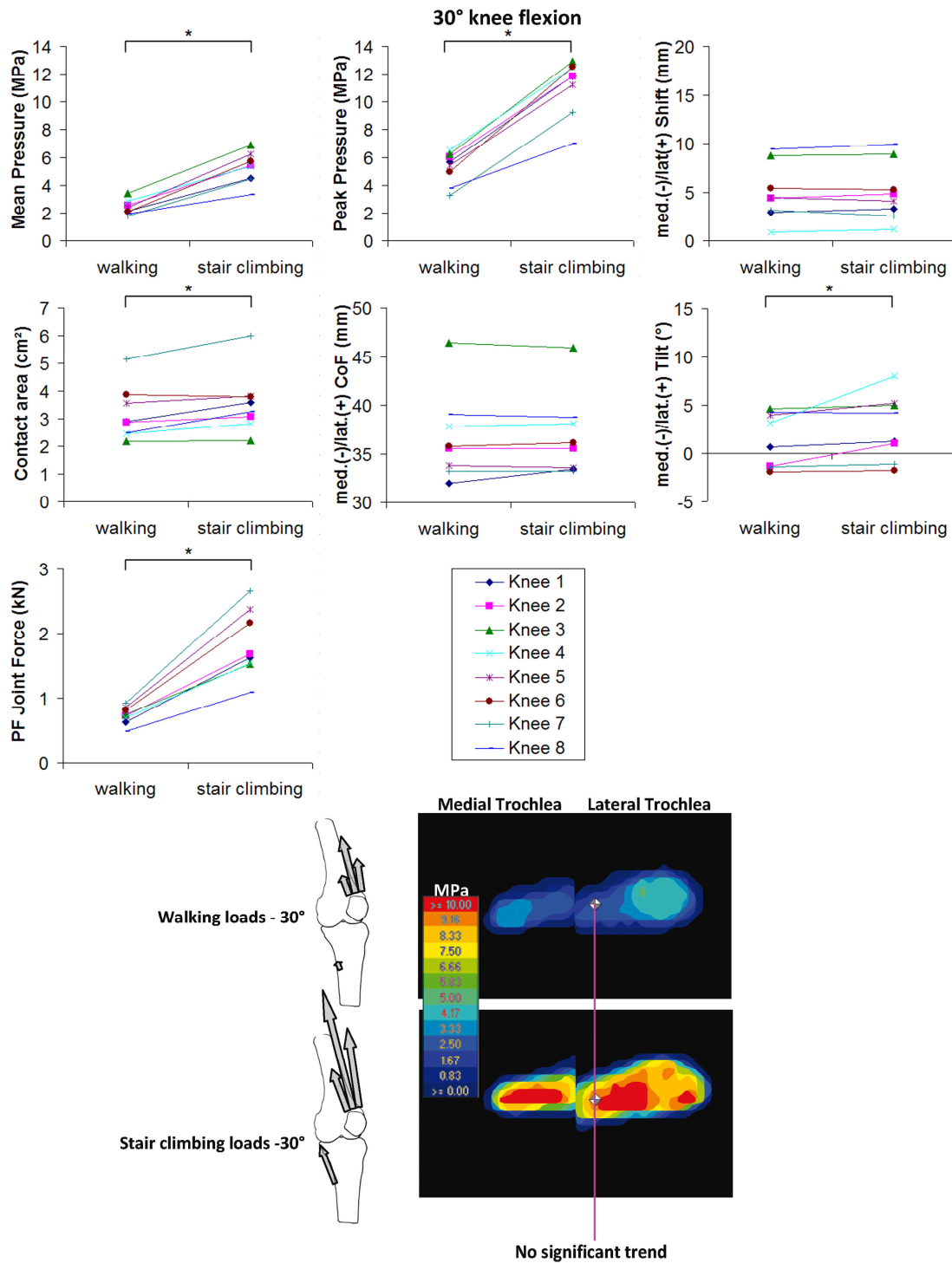


Figure 26: Comparison of patellofemoral mean and peak pressures, contact area, joint force, medial-lateral position of the centre of force on the trochlea (CoF), patellar shift and tilt between a walking and a stair climbing load case at 30° knee flexion. Representative data of pressure distribution, contact area and medial-lateral position CoF on the trochlea are presented graphically for each load case.

Table 3: Results of patellofemoral contact mechanics and kinematics analysis: Median (Range)

Results of patellofemoral contact mechanics and kinematics analysis: Median (Range)								
Knee Flexion (°)	Load case	Patellofemoral contact mechanics				Patellar kinematics		
		Mean pressure (MPa)	Contact area (cm ²)	Joint Force (N)	Peak pressure (MPa)	CoF med./lat. ^a (mm)	Lateral shift (mm)	Lateral tilt (°)
12	Walking	2.39 (1.63, 2.89)	1.48 (1.19, 2.82)	343 (242, 483)	6.19 (4.47, 7.21)	40.6 (33.3, 48.9)	6.0 (1.8, 16.1)	7.5 (-0.8, 11.8)
	Stair climbing	2.56 (1.51, 3.33)	1.52 (1.14, 2.62)	360 (229, 537)	7.05 (5.26, 9.54)	41.8 (34.6, 49.4)	6.4 (1.5, 16.2)	9.2 (-0.5, 13.1)
30	Walking	2.28 (1.79, 3.39)	2.87 (2.19, 5.16)	735 (487, 925)	5.54 (3.29, 6.53)	35.7 (32.0, 46.4)	4.4 (0.9, 9.4)	1.9 (-1.9, 4.6)
	Stair climbing	5.40 (3.34, 6.89)	3.42 (2.22, 6.00)	1657 (1088, 2665)	11.85 (6.98, 12.95)	35.9 (33.2, 45.9)	4.5 (1.2, 10.0)	2.7 (-1.8, 8.0)

^a CoF: medial-lateral position of the centre of force on the trochlea - higher values indicate a more lateral CoF

Discussion

This study aimed to investigate the contact mechanics in the intact patellofemoral joint, and specifically the interaction between musculoskeletal loading and patellofemoral biomechanics in healthy joints. It was hypothesized that, compared to level walking, stair climbing – an activity that places higher demands on the knee (Andriacchi et al. 1980; Costigan et al. 2002; Mason et al. 2008; Taylor et al. 2004) and that is associated with anterior knee pain (Dye 2005) – would deliver not only higher patellofemoral pressure, but also a more lateral force distribution on the trochlea and a more lateral shift and tilt at early knee flexion. Using an in vitro set-up to apply physiological-like quadriceps loading for walking and stair climbing, this study was able to verify these hypotheses for all parameters except for patellar shift.

The results demonstrated that the mean patellofemoral pressure and contact area did not differ significantly between the walking and stair climbing loads at the initial engagement of the patella in the trochlea (12°) (Figure 25). Although this is reflected in the similar patellofemoral joint reaction forces for walking and stair climbing loads, the peak pressure was significantly higher for the stair climbing loads, indicative of a different force distribution. At the same time, stair climbing resulted in a more lateral force distribution on the trochlea and a more lateral tilt. This emphasises that the contact mechanics during stair climbing, characterized by the force distribution across the joint

and the kinematics of the patella, present a mechanically more challenging environment for the soft tissue structures of the joint.

In further knee flexion (30°), with the patella completely engaged in the trochlea, the mean and peak patellofemoral pressures, the contact area and the tilt were higher for the stair climbing loads (Figure 26). This is attributable to the fact that the total muscle load applied in stair climbing was considerably higher – approximately three times as high as that for walking. Interestingly, the medial-lateral CoF did not differ. This suggests that the patellofemoral force distribution is less sensitive to changes in muscle loading after complete patellar engagement in the trochlea occurs.

At initial patellar engagement in the trochlea, the sensitivity of both the patellar kinematics (tilt) and the force distribution (peak pressure and medial-lateral CoF) to changes in the muscle loading patterns under similar patellofemoral joint forces (Figure 25) indicates the key role of muscle activity in determining patellofemoral biomechanics at early knee flexion. In cases of patellar instability, when the ability of the ligaments (Bicos et al. 2007) and the bony anatomy (Powers 2000) to stabilize the joint is reduced, muscle activity might be of even greater importance in the determination of patellofemoral contact mechanics and kinematics. The findings of this study therefore highlight the importance of considering functionally demanding physical activities, such as stair climbing, for clinically relevant analyses of patellofemoral biomechanics.

A previous study reported, however, no statistical difference for the patellar position among three different loading patterns (sitting, squatting and constant load) at the same knee flexion angle (Sakai et al. 1996). Another study, comparing axial to multi-plane loading of the quadriceps, reported no differences in the induced tilt between the two loading conditions (Powers et al. 1998). A third study, which examined the influence of changing the direction of the axial quadriceps force, reported no impact on patellar movement (Nagamine et al. 1995a). In each of these studies, however, relatively low quadriceps forces (<300 N), were applied, due to the inability to transmit higher forces to the joint. This limitation of previous set-ups might explain the inability to differentiate the joint mechanics between different activities. Therefore, adequate loading of the patellofemoral joint seems to be a mandatory prerequisite for identifying pathological kinematic patterns associated with the patellofemoral pain syndrome, as also suggested in a recent in vivo study (MacIntyre et al. 2006). To provide adequate joint loading (Farahmand et al. 1998; Huberti and Hayes 1984; Sakai et al. 2000) a new muscle-tendon fixation technique (Schöttle et al. 2009) was used in this study to ensure sufficient transmission of high force magnitudes.

Contact area was previously found to increase progressively with knee flexion (Eilerman et al. 1992; Hungerford and Barry 1979; Patel et al. 2003; Salsich et al. 2003) and with higher patellofemoral forces (Besier et al. 2005; Matthews et al. 1977; Mesfar and Shirazi-Adl 2005). The findings of the current study agree with both findings (Table 3). However, in the case of two knees (knees 3 and 6, Figure 26), only a marginal change in contact area was observed for stair climbing compared to walking, at 30° knee flexion (0.03 and -0.09 cm², respectively). Although the loads for stair climbing were approximately three times higher than for walking at this flexion angle, the unchanged contact area indicates that its maximum was already achieved in those two knees under walking loads. This can be attributed to the fact that the walking loads were already substantial, with a total muscle force of over 1100 N. A previous study in the feline patellofemoral joint suggested that there is a lower rate of increase in contact area in the high load spectrum (Clark et al. 2002). The current findings might further indicate that above a specific load level, a further increase in contact area is no longer possible. The change of patellofemoral contact area at the high end of the force spectrum should thus be further investigated to elucidate this interaction.

The previously described general pattern of medialisation of the patellar tilt with early knee flexion (Katchburian et al. 2003) was corroborated by the results of the current study. A novel aspect revealed in our study was that this pattern was evident for both walking and stair climbing between 12° and 30° knee flexion, with a similar range of tilt medialisation in both activities (Table 3). Furthermore, this change in motion was accompanied by a medialising trend in the patellofemoral kinetics in the form of a more medial CoF, which was again observed in both activities. A general pattern of medial patellar shift, as described earlier (Ahmed et al. 1999; Amis et al. 2006; Nagamine et al. 1995a; van Kampen and Huiskes 1990), was not evident from the results of this study. Our findings therefore indicate that a change in the medial-lateral CoF, even if accompanied by a change in patellar tilt, is not necessarily linked to a medial-lateral translation of the patella.

Although physiological-like muscle loading was achieved in the current study, certain limitations should be mentioned concerning the loading conditions used, the test set-up and the sample size. The muscle loading was obtained from a numerical model which itself was based upon certain assumptions (Heller et al. 2001b). However, the muscle activity predicted by the model was shown to be in general agreement with typical muscle activity profiles (Sutherland 2001). Furthermore, validation of the contact forces calculated at the hip using this model against in vivo measured forces (Heller et al.

2001b) lends further credibility to the model's prediction. Although muscle activation during a complete gait cycle is complex, and forces in hamstring muscles other than the semimembranosus and semitendinosus were also predicted by the model, only the latter muscles were modelled in vitro, since they provided the largest contribution to the knee joint forces.

In order to safely and reproducibly apply the high loads with peak quadriceps forces in excess of 3000 N to the knee, the set-up enabled the computer-controlled, synchronous application of the muscle forces (Kassi et al. 2005; Schöttle et al. 2009).

Whilst the contact mechanics of the patellofemoral joint certainly depend on the specific boundary conditions imposed upon the joint, the set-up accurately replicated the pose of the knee as measured during the gait analysis and the muscle loading to exert the extension forces acting at this instance of the cycle. Here, the precise application and regulation of the muscle forces in a quasi-static manner was favoured over allowing dynamic equilibrium to be obtained in a fully unconstrained manner. Even though such a set-up would be more physiological, the test protocol employed in the current study was considered to be both a crucial and necessary adaptation for the safe and reproducible application of muscle forces representative of the in vivo magnitudes experienced during walking and stair climbing. Whilst a major aim of this work was to provide realistic muscle loading conditions to the patellofemoral joint, the aim was not to fully reproduce the dynamics and kinematics of the entire knee joint for a complete gait cycle. The set-up rather simulated pre-determined instances of the cycles as quasi-static, independent events. Furthermore, the set-up was not designed to allow a detailed analysis of the tibiofemoral joint load distribution, and the regulation of additional external forces was not part of the test protocol. Although under these high forces, the influence of further external forces was considered to have only a limited effect on the biomechanics of the patellofemoral joint, future studies should examine their additional influence.

This study focused on the analysis of the conditions close to knee extension. However, not only did the peak forces during walking occur at early knee flexion, but also approximately 95% of the peak forces during stair climbing were reached at 30° of flexion (Taylor et al. 2004). Thus, the comparison at identical flexion angles of both 12° and 30° allowed the influence of challenging muscle loading conditions to be better isolated, minimized experimental error and, most importantly, represented two key instances of both the walking and stair climbing cycles.

A possible drawback of TekScan sensors is that the periphery of the contact area may not be recorded if the pressure is below the working threshold of the sensor. This did not limit comparisons between conditions within our study. The two pads of the pressure sensor (medial and lateral) enabled a conforming coverage of the concave surface of the trochlea. A possible minor overlapping of the pads in the central trochlea could thus have resulted in a slight overestimation of the contact area and forces. Furthermore, whilst a small proximal-distal alignment error between the two pads could not be excluded, this did not affect the medial-lateral CoF (Fig. 25 and 26).

Due to the small sample size ($n=8$), ad hoc adjustments for multiple comparisons were not applicable, providing a descriptive character to the reported p values. In all but two cases where significant changes were observed, however, all eight knees followed a consistent trend, which was also reflected in the lowest possible p value for the given sample size ($p=0.012$).

This study has demonstrated that stair climbing, as a more demanding activity, results in more challenging patellofemoral contact mechanics and kinematics compared to level walking at early knee flexion, as characterized by significantly higher patellofemoral pressure, a more lateral force distribution on the trochlea and a more lateral tilt of the patella. Higher patellofemoral pressure (Dye 2005; Felson 2004), more lateral force distribution (Doucette and Goble 1992) and higher tilt (Fulkerson 2002; Grelsamer 2000) have all been previously associated with patellofemoral pathologies. Not only did the findings of this study provide a possible biomechanical explanation for the association of stair climbing with patellofemoral pain, they also indicate that the use of in vitro set-ups that are capable of simulating physiological-like musculoskeletal loading seems to be of key importance for assessing surgically induced changes in patellofemoral joint kinematics and contact mechanics under clinically relevant conditions. These findings further indicate that the loading conditions in the patellofemoral joint, specifically under challenging activities such as stair climbing, should be included in analyses that aim to investigate the effects of femoral component malalignment in TKA.

2.4 In vivo assessment of collateral ligament function in the healthy knee

König C, Matziolis G, Taylor WR, Sharenkov A, Graichen H, Hinterwimmer S, Duda GN, Heller MO. 2007, DGfB Jahrestagung

Many post-operative complications in TKA are related to joint stability. However, there is little knowledge to date on the effects of femoral component malalignment on the function of the collateral ligaments. A suggested approach is to analyse the distance between the ligaments' bony insertions (Park et al. 2005; Van de Velde et al. 2007). This initial analysis aims to characterize in vivo collateral ligament function in the healthy knee joint.

Materials and methods

MRT scans of the knee joints of 12 healthy volunteers were acquired at flexion angles of 0°, 30° and 90°, under both passive and active muscle conditions (von Eisenhart-Rothe et al. 2004). After image acquisition, semi-automated segmentation of the femur and tibia was performed, based on a grey-value oriented region-growing algorithm

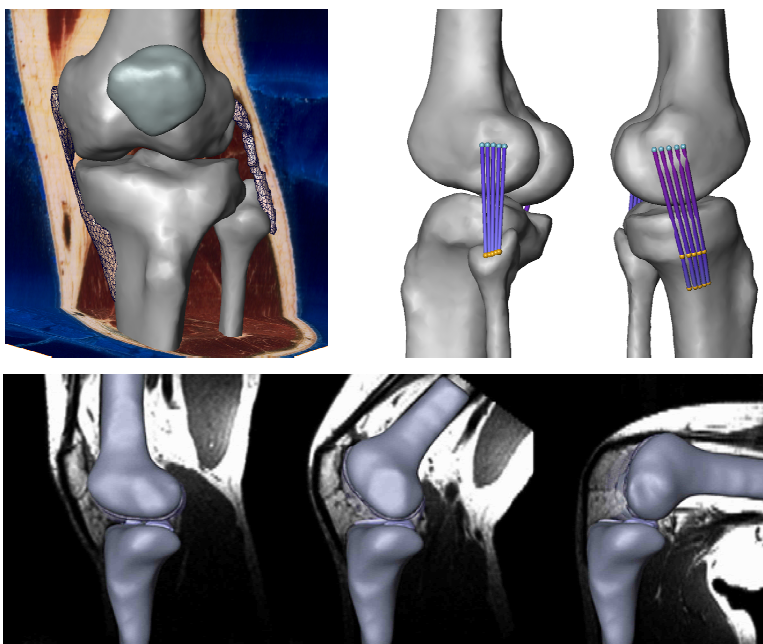
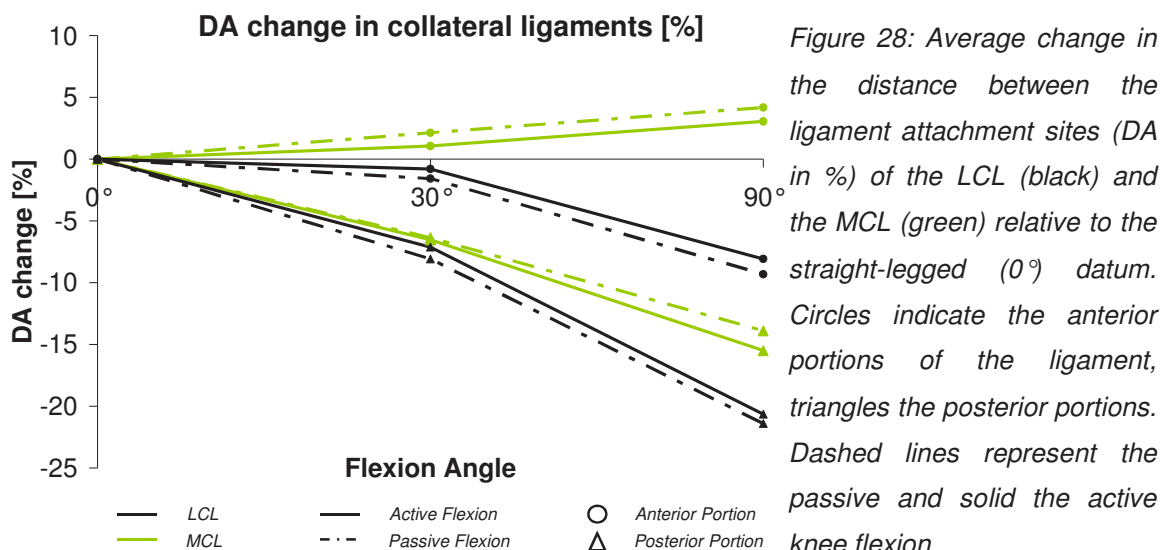


Figure 27: Collateral ligament function was derived using 3D models of the ligaments reconstructed from the Visible Human dataset (upper left). Landmarks were placed to define the proximal (blue) and distal (yellow) insertion sites of the lateral (upper middle) and the medial (upper right) collateral ligaments. Joint kinematics were obtained from MRI images at 0°, 30° and 90° knee flexion (bottom)

(Bringmann et al. 2000). Using a marching cube algorithm, surface models of the bony structures were created, to derive in vivo joint kinematics. Landmarks were placed at the insertion sites of both the lateral (LCL) and the medial (MCL) collateral ligaments, using data augmented by high-resolution colour images of the Visible Human dataset (Spitzer et al. 1996). These landmarks were transferred to each subject, using the individual length of the transepicondylar axis as a patient-specific scaling factor. The landmarks were then transformed from the 0° tibial datum into the 30° and 90° flexed positions, using transformation matrices obtained by registering the femur using an iterative closest point transform algorithm (Besl and McKay 1992) implemented within the visualization and volume modelling software, AMIRA (Mercury Computer Systems Inc., MA, USA) (Figure 27). In the anterior and posterior regions of the MCL and the LCL, the distance between the ligament attachment sites (DA) was evaluated for the 30° and 90° positions relative to the straight knee. A Wilcoxon test was performed to detect significant differences in DA during flexion and to find differences in DA characteristics between the regions of the ligament.

Results

A significant difference ($p < 0.05$) was observed in the DA between the anterior and posterior regions of the LCL and the MCL throughout flexion (Figure 28). The LCL DA progressively decreased for both active and passive knee flexion. Whilst no difference was observed in the anterior region until 30°, a statistically significant decrease was



seen between 30° and 90°. For active flexion, the DA change for the anterior portions (-0.8±2.7% and -8.1±5.4% at 30° and 90° respectively) was less than for the posterior portions (-7.1±3.4% and -20.7±8.5%)

Discussion

The in vivo data for healthy knees presented in this study define a reference for ligament characteristics during both passive and active flexion. Their accepted role as stabilizers in the extended knee was underlined by a reduced DA in most of the ligament regions with increasing flexion. The anterior parts of the MCL, however, showed an increased DA with increasing flexion, possibly resisting anterior tibial loads (Sakane et al. 1999). The application of the methodology presented in this study can help provide a better understanding of the conditions in patients undergoing TKA.

3 THE EFFECT OF JOINT LINE ELEVATION ON JOINT CONTACT FORCES

König C, Sharenkov A, Matziolis G, Taylor WR, Perka C, Duda GN, Heller MO. 2010, J Orthop Res. 2010 Jan;28(1):1-5.

This chapter describes the adaptation of the musculoskeletal models to the conditions after a total knee replacement is described. These models are then utilized to analyse the effects on the joint contact forces of the elevation of the joint line – a specific malalignment of the femoral component that has been associated with post-operative complications.

3.1 Introduction

The influence of an elevated joint line on the post-operative outcome of total knee arthroplasty (TKA) remains a controversial topic. Although several studies have found no correlation between joint line elevation and clinical outcomes (Bellemans 2004; Ritter et al. 1999; Selvarajah and Hooper 2009), others have linked an elevated joint line to inferior clinical and functional results (Chiu et al. 2002; Figgie et al. 1986; Laskin 1998; Martin and Whiteside 1990; Partington et al. 1999; Porteous et al. 2008). In particular, it was found that joint line elevation can be associated with patellofemoral problems (Laskin 1998), lower knee scores (Figgie et al. 1986; Partington et al. 1999; Porteous et al. 2008), limited knee flexion capability (Chiu et al. 2002) and mid-flexion joint instability (Martin and Whiteside 1990) – all factors that can lead to revision surgery. Even though restoration of the joint line in primary and revision TKA seems to be possible within an accuracy of 5 mm (Mahoney and Kinsey 2006; Rouvillain et al. 2008; Wyss et al. 2006), recent studies have shown that, despite the possible clinical complications associated with a joint line elevation, the joint line remains elevated by more than 5mm in over 36% of revised TKAs (Laskin 2002; Porteous et al. 2008). Besides difficulties in estimating the physiological location of the joint line (Laskin 2002) and an overly cautious tibial resection (Grelsamer 2002; Laskin 2002), a common reason for an elevated joint line is the way in which distal femoral bone loss is managed in revision situations (Bellemans 2004; Laskin 2002; Porteous et al. 2008). While the joint line can be restored using femoral augments (Bellemans 2004; Laskin 2002), this procedure produces additional implant costs, for the augments as well as the associated stem. Addressing distal and posterior femoral bone loss with a proximalization and undersizing of the femoral component is therefore common (Bellemans 2004; Scuderi and Insall 1992). However, the necessity to fill the resulting larger flexion or extension gaps with a thicker insert leads to an elevated joint line (Laskin 2002; Porteous et al. 2008).

To date, the effect of an either intended or unintended joint line elevation on knee biomechanics, and in particular on the loading conditions at the joint, has received little interest. Increased joint loading is thought to have an influence on the development of osteoarthritis (Wu et al. 2000), and has been related to both pain (Dye 2005; Dye et al. 1998; Grana and Kriegshauser 1985; Heino Brechter and Powers 2002) and the wear rate of polyethylene inserts (Estupinan et al. 1998) after TKA. Altered contact forces that are induced by changing the joint line position in TKA are therefore likely to have an

effect on the post-operative outcome. In the broad spectrum of human motion, these altered contact forces would have the largest effect during activities that are physically challenging and frequently performed. Stair climbing is such an activity that already exposes the knee to considerable contact forces (Costigan et al. 2002; D'Lima et al. 2005b; Taylor et al. 2004). Any further increase to the contact forces may lead to overloading conditions in the joint, possibly contributing to the increased incidence of post-TKA patellofemoral pain during this activity (Mayman et al. 2003). In addition, prevalent daily activities such as normal walking (Morlock et al. 2001) may be subject to the risk of permanent overloading, which can increase polyethylene wear and contribute to aseptic loosening of the implants.

Understanding the biomechanical situation after joint line elevation, in walking and stair climbing activities, is an important step towards comprehending the role that restoration of the joint line plays in the clinical outcome, and for determining whether surgical procedures that cause a joint line elevation should be avoided. The aim of this study was therefore to analyse the effects of an elevation of the joint line on the tibio- and patellofemoral joint contact forces during stair climbing and normal walking.

3.2 Methods

Musculoskeletal model

To calculate joint contact forces, we used a previously validated musculoskeletal model of the human lower limb (Bergmann et al. 2001; Bergmann et al. 1988; Heller et al. 2001b). Locations of the joint contact forces and muscle attachments were determined by scaling a computer model of the human lower limb to match each subject's anatomy. Muscles were modelled as straight lines spanning between the origin and insertion, and bony wrapping points were introduced where necessary to represent a more realistic curved path of the muscle. The physiological cross-sectional area of each muscle was obtained from the literature (Brand et al. 1986; Duda et al. 1996) and scaled to the patients' body weights (Heller et al. 2001b). Intersegmental resultant forces were calculated by an inverse dynamics approach using measured ground reaction forces and gait data from four subjects. Since tracking of the patella was not possible during gait analysis, the motion of the patella was derived from an in vitro simulation of a complete flexion-extension cycle (Durselen et al. 1995) of an intact knee joint and integrated into the musculoskeletal model.

To calculate the joint contact forces, quasi-static optimization was performed with the goal of minimizing the sum of the square of the muscle stresses (Taylor et al. 2004). The sum of all muscle forces acting on a joint, together with the intersegmental resultant forces from the inverse dynamics analysis, defined the joint contact forces. Specifically at the patella, the patellofemoral joint contact forces were the sum of the forces of the patellar ligament and the muscle forces that were calculated for the vastus medialis, vastus lateralis, vastus intermedius and the rectus femoris. Instrumented femoral prostheses in the same four subjects gave access to in vivo hip contact forces during normal walking and stair climbing activities, allowing the validation of the calculated joint contact forces at the hip (Bergmann et al. 2001; Bergmann et al. 1988; Heller et al. 2001b).



Figure 29: CAD model of the assembled ultra-congruent implant used in the study consisting of the femoral component, the tibial insert and the tibial component (Aesculap Columbus UC)

A TKA with an ultra-congruent, fixed bearing and cruciate sacrificing implant design (Figure 29) (Columbus UC, Aesculap AG, Tuttlingen, Germany) was virtually performed on the musculoskeletal models of the same four subjects, to simulate the post-operative anatomy and allow surgical variation to be investigated. CAD models of the tibial and femoral components were orientated in the sagittal, coronal and axial planes according to standard surgical procedures (Figure 30) using visualization and volume modelling software (AMIRA, Mercury Computer Systems Inc., MA, USA). The correct sizing and positioning of the components was supervised by an experienced orthopaedic surgeon (GM).

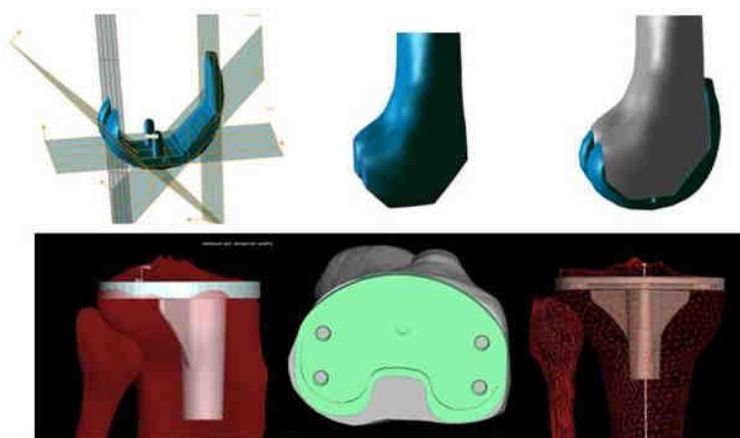


Figure 30: Virtual TKA surgery using 3D surface models of the tibia and the femur, as well as CAD models of the tibial and femoral components.

Kinematic adaptation

In the original study, a clinical gait analysis was performed to capture the lower limb kinematics for walking and stair climbing activities (Heller et al. 2001b). To adapt this kinematic data to a post-TKA situation, a generic kinematic model of tibiofemoral motion based on the geometry of the ultra-congruent prosthesis' articulating surfaces was developed in the sagittal plane.

Tibiofemoral kinematics were modelled using three flexion angle-dependent rotation axes. The locations of these axes were determined by creating sagittal cross-sections of the femoral component in the centre of each condyle. Three arcs were fitted in each the medial and lateral articulating contour (NX3, Siemens PLM Software) (Figure 31). The axis connecting the corresponding medial and lateral centres of these arcs defined the flexion axes. The first axis defined the component rotation from hyperextension up to 17° knee flexion, at which point the radius of the second took over from 17° to 52°, and likewise the third from 52° to maximum flexion. To determine the complete tibiofemoral kinematics during walking and stair climbing, this kinematic model was then driven using

the knee flexion angles determined from the gait analysis data. For both activities, adaptations in tibiofemoral kinematics were reflected in the hip joint, whilst the ankle joint was not affected.

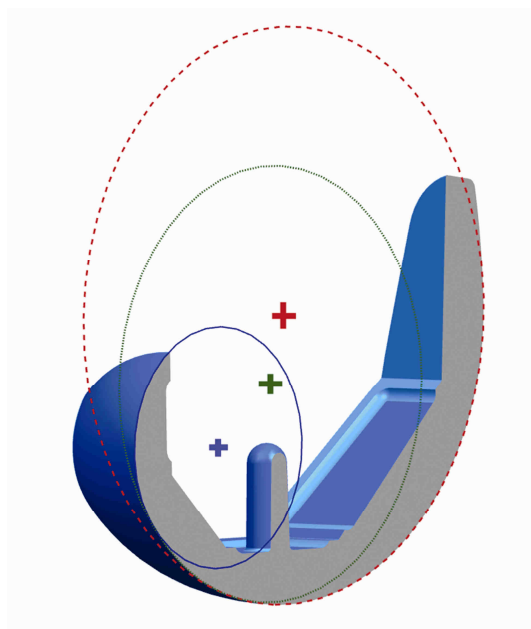


Figure 31: Cross-sectional view of a femoral component (Columbus UC, Aesculap AG, Tuttlingen, Germany). Centres of circles that were fitted to the articulating surfaces on the medial and lateral condyle defined the flexion axes of the femoral component.

The virtual TKA aimed to provide an optimal anterior-posterior position of the femoral component and to avoid varus-valgus or internal-external rotation errors. Under these conditions, the trochlear groove of the femoral component with a sulcus angle of 7° was considered to closely approximate the natural trochlea. The patellar kinematics of the intact knee was therefore considered to provide a good first approximation of the post-operative situation.

Variation of the joint line

Loss of bone stock in the distal femur, a too-small tibial resection, or the use of a too-thick inlay – all situations resulting in joint line elevation – were simulated by modifying the cranial-caudal position of the femoral and tibial prosthesis components and the size of the inlay. The anatomical femoral and tibial axes were used as a reference for the respective component translations. A joint line distalization was also simulated by distalizing both the femoral and tibial components. Leg length was not altered in the process.

The joint line was distalized 5 mm from its anatomical location, as well as being elevated by 10 and 15 mm (Figure 32). The length of the ligamentum patellae remained unchanged, thus creating a pseudo patella baja in the case of an elevated joint line (Grelsamer 2002).

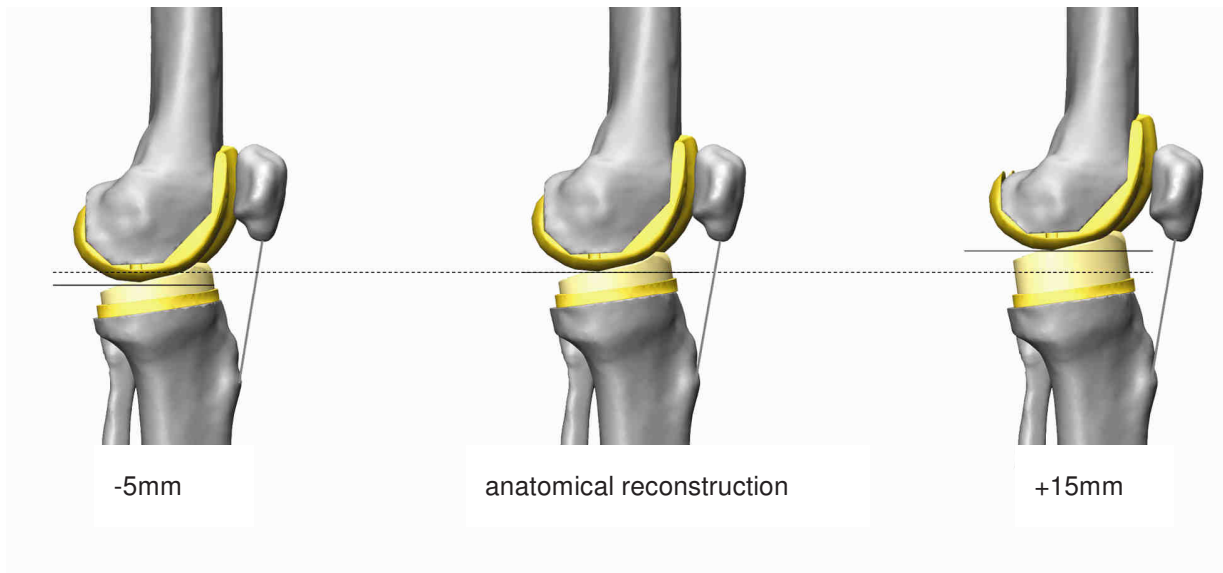


Figure 32: The joint line level was simulated between a 5 mm distalization (left), the anatomical reconstruction (centre) and up to 15 mm elevation (right).

Joint contact forces

Patellofemoral and tibiofemoral joint contact forces were calculated for repeated trials of

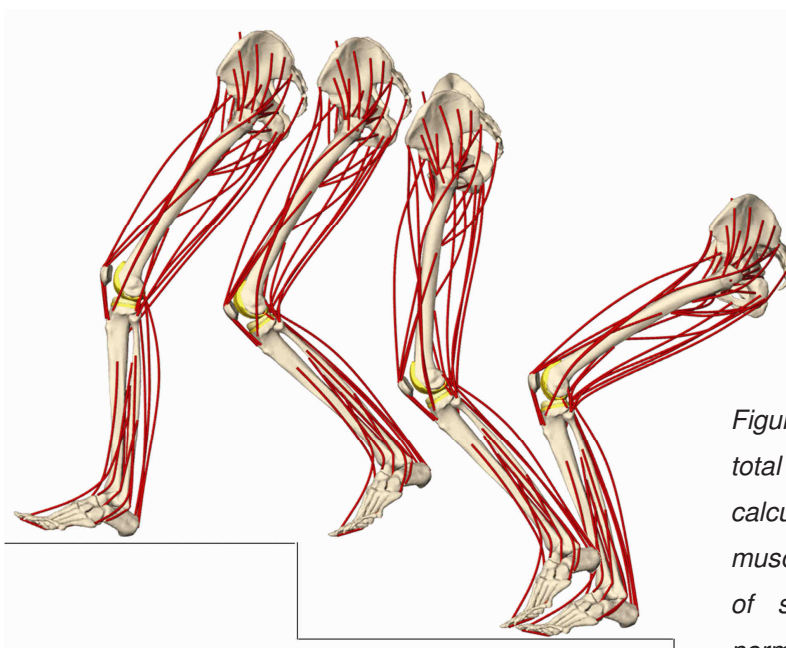


Figure 33: Joint contact forces after total knee arthroplasty were calculated using a validated musculoskeletal model for instances of stair climbing (displayed) and normal walking.

normal walking and stair climbing for all four subjects and all joint line variations, using inverse dynamics and optimization algorithms incorporated in the musculoskeletal model (Heller et al. 2001b; Heller et al. 2007b) (Figure 33).

Using the condition of an anatomically reconstructed joint line as a reference for the situations with an altered joint line, the time-point at which the peak contact force occurred was identified within each activity cycle and the maximal deviations in contact force were determined for all subjects at all altered joint line levels. A Student's *t*-test was performed to verify the reproducibility of the calculated contact force deviations within the repeated trials of each individual subject. Significance was assumed at $p < 0.05$.

3.3 Results

Elevating the joint line increased the contact forces in both the patello- and tibiofemoral joints in almost all cases (Figures 34, 35). The patellofemoral joint was more affected than the tibiofemoral joint, and in both joints, stair climbing caused a larger increase in contact force than walking.

A joint line elevation of 10mm caused an increase in the patellofemoral joint contact force of 60% of the subject's body weight (BW) during stair climbing and 30% BW during normal walking. At the tibiofemoral joint, only a slight increase of less than 10% BW was observed in both activities. A further elevation of the joint line from 10mm to 15mm only minimally affected the tibiofemoral joint in either activity, with an additional increase in the contact force of less than 6% BW. In the patellofemoral joint, however, this additional joint line elevation further increased the contact forces by about 30% BW during stair climbing, resulting in a total increase of 90% BW relative to the anatomically reconstructed joint line. During normal walking, the additional joint line elevation increased the patellofemoral contact forces by about 10% BW, resulting in a total increase of 40% BW.

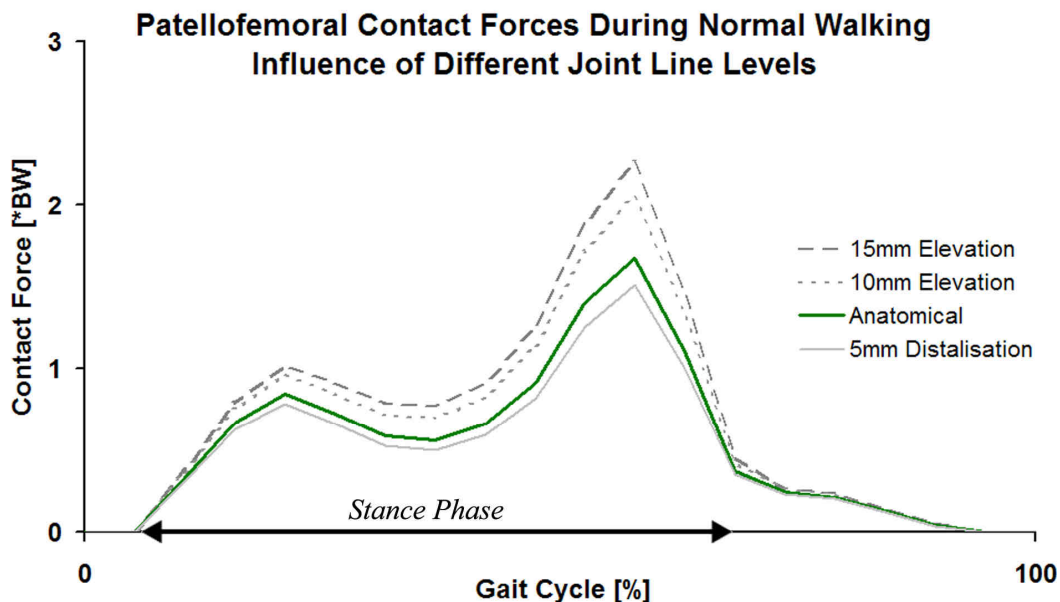


Figure 34: Exemplary patellofemoral joint contact force pattern during a cycle of normal walking, calculated for one patient (thick solid line). The contact forces were recalculated after simulating joint line elevations of 10 and 15mm (dashed lines) and a joint line distalization of 5mm (thin solid line).

Distalizing the joint line by 5mm reduced the contact forces in both the tibio- and patellofemoral joints. The tibiofemoral contact forces during normal walking and stair climbing, however, were only minimally affected, being reduced by less than 6% BW. A larger effect was seen in the patellofemoral joint, where a 5mm joint line distalization resulted in a reduction of contact forces of 11% BW during normal walking and up to 30% BW during the stair climbing activity.

At the same joint line levels, there were consistent findings for contact forces in all repeated trials of the individual subjects and between the individual subjects ($p < 0.05$).

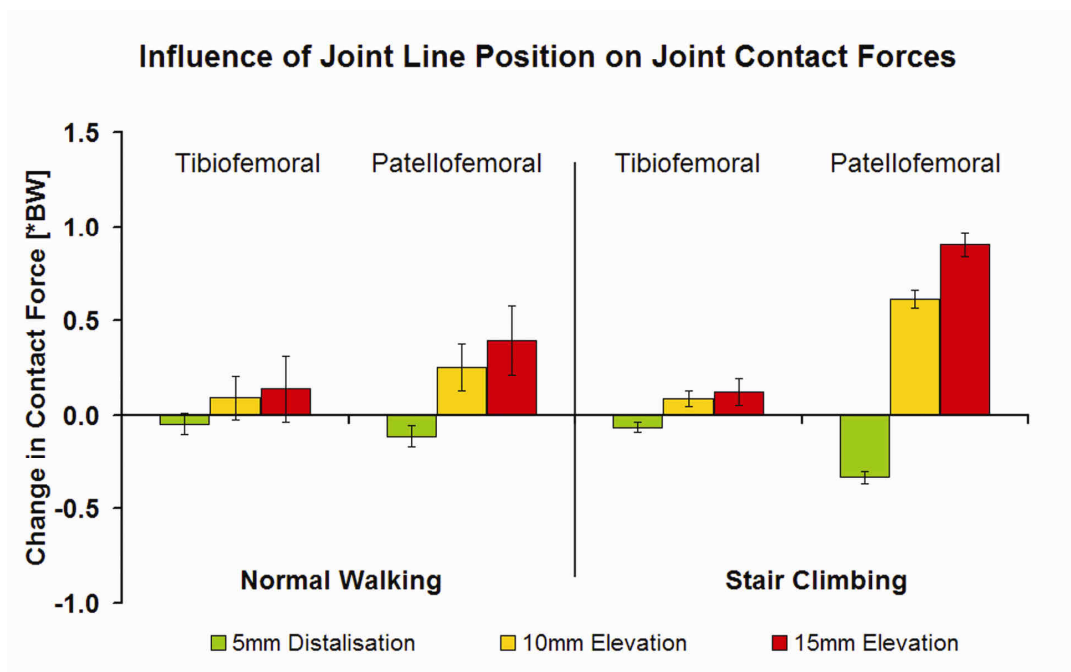


Figure 35: The average changes and the respective standard deviations in the patellofemoral and tibiofemoral contact forces of four subjects, caused by a distalization (green bars) or elevation (yellow and red bars) of the joint line, shown in multiples of body weight (BW) relative to the contact forces in the situation of an anatomically reconstructed joint line.

3.4 Discussion

Recent studies have shown that in more than 36% of all revision TKAs, the joint line remains elevated by more than 5mm (Laskin 2002; Porteous et al. 2008). Although clinical observations have indicated that an elevation of the joint line is associated with inferior clinical results (Figgie et al. 1986; Laskin 1998; Laskin 2002; Partington et al. 1999; Porteous et al. 2008), the effects of joint line elevation on knee biomechanics remain relatively unknown. However, this knowledge is essential for understanding the observed inferior clinical results. For the first time, we have shown that elevating the joint line can lead to an increase in joint contact forces in both the tibio- and patellofemoral joints during walking and stair climbing – activities prevalent in daily living (Morlock et al. 2001) and known to expose the knee to considerable internal loading (Costigan et al. 2002; D'Lima et al. 2005b; Taylor et al. 2004).

The patellofemoral joint was particularly affected during stair climbing activities, in which the contact forces increased by more than half of a patient's body weight (60% BW) at 10mm of joint line elevation – a displacement that can commonly occur in revision surgery (Partington et al. 1999). An even more pronounced increase in contact forces was observed when the joint line was further elevated to 15mm: during stair climbing, our calculations showed patellofemoral joint contact forces of up to 90% BW more than the contact forces that occur in an anatomically reconstructed knee. Thus, a patient of 85kg could experience an *increase* in patellofemoral contact forces of up to 750N. Increased forces at the patellofemoral joint were also observed during walking, although the contact force increase was always less than during stair climbing. However, due to the prevalence of walking (Morlock et al. 2001), even the 30% BW increase calculated at 10mm joint line elevation further contributes towards a considerable and constant overloading situation in the load-bearing structures. Overloading of the patellofemoral joint can increase the risk of patellar degeneration and can also put a patellar replacement at risk of early failure due to an increased wear rate of the polyethylene insert (Estupinan et al. 1998).

Overloading conditions have also been associated with pain in several studies (Dye 2005; Dye et al. 1998; Grana and Kriegshauser 1985; Heino Brechter and Powers 2002). While a number of other factors, such as instability or patellar overstuffing can also contribute to anterior knee pain, the results of our analyses indicate that the clinically observed complications in patients with an elevated joint line (Chiu et al. 2002;

Figgie et al. 1986; Martin and Whiteside 1990; Partington et al. 1999; Porteous et al. 2008) may well be linked to the increase in patellofemoral contact forces. Specifically, Porteous and co-workers (Porteous et al. 2008) reported that patients with a joint line elevated by more than 5mm had a lower Bristol Knee Score – a score that has a high sensitivity to pain levels. A study by Figgie and co-workers (Figgie et al. 1986) showed that joint line elevation correlated with lower functional knee scores, patellofemoral pain and the need for revision. Avoiding an elevation of the joint line and thus avoiding an overloading of the load-bearing structures in the knee may therefore be crucial for further improving the post-operative outcome in revision TKA.

Even though direct measurements of in vivo loading conditions in the knee have been performed previously (D'Lima et al. 2005a; Heinlein et al. 2007; Wallace et al. 1998; Wasielewski et al. 2005; Zhao et al. 2007), a study of anatomical variation such as the elevation or distalization of the joint line in an individual is not possible in vivo. The approach used in this study, utilizing validated musculoskeletal models, is an established procedure to gain information about the loading conditions in structures that are barely accessible for in vivo measurements, and also to investigate the effects of anatomical variations (Heller et al. 2001a; Heller et al. 2003).

Several studies have investigated tibiofemoral kinematics after TKA (Dennis et al. 2003; Dennis et al. 2004; Nilsson et al. 1990; Zihlmann et al. 2006). However, no general kinematic patterns have been identified so far. Dennis et al. (Dennis et al. 2003; Dennis et al. 2004) showed that post-operative kinematics depend upon the implant type used and on the surgeon performing the surgery. To allow standardization and comparative results, a geometric approach was chosen for this study, to derive a generic kinematic pattern for the ultra-congruent, fixed bearing prosthesis design. Whilst this modelling approach of describing tibiofemoral kinematics in the sagittal plane reflects the guiding characteristics of this specific prosthesis design, a certain variation of this generic kinematic pattern is likely to occur in vivo (Dennis et al. 2004).

The sensitivity of the patellofemoral joint contact forces to the joint line location, as shown in this study, highlights the importance of carefully considering joint line reconstruction, especially in revision TKA. The results from this study indicate that an elevated joint line, creating a pseudo patella baja (Grelsamer 2002), can expose the patient's patellofemoral joint to unphysiologically high contact forces, and thus expose the patient to a high risk of developing clinical and functional problems. Orthopaedic surgeons should therefore be aware of the procedures in TKA that may lead to an elevated joint line (Bellemans 2004; Figgie et al. 1986; Scuderi and Insall 1992). Our

data suggests that distal femoral defects should be addressed with augmentation (Bellemans 2004) rather than proximalizing and undersizing the femoral component and using a thicker tibial insert. Since errors in joint line reconstruction have a significant impact on joint contact forces, the correct level of the tibial resection (Grelsamer 2002; Laskin 2002) should be verified using robust methods to identify the location of the natural joint line (Mason et al. 2006; Rouvillain et al. 2008). Especially in revision situations, navigation systems could be of great benefit in assisting the surgeon to restore the natural joint line.

In conclusion, the contact forces in the knee, particularly in the patellofemoral joint, are sensitive to joint line reconstruction. Elevating the joint line in revision TKA can increase the joint contact forces and should be therefore avoided where possible, in order to minimize the risk of biomechanically induced post-operative complications.

4 THE EFFECT OF JOINT LINE ELEVATION ON COLLATERAL LIGAMENT FUNCTION IN MID-FLEXION AFTER TKA

König C, Matziolis G, Sharenkov A, Perka C, Duda GN, Heller MO 2010. Med Eng Phys (cond. accepted)

In addition to the complications in TKA that might be associated to with increased joint contact forces, a large proportion of TKA revisions are stability-related. With the collateral ligaments as the main remaining soft-tissue stabilizers in the post-operative joint, successful total knee replacement with non- or semi-constrained implants depends on the ligaments' functional integrity after joint replacement. A model to evaluate ligament function in the joint after total knee arthroplasty is introduced in the following chapter.

To specifically address “mid-flexion” instability – an instability phenomenon with speculated links to an elevation of the joint line – this model is then used in combination with the model established in chapter three, allowing the simulation of femoral component malalignment.

4.1 Introduction

Careful balancing of the soft tissue stabilizers is essential for the success of total knee arthroplasty (TKA) (Pape and Kohn 2007; Peters 2006; Whiteside 2002). Particularly in non- or semi-constrained implants, the lateral collateral ligament (LCL) and the medial collateral ligament (MCL) ensure the knee's varus / valgus stability, while the MCL also resists external rotation and anterior–posterior translation (Gardiner et al. 2001; Harfe et al. 1998). Even though gap- and ligament balancing techniques have been established to create a stable joint in extension and flexion (Dorr and Boiardo 1986; Insall et al. 1985; Krackow and Mihalko 1999; Peters 2006; Whiteside 2002), joint stability-related problems account for a significant portion of TKA revisions (Fisher et al. 2007; Gioe et al. 2004; Yercan et al. 2005).

The instability in mid-flexion (MFI) is one of these problems and it has not been fully understood so far. Even knees that have been carefully balanced in extension and at 90° flexion can exhibit MFI. An elevation of the joint line (JLE) in the course of TKA is one of the reasons that have been discussed to cause MFI (Martin and Whiteside 1990; Parratte and Pagnano 2008).

An interesting approach towards a better understanding of MFI is the work of Amis and co-workers (Amis and Zavras 1995). In the context of the length change patterns of the cruciate ligaments during knee flexion they reported that the location of the cruciate ligaments' femoral attachment sites relative to a femoral flexion axis significantly influences the length change patterns of these ligaments (Amis and Zavras 1995).

Since JLE is altering the knee's flexion axis relative to the location of the collateral ligaments' femoral attachment sites, it is therefore likely that JLE can induce an altered lengthening or shortening characteristics of the collateral ligaments throughout flexion as well (Churchill et al. 1998; Nietert 1977).

Computer modelling opens the possibility to systematically study the influence of selected parameters and has the advantage that it can further be applied to a number of subjects. Specific musculoskeletal models can thus be utilized to investigate whether JLE results in a distance decrease between the femoral and tibial collateral ligament attachment sites in mid-flexion relative to the reconstructed joint. Such a finding could then indeed provide an explanation for MFI.

We hypothesised that JLE and the subsequent change in the position of the femoral collateral ligament attachment sites relative to the femoral articulating surface alters the length change patterns of the collateral ligaments during knee flexion, specifically in mid-flexion. The aim of this study was therefore to analyze the length change patterns of the collateral ligaments during knee flexion for situations of JLE after TKA in order to assess whether JLE can indeed contribute to mid-flexion instability.

4.2 Methods

Musculoskeletal model

The computer model that formed the basis for this study was derived from the Visible Human (VH) CT dataset (Spitzer et al. 1996) and data from the literature (Duda et al. 1996), containing bony structures, muscles and simplified representations of the ligament insertion sites of the lower limb (Heller et al. 2001b).

To analyse the length change patterns of the collateral ligaments during knee flexion, the musculoskeletal model now needed to be complemented with a more detailed description of the collateral ligaments. We therefore used the high resolution colour images (resolution 0.32 x 0.32 x 1 mm) from the same VH dataset that was used to create the reference musculoskeletal model. In these high-resolution colour images, soft tissue structures were identified (Amis et al. 2003; Otake et al. 2007; Putz et al. 2007; Robinson et al. 2004a; Robinson et al. 2004b; Seebacher et al. 1982), allowing the 3D modelling

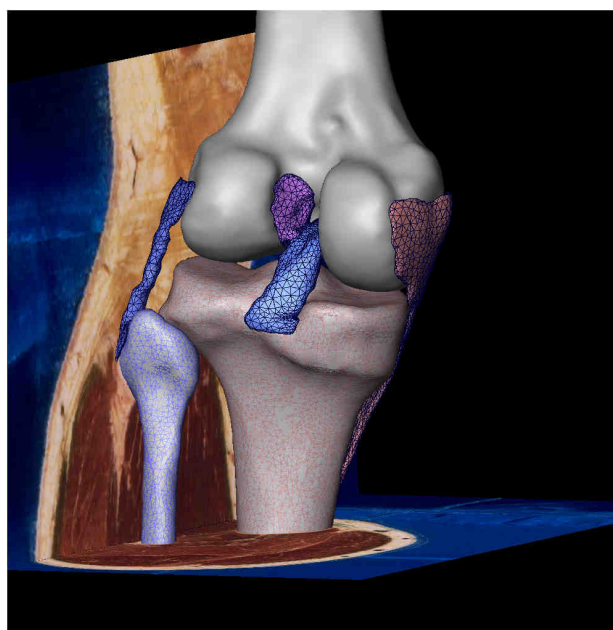


Figure 36: The medial and lateral collateral ligaments (here displayed together with the cruciate ligaments) were modelled using high-resolution cross-sectional images of the Visible Human dataset.

of the medial and lateral collateral ligaments by using 3D visualization and volume modelling software (Amira, Visage Imaging, Inc., San Diego, CA) (Figure 36). In the combined 3D models of the tibia, femur and the collateral ligaments, the bony attachment sites of the medial and lateral collateral ligaments were each modelled as five portions, to better characterize their functional behaviour throughout knee flexion. The origin and insertion of each portion was marked with landmarks (Figure 37)(Amis et al. 2003; Otake et al. 2007; Park et al. 2005; Putz et al. 2007; Robinson et al. 2004a;

Robinson et al. 2004b; Seebacher et al. 1982). For the MCL, additional static wrapping points were defined at the proximal tibia.

This now more detailed reference model was then adapted to match the anatomy of the four participating subjects by linear scaling (Heller et al. 2001b; Taylor et al. 2004). As a result of adapting the reference models' femur and tibia using subject-specific scaling parameters, variation in the insertions of the knee ligaments across the four subjects was captured in the models. Subsequently, a virtual total knee arthroplasty, using an ultra-congruent, fixed bearing and cruciate-sacrificing implant design (Columbus UC, Aesculap AG, Tuttlingen, Germany), was performed on the same four musculoskeletal models (König et al. 2010). While the bone sizes of the four subjects varied somewhat as a result of the subject-specific scaling factors, a single implant size was found to be adequate for all four subjects when the virtual implantation was performed and verified by an experienced surgeon.

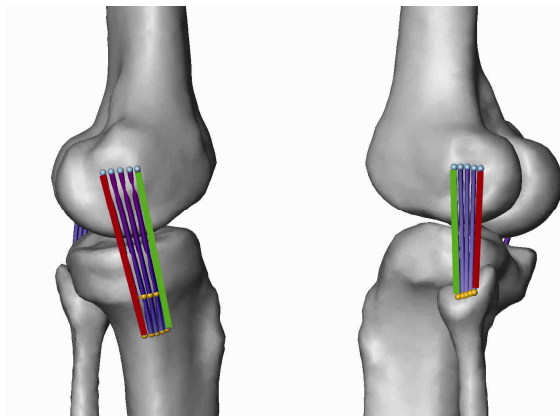


Figure 37: The medial and lateral collateral ligaments were each modelled as five portions, to better characterize their functional behaviour throughout flexion. To this end, the femoral origin and tibial attachment sites of the medial (left) and the lateral (right) collateral ligaments were marked with landmarks. For the MCL, static wrapping points were introduced at the proximal tibia. The current study focussed on the analyses of the most anterior and posterior ligament regions (thick lines).

Variation of the joint line

JLE can result from a number of different conditions, for example, in the case of distal femoral bone loss, a too-small tibial resection, the use of a too-thick inlay, or combinations of these. For the current study, it was assumed that the tibial cut was adequate and JLE was a result of modifying the cranial-caudal position of the femoral component and the height of the inlay (König et al. 2010). According to the manufacturer's recommendation, the femoral component was downsized with JLE.

Thus, the component's anterior-posterior dimension was reduced by the same amount as the JL was elevated, in order to avoid the tightening of the flexion gap that would otherwise result from JLE. In this study, JLE of 5 mm and 10 mm were simulated. The leg length remained unchanged in all simulations.

Kinematic adaptation

To adapt the tibiofemoral kinematics of the four subjects to the post-operative situation, the motion of the implanted knee joint was driven by a kinematic model that reflected the geometry of the ultra-congruent prosthesis' articulating surfaces (König et al. 2010). This model used three distinct axes of rotation to describe the relative positions of the components throughout the range of knee flexion and was constrained to motion in the sagittal plane. However, as a result of using three distinct flexion axes, the model also included the anterior-posterior motion that occurred with flexion.

Collateral ligament length change

To assess the length change in the anterior and posterior regions of the MCL and LCL, the distances between the landmarks representing these individual regions were analysed in both ligaments (Park et al. 2005; Van de Velde et al. 2007). Initially, in the anatomically reconstructed knee, the distance between the attachment sites (DA) was computed for all four subjects during knee flexion from 0° to 90°, using an increment of 15°. The change in this distance relative to the extended knee (0°) position was then calculated. These calculations were repeated for all modifications of the JL as described above, resulting in a simulation of 12 cases in total (four subjects, three conditions each). Furthermore, at every analysed flexion angle, the DA changes that occurred during flexion with an elevated JL were compared to the DA changes in the anatomically reconstructed knee.

4.3 Results

Anatomical reconstruction

If the JL was anatomically reconstructed, the distance between the femoral and tibial attachments in the anterior MCL increased by $13.5 \pm 0.4\%$, compared to its reference length at extension, when flexing the knee from 0° to 90° (Figure 38). During the same knee flexion cycle, the MCL's posterior regions experienced a distance decrease of $8.1 \pm 1.1\%$ relative to the reference length at full extension. In the anterior region of the LCL, the DA remained approximately constant, while the posterior LCL experienced a $14.6 \pm 2.2\%$ decrease in distance, compared to its reference length at full extension, when the knee was flexed to 90° .

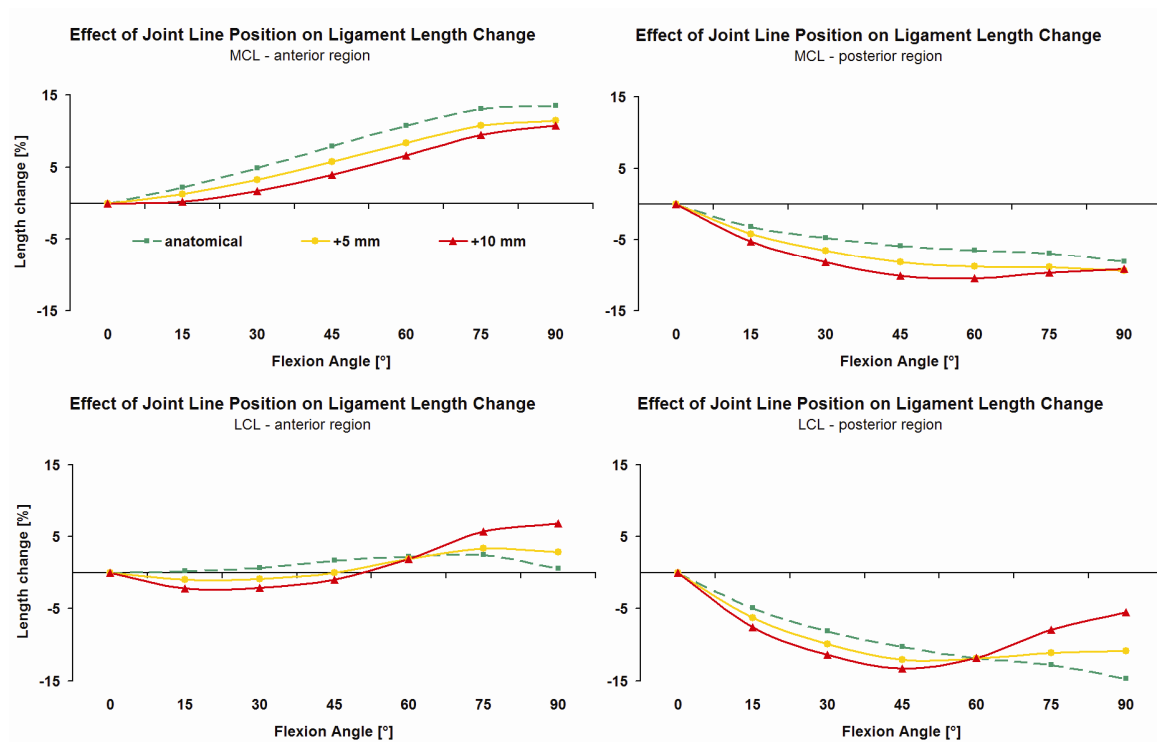


Figure 38: Length change patterns of the anterior (left) and posterior (right) regions of the medial (top) and lateral (bottom) collateral ligaments, as observed from extension to 90° of knee flexion. The dashed curve represents the anatomical reconstruction of the joint line, while the yellow and the red curve represent joint line elevations of 5 and 10 mm respectively.

Effect of JLE on DA relative to the anatomical reconstructed condition

In the anterior MCL at 90° flexion, elevating the JL lead to a DA decrease in both, the 5mm and 10mm JLE condition. Compared to the anatomical reconstructed condition at this flexion angle the DA decreased about $2.0\pm 0.2\%$ at 5mm JLE and $2.8\pm 0.5\%$ at 10mm JLE. In the posterior MCL JLE also decreased the DA relative to the anatomical reconstructed condition. At 90° flexion this decrease was $1.2\pm 0.4\%$ at 5mm JLE and $1.0\pm 0.9\%$ at 10mm JLE.

In the LCL JLE also caused a DA decrease relative to the anatomically reconstructed conditions, but only at smaller flexion angles. Knee flexion beyond 60° caused a DA increase. At 90° flexion, the DA increase in the anterior LCL was $2.3\pm 0.7\%$ at 5mm and $6.3\pm 1.5\%$ at 10mm JLE. In the posterior LCL at the same flexion angle a DA increase of $3.7\pm 1.0\%$ and $9.1\pm 2.1\%$ was observed in the posterior LCL at 5 and 10mm JLE.

In mid-flexion JLE resulted in a reduced DA in the anterior and posterior regions of both collateral ligaments relative to the anatomically reconstructed knee. In the anterior MCL the DA decreased about $4.0\pm 0.1\%$ at 10mm JLE and 45° knee flexion and was thus larger than the DA decrease observed at 90° flexion. In the posterior MCL the DA decrease was also more pronounced in mid-flexion than at higher flexion angles ($-4.2\pm 0.1\%$ at 10mm JLE and 45° flexion).

JLE in the anterior LCL resulted in a slight DA decrease in mid-flexion of $2.6\pm 0.1\%$ at 10mm JLE and 45° flexion. The DA in the posterior regions of the LCL also decreased in mid-flexion ($1.9\pm 0.03\%$ at 5mm and $3.0\pm 0.1\%$ at 10mm JLE, both at 45° flexion).

Effect of JLE on DA relative to the extended knee

Despite in mid-flexion the DA in the anterior MCL was reduced by JLE in comparison to the DA in the reconstructed condition, the DA did not get below the DA observed in the extended knee. In the anterior LCL the DA in mid-flexion at 10mm JLE got below the DA in extension ($-2.1\pm 0.6\%$ at 30° and $-1.0\pm 1.1\%$ at 45° flexion), while the DA at 5mm JLE was the same as in extension at 45° and $-0.9\pm 0.6\%$ at 30°.

In the posterior regions of the MCL and the LCL the DA was always found to be below the DA in the extended knee in both conditions: the anatomical reconstructed knee and after JLE. JLE however caused a further decrease in DA specifically in mid-flexion.

4.4 Discussion

Even though gap and ligament balancing techniques are established elements in TKA, to create a stable joint in both static and dynamic conditions (Dorr and Boiardo 1986; Insall et al. 1985; Krackow and Mihalko 1999; Peters 2006; Whiteside 2002), stability-related problems are still a major reason for a revision TKA (Fisher et al. 2007; Gioe et al. 2004; Yercan et al. 2005). It has been speculated that an elevated JL might contribute to mid-flexion instability (Martin and Whiteside 1990; Parratte and Pagnano 2008). However, little is known on whether the elevation of the JL has an effect on the collateral ligaments – key passive stabilizers of the knee – specifically in mid-flexion.

Using four musculoskeletal models of the lower limb in post-TKA condition (König et al. 2010), we have demonstrated for an ultra-congruent implant design that an elevation of the JL resulted in a reduced distance between the attachment sites of the anterior and posterior regions in both collateral ligaments during mid-flexion, in comparison to the conditions observed for an anatomically reconstructed knee joint. However, despite this generally observed distance decrease in DA as a result of JLE, the anterior MCL still exhibited a distance increase between the attachment sites if compared to its reference length in extension. In the intact knee, the MCL is known to be tensed throughout flexion and to become tighter with progressive flexion (Van de Velde et al. 2007). The data of our study suggested that even in conditions of JLE after TKR, the MCL still displayed the characteristics of a tensed ligament in mid-flexion. The anterior LCL, which is taut throughout flexion in the intact knee (Gardiner et al. 2001), was also affected by JLE and experienced a distance decrease in mid-flexion, compared to the conditions of the anatomically reconstructed JL. But in contrast to the result for the anterior MCL, we found that the DA in the anterior LCL decreased even below the reference DA in the extended knee. However, even if the anterior LCL was just taut and not pre-tensioned in extension, and would therefore become slack as a result of the observed 2.1% DA decrease, a simplified calculation using an average ligament length of 60 mm and a knee width of 55 mm would suggest that such a small DA decrease would result in a potential increase in varus / valgus laxity of less than 1.5°. Our model further predicted that the posterior regions of both the MCL and LCL slacken with increasing knee flexion for an anatomically reconstructed knee – a finding that is consistent with the results of previous studies on the function of the collateral ligaments (Gardiner et al. 2001; Harfe et al. 1998; Robinson et al. 2004b; Van de Velde et al. 2007). In JLE conditions, this

effect of collateral ligament slackening was intensified in mid-flexion. However, as those fibres are already slack in the anatomically reconstructed joint, it is rather unlikely that an increased slackening of the posterior fibres would contribute to mid-flexion instability.

JLE therefore did not seem to be a major contributor to mid-flexion instability when using the Columbus ultra-congruent prosthesis design. Nevertheless, while the observed alterations in collateral ligament length change patterns in cases of JLE could not be related to mid-flexion instability, they still may have an impact on the overall ligament function, and should therefore be the subject of further investigation. The generally observed decreased DA at lower flexion angles, and the additional decreased DA found in case of the MCL at higher flexion angles, may imply that fewer regions of the ligaments can contribute to load sharing, possibly increasing the risk of overloading within those remaining structures carrying the load. The anterior fibres of the LCL are thought to be taut in extension. Therefore, the DA increase observed as a result of JLE in the anterior LCL at higher flexion angles, with DAs that were even larger than the reference DA of the extended knee, may offer a possible cause for soft tissue complications.

Further complications may also arise when the JL is moderately elevated and the femoral component is not downsized accordingly. Compared to the anatomically reconstructed joint, the DA in 90° for a JLE of 5mm increased in the anterior MCL by $4.7 \pm 0.5\%$ to a total of $18.2 \pm 0.5\%$ and to a total of $9.9 \pm 0.8\%$ in the anterior LCL (Figure 39). Considering that the collateral ligaments are taut in extension (Gardiner et al. 2001; Harfe et al. 1998; Putz et al. 2007; Robinson et al. 2004b), it seems safe to assume that any further increase in DA would be linked to an increase in the ligament strain. It is therefore reasonable to assume that the DA increase observed in this study, specifically in the anterior MCL, is indicative of a strain increase in this portion of the ligament. While the absolute ligament strain cannot be determined with the methods presented here, it is very likely that, as a result of DA increases as large as 18%, JLE may cause strains in the ligaments that approach the magnitude of the maximum tensile strain of ligaments, reported to be between 13 and 17% (Butler et al. 1986; Quapp and Weiss 1998).

Even though pre-operative lower limb kinematics for walking, stair climbing and knee bend activities were originally captured for the same four subjects using a gait analysis system (Heller et al. 2001b), no general post-operative in vivo kinematic patterns have yet been presented in the literature, allowing for an individual modelling of post-operative kinematics (Dennis et al. 2003; Dennis et al. 2004; Nilsson et al. 1990; Zihlmann et al. 2006). Therefore the current study used a kinematic model that was

constrained to sagittal plane motion. By considering the specific geometry of the prosthesis components, the model also captured the anterior-posterior motion that occurred with flexion. While internal-external rotation was not included, preliminary fluoroscopic analyses performed in our lab indicate that there might indeed be only very little internal-external rotation occurring in vivo with such an ultra-congruent fixed bearing design. An isolated axial rotation of 5° would e.g. result in a DA increase of only approximately 0.3% (assuming an average ligament length of 60 mm, a knee width of 55 mm and an eccentric rotation axis), and therefore considering full 3D motions would not seem to have a substantial effect on the results.

While the knee kinematics were thus generic to the implant rather than subject-specific, the individual scaling of the musculoskeletal models reflected the anatomical variation in the relative positions of the ligament attachment sites with respect to the femoral component across the four subjects. Therefore, the models included essential subject-specific variations in those musculoskeletal structures that were key for the present study.

Observing the distance between ligament attachment sites to characterize the function of the ligaments (Park et al. 2005; Van de Velde et al. 2007) has the limitation that the zero-strain conditions of the ligaments are difficult to obtain (Harfe et al. 1998) and neither any initial strain within the ligament nor the condition of a slack ligament are considered. However, since the extended knee, in which the collateral ligaments are taut or strained (Gardiner et al. 2001; Harfe et al. 1998; Putz et al. 2007; Robinson et al. 2004b) is used as a reference in this study, any assumptions on ligament strains would be under- rather than overestimated.

Amis and co-workers (Amis and Zavras 1995) already emphasized the importance of the location of the ligament attachment sites relative to the femoral flexion axes, as the length change patterns of the ligaments are dependent on this relative position. Implant designs with different condyle radii and different sizing of the implant, as well as patient-specific variation in the locations of ligament attachment zones, may further alter the ligament length change patterns in mid-flexion and warrant further investigation.

The influence of the dynamics of the tibial wrapping points was not further analyzed in this study, since the main influence of JLE on the ligaments' DA is the changing position of the femoral ligament attachments relative to the rotation axis of the femoral component.

In this study, we assumed that a well balanced knee was achieved for the reference implantation in all subjects, without requiring excessive soft-tissue management. Furthermore, in the specific cases of 5 and 10 mm JLE, the tightening of the flexion gap can be exactly compensated by an equivalent reduction of the femoral components' anterior-posterior dimension through the implantation of a smaller prosthesis. In real life, the amount of JLE would not always exactly match the available implant sizes, and would thus most likely necessitate some additional soft tissue balancing. In practice, a surgeon would try to balance the soft tissues in both extension and 90° flexion during TKA by appropriate release techniques. However, the possibilities to accurately simulate these finer details of the surgical release techniques in silico are certainly limited.

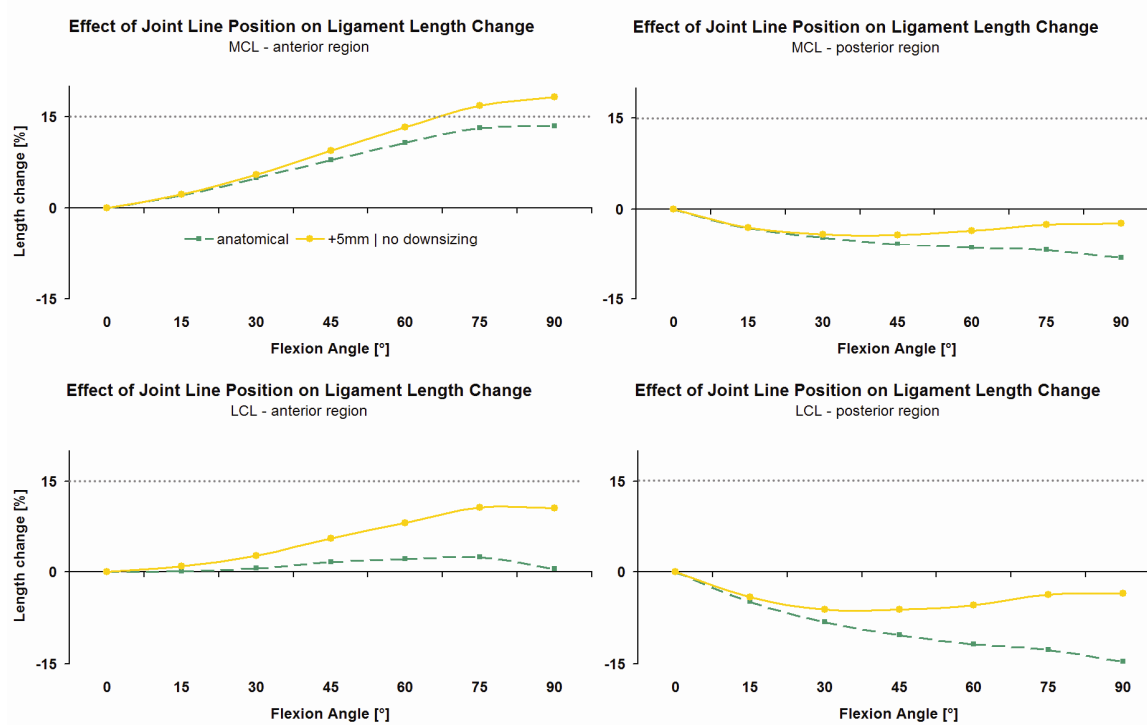


Figure 39: Length change patterns of the collateral ligaments for the conditions of joint line elevation and no downsizing of the femoral component. The graphs show the length change patterns for the anterior (left) and posterior (right) regions of the medial (top) and lateral (bottom) collateral ligaments, as observed from extension to 90° flexion. The dashed curve represents the anatomical reconstruction of the joint line, while the solid curve represents a joint line elevation of 5mm. The horizontal dotted line represents an average value for the maximum tensile strain of the collateral ligaments as reported in the literature.

The conditions analyzed here therefore represent a rather specific situation for which no additional soft tissue balancing is required. However, by focusing the study on JLE values that could be matched by appropriate changes in the anterior-posterior implant dimension, the number of unknown parameters was minimized. This facilitated the study of the influence of JLE on the behaviour of the collateral ligaments under well controlled conditions, and was therefore considered an acceptable approximation of the clinical situation.

In conclusion, our findings indicate that JLE, as hypothesised, did alter the length change patterns of the collateral ligaments during knee flexion. However, analysing the Columbus UC implant design, our findings did not support the idea that JLE is a major contributor to mid-flexion instability.

5 THE EFFECT OF COMBINED FEMORAL COMPONENT MALALIGNMENT ON JOINT CONTACT FORCES

König C, Matziolis G, Sharenkov A, Taylor WR, Perka C, Duda GN, Heller MO. 2010, The Knee (manuscript in preparation)

In chapter three it was shown that the cranial-caudal position of the femoral component, which defines the location of the joint line, has a significant influence on the contact forces acting at the knee. These findings provide a biomechanical explanation for the clinical observations that patients with an elevated joint line are likely to experience post-operative complications. In a preliminary approach to assess stability-related complications it was shown in the previous chapter that a manipulated joint line alone does not seem to be a major contributor to such complications – specifically not in mid-flexion, where instability is often clinically encountered but not yet fully explained.

Having established the musculoskeletal models, which are now capable of analysing the effects of femoral component cranial-caudal malalignment on joint contact forces and ligament function, this chapter sets out to investigate a clinically more likely scenario, i.e. combined malalignment in all six degrees of freedom and its effect on the contact forces in the joint. Such a comprehensive analysis may help to understand which of the six malalignment parameters most strongly influence the contact forces and therefore require careful intra-operative monitoring. The knowledge gained from such analyses can then be used to identify more complex malalignment conditions that can lead to critically increased contact forces and should thus be avoided.

5.1 Introduction

There is great interest in understanding the mechanisms leading to unsatisfactory clinical and functional results after total knee arthroplasty (TKA), with revision rates of up to 12% of all performed TKAs in a 10-year, and up to 18% in a 15-year follow-up (Attar et al. 2008; Burnett et al. 2004; Dixon et al. 2005; Hardeman et al. 2006; Ishii et al. 2005; Mangaleshkar et al. 2002; Mayman et al. 2003). Several studies have shown that malalignment of the femoral component affects the post-operative outcome and can ultimately lead to revision (Akagi et al. 1999; Barrack et al. 2001; Berger et al. 1998; Catani et al. 2006; Choong et al. 2009; Dennis et al. 2001; Eckhoff et al. 1995; Hofmann et al. 2003; Insall et al. 2002; Jeffery et al. 1991; Lewis et al. 1994; Liao et al. 2002; Nagamine et al. 1995b; Romero et al. 2003; Sharkey et al. 2002; Takahashi et al. 1997; Wasielewski et al. 1994; Zihlmann et al. 2005).

From the six degrees of freedom (DOF) in which femoral component malalignment can occur, it is known that e.g. an internal rotation of the femoral component of more than 3° can cause patellofemoral complications such as instability, limited range of motion and pain (Barrack et al. 2001; Berger et al. 1998; Hofmann et al. 2003)(Figure 40). Moderate external rotation is, however, not considered critical (Berger et al. 1998; Nagamine et al. 1995b). The influence of flexion errors during femoral component placement have received little attention, while coronal plane malrotation (varus–valgus malalignment) has also been associated with poorer implant survival (Choong et al. 2009; Jeffery et al. 1991) and increased joint loading (Heller et al. 2003). A cranio-caudal malpositioning of the femoral component, which determines the location of the joint line, is observed relatively often, particularly in revision TKA (Partington et al. 1999), and was shown to contribute to post-operative functional and clinical deficits (Figgie et al. 1986; König et al. 2010; Laskin 2002; Porteous et al. 2008).

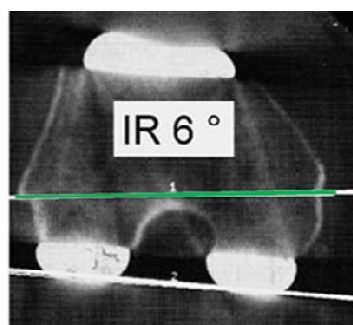


Figure 40: Post-operative radiological assessment of femoral component placement showing an internal rotation of 6° relative to the transepicondylar axis (green line). Internal rotations of more than 3° may lead to complications (Barrack et al. 2001; Berger et al. 1998; Hofmann et al. 2003).

In most of these studies, however, only the effects of a single factor, i.e. malalignment in only one DOF, has been analysed. As yet, little is known of how clinically more likely scenarios of femoral component malalignment in more than one DOF affect the knee joint's biomechanics – particularly the joint contact forces, which have been shown to affect the post-operative outcome (Dye 2005; Dye et al. 1998; Estupinan et al. 1998; Grana and Kriegshauser 1985; Heino Brechter and Powers 2002; Shelbourne et al. 1996; Skutek et al. 2001; Wu et al. 2000). Especially during physically challenging activities, such as stair climbing, the knee is exposed to significant contact forces (Costigan et al. 2002; D'Lima et al. 2005b; Taylor et al. 2004) and any further contact force increase caused by femoral component malalignment could lead to overloading conditions in the joint (Figure 41). Understanding the effects of femoral component malalignment on the loading conditions in the knee is a basis to identify the most influential alignment parameters. The precise perioperative acquisition and monitoring of these parameters may then help to identify and also avoid possible overloading conditions.

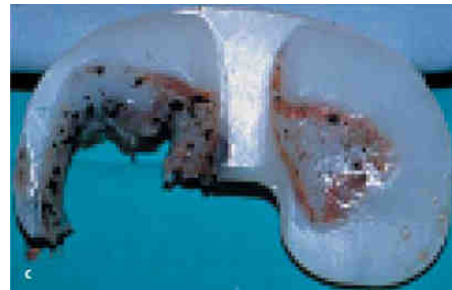


Figure 41: Failed tibial polyethylene insert showing signs of intense mechanical destruction, indicative of an overloading condition in the knee.

It was hypothesized that analysing individual femoral component malrotations or translations in just one DOF is insufficient to assess the effect of malalignment on the post-operative joint contact forces, and that a more extensive analysis of malalignment in all six DOF is necessary. Furthermore, it was hypothesized that the negative effect of an individual malalignment on joint contact forces can, in certain conditions, be compensated by the manipulation of the remaining alignment parameters.

By investigating the effect of femoral component malalignment in more than one DOF on the joint contact forces in the tibio- and patellofemoral joints, during stair climbing and normal walking, the aim of this study was to determine the malalignment parameters that have the greatest influence on the joint contact forces. It was further sought to identify combinations of malalignment that can lead to critical contact force increases and which parameters should therefore be carefully monitored.

5.2 Methods

Musculoskeletal model

Validated musculoskeletal models of four subjects, as described in more detail in the previous chapters, were used for the calculation of the tibio- and patellofemoral contact forces for walking and stair climbing. Prior to the calculations, these models were adapted to a post-TKA condition, by virtually performing a TKA with an ultra-congruent, fixed bearing and cruciate sacrificing implant design (Columbus UC, Aesculap AG, Tuttlingen, Germany), using visualization and volume modelling software (AMIRA, Mercury Computer Systems Inc., MA, USA). The prosthesis' components were orientated in the sagittal, coronal and axial plane according to standard surgical procedures. An experienced orthopaedic surgeon (GM) supervised the correct sizing and implantation of the components.

Simulation of femoral component malalignment

Using the optimal TKA implantation as a reference, femoral component malalignment was simulated in the musculoskeletal model of each subject. The position and the orientation of the implant were varied in all six DOF within a clinically likely range, which was defined with reference to the literature (Bankes et al. 2003; Barrack et al. 2001; Berger et al. 1998; Catani et al. 2006; Figgie et al. 1986; Hofmann et al. 2003; Jeffery et al. 1991; Laskin 2002; Partington et al. 1999; Porteous et al. 2008; Zihlmann et al. 2005) and confirmed by a group of experienced surgeons.

Joint line variation was simulated by modifying the cranial-caudal position of the femoral and tibial prosthesis components relative to the anatomical femoral and tibial long axes defined in the musculoskeletal model (Heller et al. 2001b). The size of the inlay was adjusted accordingly. To avoid a too-tight flexion gap under elevated joint line conditions, the femoral component was downsized according to the manufacturer's recommendation. The joint line was modified from the reference position to 10 mm distalization and 10 mm elevation using a step size of 1 mm. The leg length and the length of the ligamentum patellae remained unchanged. The medio-lateral and the antero-posterior variations of the femoral component placement were simulated by varying the position of the component in these directions, alongside the corresponding femoral axes, by up to 5mm in each direction, in steps of 2.5 mm.

The flexion-extension of the femoral component was altered by 5° towards extension and 5° towards a more flexed orientation. Here, the component was rotated in the sagittal plane about the prosthesis' medio-lateral axis. A malalignment in the frontal plane was simulated by rotating the femoral component 10°, in varus and valgus directions, about the component's antero-posterior axis. The rotation of the femoral component in the axial plane was varied up to 5° external and 10° internal rotation relative to its orientation in the reference TKA. Here the femoral component's superior-inferior axis was used as rotation axis. All rotations were simulated using a step size of 2.5°. The range of the simulated femoral component placement is summarized in table 4 and illustrated in figures 42a and 42b.

Table 4: Simulated femoral component malalignment ranges and increments.

	Cranial- Caudal Position	Medio- Lateral Position	Antero- Posterior Position	Flexion– Extension	Valgus- Varus	External- Internal Rotation
Simulated Range	±10mm	±5mm	±5mm	±5°	±10°	-5° to 10°
Increment	1mm	2.5mm	2.5mm	2.5°	2.5°	2.5°

Figure 42a: The variation of femoral component placement was simulated in six degrees of freedom (DOF): 3 translational DOFs (green) and 3 rotational DOFs (blue).

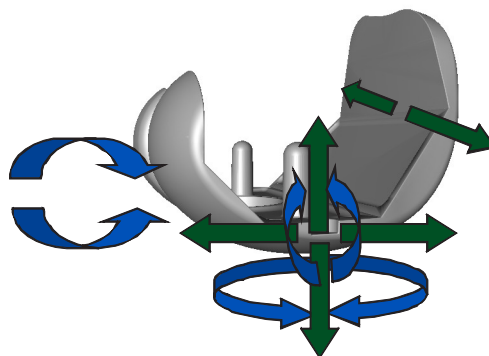


Figure 42b: Exemplary visualization of a simulated femoral component malalignment. The rotation in the axial plane was varied between 5° external rotation (left), the anatomical reconstruction (centre) and up to 10° internal rotation (right).

Kinematic adaptation

Lower limb kinematics for walking and stair climbing activities were captured in a clinical gait analysis by Heller and co-workers (Heller et al. 2001b). In chapter three, a reference kinematic model was introduced which - based on the geometry of the ultra-congruent prosthesis' articulating surfaces - adapted this gait data to a post-TKA situation (König et al. 2010). In brief, three individual flexion axes were defined by the centres of three circles that were fitted to sections of the femoral component's articulating surface on the medial and lateral condyles. According to the flexion angles derived from gait analysis, the femoral component kinematics were now described by using the component's flexion axes. Here it was assumed that the femoral component always achieved complete contact with the ultra-congruent tibial inlay.

In the initial simulation of an optimal TKA, the groove of the femoral component was orientated with a sulcus angle of 7° and represented a close reconstruction of the natural trochlea. Therefore the patellar kinematics obtained for the intact knee (Durselen et al. 1995) were considered to provide a good approximation of the patellofemoral kinematics in the anatomically reconstructed joint.

Joint contact forces

The anatomically reconstructed joint served as a reference to calculate the patello- and tibiofemoral joint contact forces for repeated trials of normal walking and stair climbing in all four subjects, using inverse dynamics and optimization algorithms (Heller et al. 2001b; Heller et al. 2007b). The peak contact forces were identified within each activity cycle. These calculations were repeated for all possible implant positions defined by the combination of all malalignment parameter values. For further processing, the calculated contact forces were stored in a database, which contained the subject identification number, the activity, the trial, the values of each of the six malalignment DOF and the resulting patello- and tibiofemoral contact forces.

Data analysis

To investigate whether femoral component malalignment can cause potential overloading situations, the analysis tested for a contact force increase above a fixed threshold in the patello- and tibiofemoral joints.

Using the previously established contact force database, the relative influence of each malalignment DOF on the total joint contact force was then further analysed. The contact force F is a function of the six malalignment parameters $P_{1..6}$. For each entity of the database, the difference in contact force was calculated relative to the entity in which the observed parameter was set to "0", i.e. remaining in its original state of the anatomically reconstructed joint.

For each observed parameter, $P_{1..6}$, these differences were then summed, representing the error-sum for this parameter, i.e. for (P_1) this error sum would be:

$$Err_{P_1} = \sum_{P_1, P_2, P_3, P_4, P_5, P_6} |(F(P_1, P_2, P_3, P_4, P_5, P_6) - F(0, P_2, P_3, P_4, P_5, P_6)) / F(0, P_2, P_3, P_4, P_5, P_6)|$$

The contribution of each individual parameter's error-sum to the total error-sum of all parameters then defined the relative influence of a specific alignment parameter on the joint contact forces.

$$Err_{P_i}^{relative} = Err_{P_i} / \sum_{n=1..6} Err_{P_n}$$

The magnitude at which an individual malalignment DOF contributes to increased loading conditions was further assessed. For every simulated magnitude of each malalignment DOF, it was calculated how often a variation of the remaining DOFs across their ranges would lead to a contact force increase of more than 10%.

Finally, all malalignment combinations that led to contact force increases of 50% and above were extracted.

5.3 Results

165375 different placements of the femoral component were simulated for each patient, and the patello- and tibiofemoral contact forces were calculated for both activities and all trials.

The relative influence of individual malalignment parameters on total contact forces

Patellofemoral joint

During normal walking the malalignment DOF with the largest relative error-sum – hence, the most influential DOF on the total joint contact forces in this joint – was the internal-external rotation of the femoral component. Here, the relative error-sum was 46% (Figure 43). Of large relative influence were also the varus-valgus malalignment (20%), the antero-posterior location (14%) and the location of the joint line (13%). The flexion-extension and the medio-lateral position were not as influential (6% and below).

In the stair climbing activity, the joint line had the strongest influence (29%), which was 16% higher than the joint line's influence in normal walking (Figure 43). The antero-posterior position (24%), the varus-valgus malalignment (20%) and the internal-external rotation (18%) were each ranked similarly, while the flexion–extension and the medio-lateral position were DOFs in which a deviation from the targeted reconstruction had a smaller influence on the loading conditions (5% and below).

Tibiofemoral joint

The most influential malalignment DOF during normal walking was varus-valgus rotation (35%)(Figure 44). The internal-external rotation (19%), the joint line (18%) and the antero-posterior location of the implant (16%) were also of substantial influence. The relative error sum of the medio-lateral position was 10%, while that of the flexion-extension was 2%.

During stair climbing, varus-valgus alignment had again the greatest impact on the tibiofemoral contact forces (28%)(Figure 44). The joint line also had a significant influence (27%) on the contact forces, as well as the internal-external rotation (21%).

With values of 12% (antero-posterior location) and below (medio-lateral position 10%, flexion-extension 2%), the other parameters' influence was rather small.

Malalignment scenarios that caused contact force increases of 10% and more

Femoral component malalignment caused contact force increases of 10% and more in both joints and during both activities (Figures 43 and 44). Maximum joint contact forces with magnitudes of 70% higher than in the anatomically reconstructed joint were found to occur in the simulated malalignment. The number of incidences in which malalignment caused such extreme contact force increases of 50% or more varied between the subjects analysed, reaching a maximum of 1.2% of all simulated malalignment conditions. Interestingly, in 95% of these cases, an internal rotation above 5° was present in combination with a varus malalignment above 5°.

The 10% contact force increase threshold was exceeded in at least one joint in an average of 28±1% of all analysed cases, with more incidences in the patellofemoral joint (36±9%) than in the tibiofemoral joint (20±1%). Such contact force increases of 10% or more can be caused by every type of malalignment. Even if an individual DOF was kept in its reference condition, malalignment in the remaining DOFs can increase contact forces beyond the threshold. The share of these cases in all identified cases of increased contact forces ranged from 6% to 45%. Some kinds of malalignment were found in more than 50% of the cases of increased contact forces; the most influential parameter was present in 92%.

Patellofemoral joint

During normal walking, the patellofemoral joint experienced, in 33±1% of all analysed cases, a contact force increase of 10% or more, which was not quite as often as in stair climbing (39±6%). An internal rotation of the femoral component of 5-10° was present in 92% (normal walking) and 65% (stair climbing) of all cases of increased contact forces (Figure 43). An overly anterior placement of the femoral component (5mm) had a 58% share in these cases during stair climbing.

Tibiofemoral joint

In the tibiofemoral joint, fewer cases of contact force increases of 10% or more were observed during normal walking (19±1%) than during stair climbing (21±1%). A varus

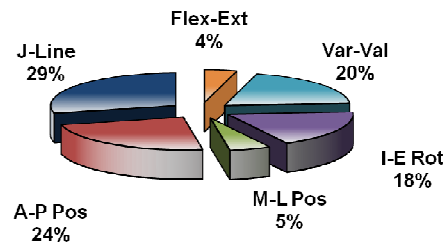
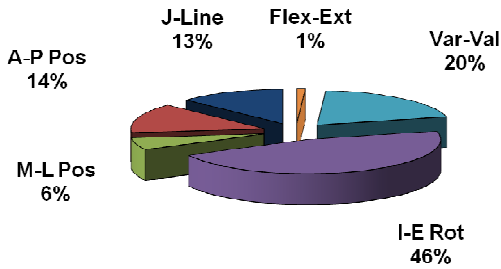
malalignment between 5° and 10° was present in 83% of all cases of a 10% contact force increase during normal walking (Figure 44). Similarly to the patellofemoral joint, an internal rotation of the femoral component between 5° and 10° had a large share in the increased contact forces during both activities (stair climbing 72%, normal walking 75%). A distalization of the joint line of 5 to 10 mm was present in 64% of all cases where a 10% contact force increase was observed in the tibiofemoral joint.

Patellofemoral

Normal Walking

Stair Climbing

Relative Influence on Joint Contact Force (JCF)



Conditions with 10% JCF Increase – Relative Share

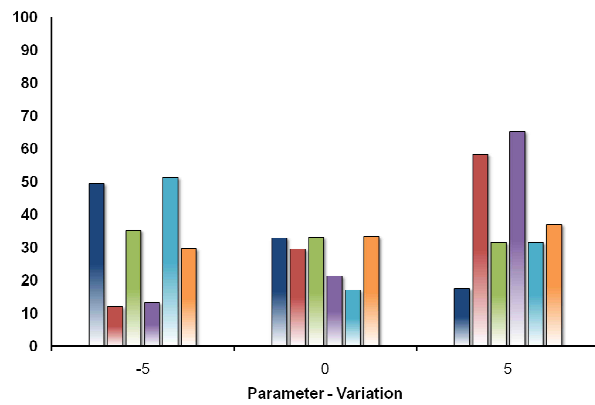
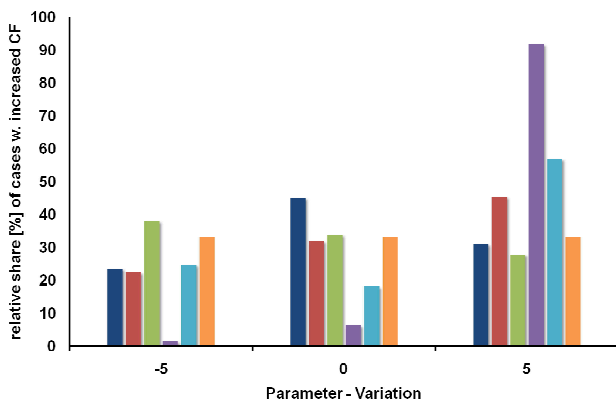


Figure 43: The relative influence of individual malalignment parameters on patellofemoral contact forces (top). Histograms show the share of the specific levels of the individual malalignments in the total number of cases in which the contact forces increased 10% or more. Values are given for normal walking (left) and stair climbing (right).

Tibiofemoral

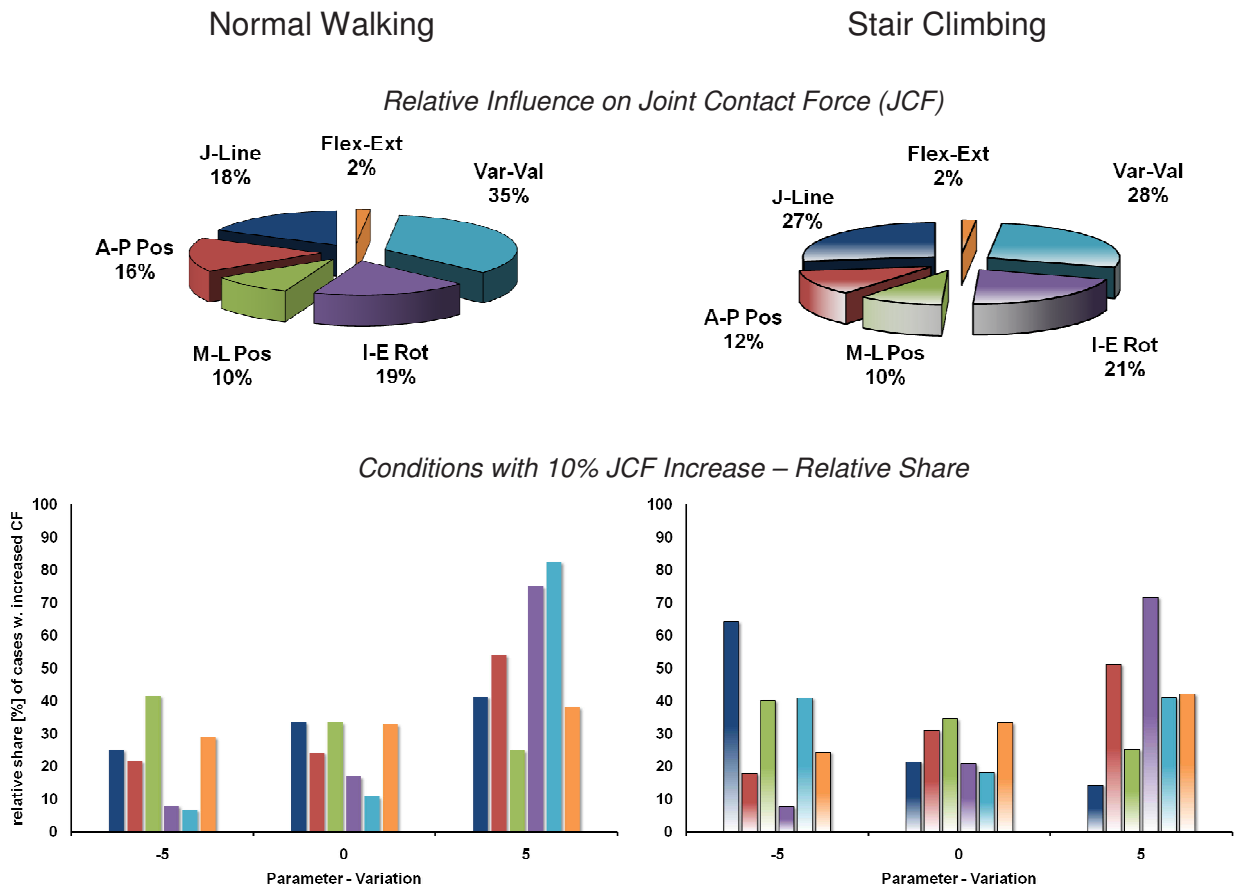


Figure 44: The relative influence of individual malalignment parameters on tibiofemoral contact forces (top). Histograms show the share of the specific levels of the individual malalignments in the total number of cases in which the contact forces increased 10% or more. Values are given for normal walking (left) and stair climbing (right).

5.4 Discussion

It is known that malalignment of the femoral component can be linked to unfavourable post-operative results in TKA and can ultimately lead to revision (Akagi et al. 1999; Barrack et al. 2001; Berger et al. 1998; Catani et al. 2006; Choong et al. 2009; Dennis et al. 2001; Eckhoff et al. 1995; Hofmann et al. 2003; Insall et al. 2002; Jeffery et al. 1991; Lewis et al. 1994; Liao et al. 2002; Nagamine et al. 1995b; Romero et al. 2003; Sharkey et al. 2002; Takahashi et al. 1997; Wasielewski et al. 1994; Zihlmann et al. 2005). Most of these studies dealing with the influence of femoral component malalignment on the TKA outcome assessed malalignment in an individual DOF only. The interactions with the remaining DOFs are poorly understood to date, and the relative importance of each malalignment DOF remains uncertain.

Using a validated musculoskeletal model, we analysed for the first time the interaction of all six DOFs in femoral component placement. The tibio- and patellofemoral contact forces during normal walking and the more challenging activity of stair climbing were calculated for a range of clinically relevant malalignment conditions (Bankes et al. 2003; Barrack et al. 2001; Berger et al. 1998; Catani et al. 2006; Figgie et al. 1986; Hofmann et al. 2003; Jeffery et al. 1991; Laskin 2002; Partington et al. 1999; Porteous et al. 2008; Zihlmann et al. 2005). We were able to show that malalignment increased joint contact forces by at least 10% in 28% of all simulated cases, reaching a maximum contact force increase of 70% higher than that in the reference implantation.

Avoiding femoral component placements that are likely to result in overloading seems a reasonable strategy, especially since increased joint loading has been related to pain (Dye 2005; Dye et al. 1998; Grana and Kriegshauser 1985; Heino Brechter and Powers 2002; Mayman et al. 2003) and the wear rate of polyethylene inserts (Estupinan et al. 1998), as well as being discussed in the context of osteoarthritis progression (Wu et al. 2000) and the development of arthrofibrosis (Shelbourne et al. 1996; Skutek et al. 2001).

However, analysing the relative effect of a variation in each malalignment parameter on the overall contact forces revealed that there is no specific parameter that is always and alone causing a contact force increase. The malalignment parameters that lead to increased contact forces are rather dependent on the joint and the activity performed.

The main contributors to altered contact forces in the patellofemoral joint are the internal-external rotation during normal walking and the joint line during stair climbing. In the tibiofemoral joint varus-valgus malalignment has the greatest impact on joint contact forces during both activities, in stair climbing being just marginally more influential than the joint line. Considering the distribution of the cases where the contact forces exceeded a 10% increase, it was apparent that even if the alignment of an individual parameter is perfectly achieved, a malalignment of the other parameters within the analysed boundaries will lead, in at least 6% and up to 45% of all these cases, to a load increase of 10% or more.

An internal rotation of the femoral component was identified as putting both joints at risk of increased contact forces. In all of the cases where a contact force increase of 10% or more occurred, up to 92% were caused by a 5° to 10° internally rotated femoral component. Our results revealed that, in such cases, an overloading can be scarcely avoided, no matter how the femoral component is positioned and orientated otherwise. These findings could be an explanation for the clinical complications often associated with an internal rotation of the femoral component (Barrack et al. 2001; Berger et al. 1998; Hofmann et al. 2003). This biomechanical data therefore emphasizes the need for careful control of the femoral component's rotation.

Varus-valgus malalignment has been clinically associated with poor implant survival (Choong et al. 2009; Jeffery et al. 1991). Our data showed that, specifically in the tibiofemoral joint during normal walking, a varus malalignment of 5° and above (limited to 10°) was present in 83% of the cases where a contact force increase of 10% or more was calculated. A previous computational analysis predicted a contact force increase in both a varus and a valgus malalignment, with a greater impact from a valgus alignment (Heller et al. 2003). While the study of Heller and co-workers (Heller et al. 2003) simulated an isolated varus-valgus deformity only, it is now apparent that the additional malalignment in the remaining DOFs increased the impact of a varus malalignment on the joint contact forces.

Our results also indicate that the joint line influences the joint contact forces, particularly during stair climbing. Joint line-related clinical complications have been typically associated with joint line elevations of 5mm and above (Figgie et al. 1986; Porteous et al. 2008). While a joint line elevation in the otherwise well aligned femoral component was indeed shown to increase joint contact forces, especially in the patellofemoral joint during stair climbing (König et al. 2010), the joint line may be even more influential when distalized in combination with malalignment in any other DOF. These findings

emphasize the necessity to consider the whole spectrum of femoral component malalignment in biomechanical analyses.

A too-anterior placement of the femoral component can also increase the risk of higher contact forces, indicating that special care should be taken to avoid an anterior overstuffing during TKA.

The analyzed moderate contact force increases of 10% can lead to small but permanent overloading conditions, and may rather have long-term effects on the post-operative results, such as the complications related to implant wear and debris. However, the observed increases of 50% or more may directly put the primary fixation of the implant at risk, which can lead to a failure of the TKA. We found that these peak forces can occur when a larger varus malalignment is combined with an internal rotation. Such combinations should therefore be avoided.

The approach chosen in this study was to use validated musculoskeletal models (Heller et al. 2001a; Heller et al. 2003). Even though direct measurements of the in vivo loading conditions in the knee have been performed previously (D'Lima et al. 2005a; Heinlein et al. 2007; Wallace et al. 1998; Wasielewski et al. 2005; Zhao et al. 2007), analysing the biomechanical effects of complex malalignment in all six DOFs is not possible in vivo. The modelling approach used in this study also comes with certain limitations. The analyses performed were limited to one implant type only – an ultra-congruent cruciate sacrificing, fixed bearing prosthesis design. The relative importance of the individual malalignment parameters might differ when using different implant types, but it is unlikely that the results would be completely different. Nonetheless, other implant designs should be the subject of further studies. Using the ultra-congruent implant design in this study had the advantage that a geometric approach could be chosen for simulating the tibiofemoral kinematics. A generic sagittal plane kinematic model was used, reflecting the guiding characteristics of this specific prosthesis design. Even though several studies have investigated tibiofemoral kinematics after TKA (Dennis et al. 2003; Dennis et al. 2004; Nilsson et al. 1990; Zihlmann et al. 2006), no general kinematic patterns have yet been identified that could have been applied in this study. The kinematic model used in this study therefore reflected only a limited spectrum of the kinematic variation that is likely to occur in vivo (Dennis et al. 2004).

Our data revealed that, during TKA surgery, it is not a simple task to minimize the risk of overloading conditions. We showed that it is not sufficient to accurately monitor only a single but influential DOF, such as the location of the joint line, to avoid the risk of

overloading, as there is a considerable risk remaining that an overloading condition is induced by additional malalignment in the remaining DOFs. The complex interactions between the individual DOFs of femoral component malalignment are also dependent on the observed joint and the activity performed, which makes it very difficult to evaluate the effect of malalignment on the post-operative loading conditions.

Navigation systems that are capable of an accurate and reproducible monitoring of the most influential parameters could identify, and possibly help to avoid, complex malalignments that cause overloading. Furthermore, integrating intra-operative biomechanical assessments in the navigation workflow can directly assist the surgeon to biomechanically evaluate and optimize the planned placement of the femoral component. Even if the optimal alignment of an influential DOF cannot be achieved surgically, the remaining DOFs could then be manipulated to compensate for the resulting negative biomechanical effects.

In conclusion, we were able to confirm our hypothesis that it is not sufficient to analyse malalignment DOFs individually, since a complex interplay exists between all six DOFs, which are also activity- and joint-dependent. Even though our simulations revealed that there are compromise options available to avoid overloading conditions, internal rotation combined with varus malalignment should be avoided, as they leave limited possibilities to avoid excessive contact force increases, possibly compromising short-term survival of the implant. Internal-external rotation, joint line and varus-valgus alignment strongly influence the joint loading conditions and should be monitored to minimize the risk of overloading conditions that could reduce the survival time of the implant in the long term.

6 SUMMARY AND CONCLUSIONS

Improving the overall function and survival time of a knee endoprosthesis is a challenging and also multidisciplinary task. In addition to, for example, minimizing the risk of peri-operative infections (Berbari et al. 1998) and optimizing the implant's design and mechanical stability (Wang and Wang 2000), an optimal placement of the implant is essential for the success of the TKA (Rousseau et al. 2008). Malalignment of the femoral component was identified in several studies as being related to post-operative complications and early failure of the implant (Akagi et al. 1999; Barrack et al. 2001; Berger et al. 1998; Catani et al. 2006; Choong et al. 2009; Dennis et al. 2001; Eckhoff et al. 1995; Hofmann et al. 2003; Insall et al. 2002; Jeffery et al. 1991; Lewis et al. 1994; Liao et al. 2002; Nagamine et al. 1995b; Romero et al. 2003; Sharkey et al. 2002; Takahashi et al. 1997; Wasielewski et al. 1994; Zihlmann et al. 2005). However, the underlying biomechanical reasons – especially in conditions of complex femoral component malalignment in several DOFs – remain relatively unknown. Such knowledge is essential, to identify and possibly avoid unfavourable biomechanical conditions resulting from femoral component malalignment.

The aim of this study, therefore, was to enhance the understanding of the effects of femoral component malalignment on knee biomechanics after TKA, specifically on the tibio- and patellofemoral contact forces and on the function of the collateral ligaments.

A mathematical approach was chosen in this study, which set out to utilize musculoskeletal models in which large numbers of malalignment conditions could be simulated. In the first stages of this study, preliminary work was performed to adapt the musculoskeletal models for such a task. A novel 3D representation of the lower limb's active and passive soft tissue stabilizers was created, allowing detailed spatial modelling of the muscular lines in the musculoskeletal model and a precise description of the knee ligaments' bony insertion sites.

To drive the musculoskeletal model, the availability of a reliable reference for tibiofemoral kinematics is required. In vivo tibiofemoral kinematics were determined for various muscular activation patterns and a kinematic model developed, which was capable of predicting complex kinematic patterns (Heller et al. 2007a). The analysis of an ultra-congruent implant design later in the study allowed the use of a more simplified

geometric approach to describe tibiofemoral kinematics. However, the new kinematic model may also allow simulation of the more complex kinematic patterns of other implant designs. The newly developed techniques by Ehrig and colleagues (Ehrig et al. 2007) are promising for obtaining the necessary kinematic reference data. Their methods reduce the effects of soft tissue artefacts in gait analysis data and may thus allow for the precise and non-invasive acquisition of tibiofemoral reference kinematics.

Besides the healthy tibiofemoral joint, the patellofemoral joint was also investigated, using a novel in vitro setup. This setup allowed the application of in vivo loading conditions, which has not been achieved before (Goudakos et al. 2010; Goudakos et al. 2009). Analysing the patellofemoral contact mechanics revealed the importance of including different activities when looking at the loading conditions in the joint. Stair climbing led to more challenging contact mechanics than normal walking. Additional load increases caused by TKA could cause patellofemoral pathologies.

Subsequently, the musculoskeletal models that were originally developed to represent an intact knee joint were adapted to reflect the conditions after a TKA. A cranial-caudal malalignment of the femoral component, which has been clinically reported to be relevant to the post-operative outcome (Laskin 2002; Porteous et al. 2008), was then simulated in this model.

Our analyses showed that an elevated joint line can indeed lead to increased contact forces, especially in the patellofemoral joint during stair climbing. Clinically, an elevation of the joint line should thus be avoided, as it can expose the patient to unphysiologically high joint contact forces, increasing the risk of developing clinical and functional problems. Specific procedures in TKA that may lead to an elevated joint line (Bellemans 2004; Figgie et al. 1986; Scuderi and Insall 1992), such as managing distal femoral defects (Bellemans 2004) or defining the level of tibial resection (Grelsamer 2002; Laskin 2002), should be handled with extra caution.

The representation of the collateral ligaments, newly integrated into the model, allowed the study of the effect of this cranial-caudal malalignment of the femoral component on the function of the collateral ligaments. A possible link to instability in mid-flexion (Martin and Whiteside 1990; Parratte and Pagnano 2008) was not found. However, an elevated joint line influences the function of the collateral ligaments in a manner that suggests a constant condition of increased loading in the anterior portions of the ligaments, possibly contributing to overloading-related soft tissue complications such as the development of arthrofibrosis (Shelbourne et al. 1996; Skutek et al. 2001).

Clinically it is more likely that malalignment occurs not only in one DOF, as simulated previously, but rather in several DOFs at the same time. Understanding the effects of a complex malalignment on joint contact forces, and how influential a malalignment DOF is in comparison to the other DOFs, is of specific interest. This knowledge is a basis for the perioperative planning and the intraoperative placement of the femoral component in a biomechanical context. The musculoskeletal model was therefore adapted to allow the simultaneous simulation of femoral component malalignment in all six DOFs.

More than 165000 malalignment conditions were simulated and the patello- and tibiofemoral contact forces calculated for subjects performing two activities. The relative influence of a variation of an individual malalignment parameter on the total contact forces was found to be dependent on the activity performed and the specific joint. Furthermore, our data indicated that even keeping an individual malalignment parameter in its reference condition could not always prevent the joint from being exposed to contact forces increased by 10% or above. The careful intraoperative monitoring of only a single parameter seems therefore not sufficient to prevent overloading conditions. However, according to our data, the risk of increased loading can be significantly reduced if specific alignment parameters, such as the internal rotation, are kept within certain limits.

Our results showed that examining malalignment in an individual orientation only, does not allow conclusions on the joint's biomechanics to be drawn if malalignment in other orientations is present. Even though our results earlier in this study suggested that a joint line distalization will decrease contact forces, it was apparent now that this was not always a valid conclusion and needed to be refined. A distalization of the joint line is therefore likely to decrease the joint contact forces, but may, in combination with malalignment in other orientations, also cause a contact force increase.

Interestingly, the contact force increase observed in the simulation of an isolated joint line elevation can be partially compensated by the presence of other malalignment. This highlights that no biomechanical conclusions can be drawn from assessing an individual malalignment alone, but rather, that at least those parameters that have been identified as highly influential should be included.

Another clinically relevant finding of this study was the identification of malalignment conditions that can lead to significantly increased loading conditions. According to our data, an internal rotation above 5° combined with a varus malalignment above 5° can result in a load increase of 50% or more. Such overloading may put the joint at risk of

early failure and should therefore be avoided. Since smaller increases of contact forces (10% and above), caused by femoral component malalignment, were found in 28% of all examined cases, possibilities should be investigated to clinically avoid these conditions as well, as they could affect the implant survival in the long term.

An intensive discussion has been held in the literature about the necessity of using navigation systems in total knee replacement (Kim et al. 2007; Lutzner et al. 2008; Matziolis et al. 2006; Matziolis et al. 2007; Spencer et al. 2007). According to our findings, a great benefit of these systems is the option to intra-operatively monitor the femoral component placement process for possible malalignment. Critical conditions such as the combination of varus and internal rotation could then be identified. However, it remains to be proven that navigation systems allow for the accurate and reproducible acquisition of FCM (Jenny and Boeri 2004).

Navigation systems may also be the key to intra-operatively identifying malalignment conditions where smaller load increases may occur. Due to the complex interplay between the six malalignment parameters, identifying such conditions is almost impossible for the surgeon without assistance. Enhancing orthopaedic navigation systems with a database such as the one created in this study, which contains a matrix of malalignment in all DOFs and the resulting contact forces for both joints and the most common activities, would allow for the intra-operative detection of increased loads. Such systems could also assist in situations when a specific malalignment is required as a surgical compromise. If, for example, the femoral component is internally or externally rotated in order to achieve a balanced flexion gap, these systems then could guide the manipulation of the remaining alignment parameters to reduce the joint contact forces.

To fully facilitate the possibility of intra-operative optimization of femoral component placement from a biomechanical point of view, in the future, routines should be integrated in the TKA procedure to reliably acquire the individual anatomy of the patient's whole lower limb. The biomechanical assessment of the planned implant placement would then advance from rather generic assumptions to a patient-specific determination of the internal loading conditions, increasing the options to individually optimize the surgical intervention.

In conclusion, this study presented enhanced musculoskeletal models to assess the effect of femoral component malalignment on collateral ligament function and the tibio- and patellofemoral contact forces in the post-TKA knee joint. The contact forces in the knee were found to be determined by a complex interplay of several alignment

parameters, also depending on the analysed joint and the performed activity. This indicated that it is not sufficient to assess only an individual malalignment parameter if biomechanical conclusions are to be drawn. The excessive contact force increases identified at higher varus and internal rotation malalignments were of particular clinical relevance. The use of the presented database of femoral component malalignments and their biomechanical consequences, or a real-time assessment of patients' individual loading conditions, are important steps towards intra-operatively minimizing the risk of increased contact forces. Avoiding excessive peak loading or a long-term smaller load increase may promote both primary stability and long-term survival of the implant.

7 REFERENCES

- Ahmad, C. S., Cohen, Z. A., Levine, W. N., Gardner, T. R., Ateshian, G. A. and Mow, V. C. (2003). "Codominance of the individual posterior cruciate ligament bundles. An analysis of bundle lengths and orientation." *Am J Sports Med* **31**(2): 221-225.
- Ahmed, A. M., Duncan, N. A. and Tanzer, M. (1999). "In vitro measurement of the tracking pattern of the human patella." *J Biomech Eng* **121**(2): 222-228.
- Akagi, M., Matsusue, Y., Mata, T., Asada, Y., Horiguchi, M., Iida, H. and Nakamura, T. (1999). "Effect of rotational alignment on patellar tracking in total knee arthroplasty." *Clin Orthop Relat Res*(366): 155-163.
- Amis, A. A., Bull, A. M., Gupte, C. M., Hijazi, I., Race, A. and Robinson, J. R. (2003). "Biomechanics of the PCL and related structures: posterolateral, posteromedial and menisiofemoral ligaments." *Knee Surg Sports Traumatol Arthrosc* **11**(5): 271-281.
- Amis, A. A., Gupte, C. M., Bull, A. M. and Edwards, A. (2005). "Anatomy of the posterior cruciate ligament and the menisiofemoral ligaments." *Knee Surg Sports Traumatol Arthrosc* **14**: 14.
- Amis, A. A., Senavongse, W. and Bull, A. M. (2006). "Patellofemoral kinematics during knee flexion-extension: an in vitro study." *J Orthop Res* **24**(12): 2201-2211.
- Amis, A. A. and Zavras, T. D. (1995). "Isometricity and graft placement during anterior cruciate ligament reconstruction." *The Knee* **2**(1): 5-17.
- Andriacchi, T. P., Alexander, E. J., Toney, M. K., Dyrby, C. and Sum, J. (1998). "A point cluster method for in vivo motion analysis: applied to a study of knee kinematics." *J Biomech Eng* **120**(6): 743-749.
- Andriacchi, T. P., Andersson, G. B., Fermier, R. W., Stern, D. and Galante, J. O. (1980). "A study of lower-limb mechanics during stair-climbing." *J Bone Joint Surg Am* **62**(5): 749-757.
- Attar, F. G., Khaw, F. M., Kirk, L. M. and Gregg, P. J. (2008). "Survivorship analysis at 15 years of cemented press-fit condylar total knee arthroplasty." *J Arthroplasty* **23**(3): 344-349.
- Bankes, M. J., Back, D. L., Cannon, S. R. and Briggs, T. W. (2003). "The effect of component malalignment on the clinical and radiological outcome of the Kinemax total knee replacement." *Knee* **10**(1): 55-60.
- Banks, S. A. and Hodge, W. A. (1996). "Accurate measurement of three-dimensional knee replacement kinematics using single-plane fluoroscopy." *IEEE Trans Biomed Eng* **43**(6): 638-649.
- Baratta, R., Solomonow, M., Zhou, B. H., Letson, D., Chuinard, R. and D'Ambrosia, R. (1988). "Muscular coactivation. The role of the antagonist musculature in maintaining knee stability." *Am J Sports Med* **16**(2): 113-122.
- Barrack, R. L., Schrader, T., Bertot, A. J., Wolfe, M. W. and Myers, L. (2001). "Component rotation and anterior knee pain after total knee arthroplasty." *Clin Orthop Relat Res*(392): 46-55.
- Beck, P., Brown, N. A., Greis, P. E. and Burks, R. T. (2007). "Patellofemoral contact pressures and lateral patellar translation after medial patellofemoral ligament reconstruction." *Am J Sports Med* **35**(9): 1557-1563.
- Bellemans, J. (2004). "Restoring the joint line in revision TKA: does it matter?" *Knee* **11**(1): 3-5.
- Bellemans, J., Robijns, F., Duerinckx, J., Banks, S. and Vandenuecker, H. (2005). "The influence of tibial slope on maximal flexion after total knee arthroplasty." *Knee Surg Sports Traumatol Arthrosc* **13**(3): 193-196.

- Berbari, E. F., Hanssen, A. D., Duffy, M. C., Steckelberg, J. M., Ilstrup, D. M., Harmsen, W. S. and Osmon, D. R. (1998). "Risk factors for prosthetic joint infection: case-control study." *Clin Infect Dis* **27**(5): 1247-1254.
- Berger, R. A., Crossett, L. S., Jacobs, J. J. and Rubash, H. E. (1998). "Malrotation causing patellofemoral complications after total knee arthroplasty." *Clin Orthop Relat Res*(356): 144-153.
- Bergmann, G., Deuretzbacher, G., Heller, M., Graichen, F., Rohlmann, A., Strauss, J. and Duda, G. N. (2001). "Hip contact forces and gait patterns from routine activities." *J Biomech* **34**(7): 859-871.
- Bergmann, G., Graichen, F. and Rohlmann, A. (1993). "Hip joint loading during walking and running, measured in two patients." *J Biomech* **26**(8): 969-990.
- Bergmann, G., Graichen, F. and Rohlmann, A. (1995). "Is staircase walking a risk for the fixation of hip implants?" *J Biomech* **28**(5): 535-553.
- Bergmann, G., Graichen, F., Siraky, J., Jendrzynski, H. and Rohlmann, A. (1988). "Multichannel strain gauge telemetry for orthopaedic implants." *J Biomech* **21**(2): 169-176.
- Besier, T. F., Draper, C. E., Gold, G. E., Beaupre, G. S. and Delp, S. L. (2005). "Patellofemoral joint contact area increases with knee flexion and weight-bearing." *J Orthop Res* **23**(2): 345-350.
- Besl, P. J. and McKay, N. D. (1992). "A Method for Registration of 3-D Shapes." *IEEE Transactions on Pattern Analysis and Machine Intelligence* **14**(2): 239 - 256.
- Beynon, B., Howe, J. G., Pope, M. H., Johnson, R. J. and Fleming, B. C. (1992). "The measurement of anterior cruciate ligament strain in vivo." *Int Orthop* **16**(1): 1-12.
- Bicos, J., Fulkerson, J. P. and Amis, A. (2007). "Current concepts review: the medial patellofemoral ligament." *Am J Sports Med* **35**(3): 484-492.
- Blaaha, J. D., Mancinelli, C. A. and Simons, W. H. (2002). "Using the transepicondylar axis to define the sagittal morphology of the distal part of the femur." *J Bone Joint Surg Am* **84-A (Suppl 2)**: 48-55.
- Blankevoort, L. and Huiskes, R. (1996). "Validation of a three-dimensional model of the knee." *J Biomech.* **29**(7): 955-961.
- Blankevoort, L., Huiskes, R. and de Lange, A. (1990). "Helical axes of passive knee joint motions." *J Biomech* **23**(12): 1219-1229.
- Brand, R. A., Crowninshield, R. D., Wittstock, C. E., Pedersen, D. R., Clark, C. R. and van Krieken, F. M. (1982). "A model of lower extremity muscular anatomy." *Journal of biomechanical engineering* **104**(4): 304-310.
- Brand, R. A., Pedersen, D. R., Davy, D. T., Kotzar, G. M., Heiple, K. G. and Goldberg, V. M. (1994). "Comparison of hip force calculations and measurements in the same patient." *J Arthroplasty* **9**(1): 45-51.
- Brand, R. A., Pedersen, D. R. and Friederich, J. A. (1986). "The sensitivity of muscle force predictions to changes in physiologic cross-sectional area." *J Biomech* **19**(8): 589-596.
- Brantigan, O. C. and Voshell, A. F. (1941). "The mechanics of the ligaments and menisci of the knee joint." *The Journal of Bone and Joint Surgery* **23**(1): 44.
- Brugem, S. J., Sierevelt, I. N., Schafroth, M. U., Blankevoort, L., Schaap, G. R. and van Dijk, C. N. (2008). "Less anterior knee pain with a mobile-bearing prosthesis compared with a fixed-bearing prosthesis." *Clin Orthop Relat Res* **466**(8): 1959-1965.
- Bringmann, C., Eckstein, F., Bonel, H., Englmeier, K. H., Reiser, M. and Graichen, H. (2000). "[A new in vivo technique for 3-dimensional analysis of the translation of femoral condyles and the menisci responding to antagonistic muscle forces]." *Biomed Tech (Berl)* **45**(10): 258-264.
- Brunner, E., Domhof, S. and Langer, F. (2002). *Nonparametric Analysis of Longitudinal Data in Factorial Experiments*. New York, Wiley.

- Buckwalter, J. A., Saltzman, C. and Brown, T. (2004). "The impact of osteoarthritis: implications for research." *Clin Orthop Relat Res*(427 Suppl): S6-15.
- Bull, A. M., Katchburian, M. V., Shih, Y. F. and Amis, A. A. (2002). "Standardisation of the description of patellofemoral motion and comparison between different techniques." *Knee Surg Sports Traumatol Arthrosc* **10**(3): 184-193.
- Burnett, R. S., Haydon, C. M., Rorabeck, C. H. and Bourne, R. B. (2004). "Patella resurfacing versus nonresurfacing in total knee arthroplasty: results of a randomized controlled clinical trial at a minimum of 10 years' followup." *Clin Orthop Relat Res*(428): 12-25.
- Butler, D. L., Kay, M. D. and Stouffer, D. C. (1986). "Comparison of material properties in fascicle-bone units from human patellar tendon and knee ligaments." *J Biomech* **19**(6): 425-432.
- Butler, D. L., Noyes, F. R. and Grood, E. S. (1980). "Ligamentous restraints to anterior-posterior drawer in the human knee. A biomechanical study." *J Bone Joint Surg Am* **62**(2): 259-270.
- Cappozzo, A., Catani, F., Leardini, A., Benedetti, M. G. and Croce, U. D. (1996). "Position and orientation in space of bones during movement: experimental artefacts." *Clin Biomech (Bristol, Avon)* **11**(2): 90-100.
- Caruntu, D. I. and Hefzy, M. S. (2004). "3-D Anatomically Based Dynamic Modeling of the Human Knee to Include Tibio-Femoral and Patello-Femoral Joints." *Journal of Biomechanical Engineering* **126**(1): 44-53.
- Catani, F., Fantozzi, S., Ensini, A., Leardini, A., Moschella, D. and Giannini, S. (2006). "Influence of tibial component posterior slope on in vivo knee kinematics in fixed-bearing total knee arthroplasty." *J Orthop Res* **24**(4): 581-587.
- Chao, E. Y. and Rim, K. (1973). "Application of optimization principles in determining the applied moments in human leg joints during gait." *J Biomech* **6**(5): 497-510.
- Chiu, K. Y., Ng, T. P., Tang, W. M. and Yau, W. P. (2002). "Review article: knee flexion after total knee arthroplasty." *J Orthop Surg (Hong Kong)* **10**(2): 194-202.
- Choong, P. F., Dowsey, M. M. and Stoney, J. D. (2009). "Does accurate anatomical alignment result in better function and quality of life? Comparing conventional and computer-assisted total knee arthroplasty." *J Arthroplasty* **24**(4): 560-569.
- Churchill, D. L., Incavo, S. J., Johnson, C. C. and Beynonn, B. D. (1998). "The transepicondylar axis approximates the optimal flexion axis of the knee." *Clin Orthop*(356): 111-118.
- Clark, A. L., Herzog, W. and Leonard, T. R. (2002). "Contact area and pressure distribution in the feline patellofemoral joint under physiologically meaningful loading conditions." *J Biomech* **35**(1): 53-60.
- Costigan, P. A., Deluzio, K. J. and Wyss, U. P. (2002). "Knee and hip kinetics during normal stair climbing." *Gait Posture* **16**(1): 31-37.
- Crowninshield, R. D. (1978). "Use of Optimization Techniques to Predict Muscle Forces." *J Biomech Engng* **100**(May): 88-92.
- D'Lima, D. D., Patil, S., Steklov, N., Slamin, J. E. and Colwell, C. W., Jr. (2005a). "The Chitranjan Ranawat Award: in vivo knee forces after total knee arthroplasty." *Clin Orthop Relat Res* **440**: 45-49.
- D'Lima, D. D., Patil, S., Steklov, N., Slamin, J. E. and Colwell, J. C. W. (2006). "Tibial Forces Measured In Vivo After Total Knee Arthroplasty." *The Journal of Arthroplasty* **21**(2): 255-262.
- D'Lima, D. D., Townsend, C. P., Arms, S. W., Morris, B. A. and Colwell, C. W., Jr. (2005b). "An implantable telemetry device to measure intra-articular tibial forces." *J Biomech* **38**(2): 299-304.
- Davy, D. T., Kotzar, G. M., Brown, R. H., Goldberg, V. M., Heiple, K. G., Berilla, J. and Burstein, A. H. (1988). "Telemetric force measurement across the hip after total hip arthroplasty." *J Bone Joint Surg Am* **70-A**: 45-50.
- Dennis, D. A., Komistek, R. D., Mahfouz, M. R., Haas, B. D. and Stiehl, J. B. (2003). "Multicenter determination of in vivo kinematics after total knee arthroplasty." *Clin Orthop*(416): 37-57.

- Dennis, D. A., Komistek, R. D., Mahfouz, M. R., Walker, S. A. and Tucker, A. (2004). "A multicenter analysis of axial femorotibial rotation after total knee arthroplasty." *Clin Orthop Relat Res*(428): 180-189.
- Dennis, D. A., Komistek, R. D., Walker, S. A., Cheal, E. J. and Stiehl, J. B. (2001). "Femoral condylar lift-off in vivo in total knee arthroplasty." *J Bone Joint Surg Br* **83**(1): 33-39.
- Dennis, D. A., Mahfouz, M. R., Komistek, R. D. and Hoff, W. (2005). "In vivo determination of normal and anterior cruciate ligament-deficient knee kinematics." *J Biomech* **38**(2): 241-253.
- Deuretzbacher, G. and Rehder, U. (1995). "[A CAE (computer aided engineering) approach to dynamic whole body modeling--the forces in the lumbar spine in asymmetrical lifting]." *Biomed Tech (Berl)* **40**(4): 93-98.
- Dixon, M. C., Brown, R. R., Parsch, D. and Scott, R. D. (2005). "Modular fixed-bearing total knee arthroplasty with retention of the posterior cruciate ligament. A study of patients followed for a minimum of fifteen years." *J Bone Joint Surg Am* **87**(3): 598-603.
- Dorr, L. D. and Boiardo, R. A. (1986). "Technical considerations in total knee arthroplasty." *Clin Orthop Relat Res*(205): 5-11.
- Dorr, L. D. and Chao, L. (2007). "The emotional state of the patient after total hip and knee arthroplasty." *Clin Orthop Relat Res* **463**: 7-12.
- Doucette, S. A. and Goble, E. M. (1992). "The effect of exercise on patellar tracking in lateral patellar compression syndrome." *Am J Sports Med* **20**(4): 434-440.
- Draganich, L. F., Jaeger, R. J. and Kralj, A. R. (1989). "Coactivation of the hamstrings and quadriceps during extension of the knee." *J Bone Joint Surg Am* **71**(7): 1075-1081.
- Duda, G. N., Brand, D., Freitag, S., Lierse, W. and Schneider, E. (1996). "Variability of femoral muscle attachments." *J Biomech* **29**(9): 1185-1190.
- Duda, G. N., Schneider, E. and Chao, E. Y. (1997). "Internal forces and moments in the femur during walking." *Journal of biomechanics* **30**(9): 933-941.
- Durselen, L., Claes, L. and Kiefer, H. (1995). "The influence of muscle forces and external loads on cruciate ligament strain." *Am J Sports Med* **23**(1): 129-136.
- Dye, S. F. (1987). "An evolutionary perspective of the knee." *J Bone Joint Surg Am* **69**(7): 976-983.
- Dye, S. F. (2005). "The pathophysiology of patellofemoral pain: a tissue homeostasis perspective." *Clin Orthop Relat Res*(436): 100-110.
- Dye, S. F., Vaupel, G. L. and Dye, C. C. (1998). "Conscious neurosensory mapping of the internal structures of the human knee without intraarticular anesthesia." *Am J Sports Med* **26**(6): 773-777.
- Eckhoff, D. G., Piatt, B. E., Gnadinger, C. A. and Blaschke, R. C. (1995). "Assessing rotational alignment in total knee arthroplasty." *Clin Orthop Relat Res*(318): 176-181.
- Ehrig, R. M., Taylor, W. R., Duda, G. N. and Heller, M. O. (2007). "A survey of formal methods for determining functional joint axes." *J Biomech* **40**(10): 2150-2157.
- Eilerman, M., Thomas, J. and Marsalka, D. (1992). "The effect of harvesting the central one-third of the patellar tendon on patellofemoral contact pressure." *Am J Sports Med* **20**(6): 738-741.
- English, T. A. and Kilvington, M. (1979). "In vivo records of hip loads using a femoral implant with telemetric output (A preliminary report)." *J Biomed Eng* **1**: 111-115.
- Estupinan, J. A., Bartel, D. L. and Wright, T. M. (1998). "Residual stresses in ultra-high molecular weight polyethylene loaded cyclically by a rigid moving indenter in nonconforming geometries." *J Orthop Res* **16**(1): 80-88.
- Eynon-Lewis, N. J., Ferry, D. and Pearse, M. F. (1992). "Themistocles Gluck: an unrecognised genius." *Bmj* **305**(6868): 1534-1536.

- Farahmand, F., Tahmasbi, M. N. and Amis, A. A. (1998). "Lateral force-displacement behaviour of the human patella and its variation with knee flexion--a biomechanical study in vitro." *J Biomech* **31**(12): 1147-1152.
- Felson, D. T. (2004). "Risk factors for osteoarthritis: understanding joint vulnerability." *Clin Orthop Relat Res* **427 (Suppl)**: 16-21.
- Felson, D. T. and Zhang, Y. (1998). "An update on the epidemiology of knee and hip osteoarthritis with a view to prevention." *Arthritis Rheum* **41**(8): 1343-1355.
- Ficat, P., Ficat, C. and Bailleux, A. (1975). "External hypertension syndrome of the patella. Its significance in the recognition of arthrosis." *Rev Chir Orthop Reparatrice Appar Mot* **61**(1): 39-59.
- Figgie, H. E., 3rd, Goldberg, V. M., Heiple, K. G., Moller, H. S., 3rd and Gordon, N. H. (1986). "The influence of tibial-patellofemoral location on function of the knee in patients with the posterior stabilized condylar knee prosthesis." *J Bone Joint Surg Am* **68**(7): 1035-1040.
- Fisher, D. A., Dierckman, B., Watts, M. R. and Davis, K. (2007). "Looks good but feels bad: factors that contribute to poor results after total knee arthroplasty." *J Arthroplasty* **22**(6 Suppl 2): 39-42.
- Frank., H. N. (1992). *Farbatlantzen der Medizin*, Georg Thieme Verlag Stuttgart-New York.
- Freeman, M. A. and Pinskerova, V. (2003). "The movement of the knee studied by magnetic resonance imaging." *Clin Orthop*(410): 35-43.
- Friederich, N. F., Müller, W. and O'Brien, W. R. (1992). "Klinische Anwendung biomechanischer und funktionell anatomischer Daten am Kniegelenk." *Orthopäde* **21**(1): 41-50.
- Fulkerson, J. P. (2002). "Diagnosis and treatment of patients with patellofemoral pain." *Am J Sports Med* **30**(3): 447-456.
- Gardiner, J. C., Weiss, J. A. and Rosenberg, T. D. (2001). "Strain in the human medial collateral ligament during valgus loading of the knee." *Clin Orthop Relat Res*(391): 266-274.
- Ghista, D. N., Toridis, T. G. and Srinivasan, T. M. (1976). "Human Gait Analysis: Determination of Instantaneous Joint Reaction Forces, Muscle Forces and the Stress Distribution in Bone Segments Part II." *Biomed Tech* **21**(3): 66-74.
- Gioe, T. J., Killeen, K. K., Grimm, K., Mehle, S. and Scheltzema, K. (2004). "Why are total knee replacements revised? analysis of early revision in a community knee implant registry." *Clin Orthop Relat Res*(428): 100-106.
- Giron, F., Cuomo, P., Aglietti, P., Bull, A. M. and Amis, A. A. (2005). "Femoral attachment of the anterior cruciate ligament." *Knee Surg Sports Traumatol Arthrosc* **10**: 10.
- Goudakos, I. G., Konig, C., Schottle, P. B., Taylor, W. R., Hoffmann, J. E., Popplau, B. M., Singh, N. B., Duda, G. N. and Heller, M. O. (2010). "Regulation of the patellofemoral contact area: An essential mechanism in patellofemoral joint mechanics?" *J Biomech* **43**(16): 3237-3239.
- Goudakos, I. G., Konig, C., Schottle, P. B., Taylor, W. R., Singh, N. B., Roberts, I., Streitparth, F., Duda, G. N. and Heller, M. O. (2009). "Stair climbing results in more challenging patellofemoral contact mechanics and kinematics than walking at early knee flexion under physiological-like quadriceps loading." *J Biomech* **42**(15): 2590-2596.
- Grana, W. A. and Kriegshauser, L. A. (1985). "Scientific basis of extensor mechanism disorders." *Clin Sports Med* **4**(2): 247-257.
- Gray, H. (1918). *Anatomy of the Human Body*. Philadelphia, Lea & Febiger.
- Grelsamer, R. P. (2000). "Patellar malalignment." *J Bone Joint Surg Am* **82-A**(11): 1639-1650.
- Grelsamer, R. P. (2002). "Patella baja after total knee arthroplasty: is it really patella baja?" *J Arthroplasty* **17**(1): 66-69.
- Grelsamer, R. P. and Weinstein, C. H. (2001). "Applied biomechanics of the patella." *Clin Orthop Relat Res*(389): 9-14.

- Hardeman, F., Vandenuecker, H., Van Lauwe, J. and Bellemans, J. (2006). "Cementless total knee arthroplasty with Profix: a 8- to 10-year follow-up study." *Knee* **13**(6): 419-421.
- Harfe, D. T., Chuinard, C. R., Espinoza, L. M., Thomas, K. A. and Solomonow, M. (1998). "Elongation patterns of the collateral ligaments of the human knee." *Clin Biomech (Bristol, Avon)* **13**(3): 163-175.
- Hasegawa, M., Sudo, A. and Uchida, A. (2009). "Staged bilateral mobile-bearing and fixed-bearing total knee arthroplasty in the same patients: a prospective comparison of a posterior-stabilized prosthesis." *Knee Surg Sports Traumatol Arthrosc* **17**(3): 237-243.
- Hawker, G., Wright, J., Coyte, P., Paul, J., Dittus, R., Croxford, R., Katz, B., Bombardier, C., Heck, D. and Freund, D. (1998). "Health-related quality of life after knee replacement." *J Bone Joint Surg Am* **80**(2): 163-173.
- HCUP-Databases (2007). Healthcare Cost and Utilization Project (HCUP). Rockville, MD, Agency for Healthcare Research and Quality, Rockville, MD.
- Heinlein, B., Graichen, F., Bender, A., Rohlmann, A. and Bergmann, G. (2007). "Design, calibration and pre-clinical testing of an instrumented tibial tray." *J Biomech* **40**(Suppl 1): 4-10.
- Heinlein, B., Kutzner, I., Graichen, F., Bender, A., Rohlmann, A., Halder, A. M., Beier, A. and Bergmann, G. (2009). "ESB Clinical Biomechanics Award 2008: Complete data of total knee replacement loading for level walking and stair climbing measured in vivo with a follow-up of 6-10 months." *Clin Biomech (Bristol, Avon)* **24**(4): 315-326.
- Heino Brechter, J. and Powers, C. M. (2002). "Patellofemoral stress during walking in persons with and without patellofemoral pain." *Med Sci Sports Exerc* **34**(10): 1582-1593.
- Heller, M. O., Bergmann, G., Deuretzbacher, G., Claes, L., Haas, N. P. and Duda, G. N. (2001a). "Influence of femoral anteversion on proximal femoral loading: measurement and simulation in four patients." *Clin Biomech (Bristol, Avon)* **16**(8): 644-649.
- Heller, M. O., Bergmann, G., Deuretzbacher, G., Durselen, L., Pohl, M., Claes, L., Haas, N. P. and Duda, G. N. (2001b). "Musculo-skeletal loading conditions at the hip during walking and stair climbing." *J Biomech* **34**(7): 883-893.
- Heller, M. O., Bergmann, G., Kassi, J. P., Claes, L., Haas, N. P. and Duda, G. N. (2005). "Determination of muscle loading at the hip joint for use in pre-clinical testing." *J Biomech* **38**(5): 1155-1163.
- Heller, M. O., Konig, C., Graichen, H., Hinterwimmer, S., Ehrig, R. M., Duda, G. N. and Taylor, W. R. (2007a). "A new model to predict in vivo human knee kinematics under physiological-like muscle activation." *J Biomech* **40** **Suppl 1**: S45-53.
- Heller, M. O., Matziolis, G., Konig, C., Taylor, W. R., Hinterwimmer, S., Graichen, H., Hege, H. C., Bergmann, G., Perka, C. and Duda, G. N. (2007b). "[Musculoskeletal biomechanics of the knee joint: Principles of preoperative planning for osteotomy and joint replacement.]." *Orthopade* **36**(7): 628-634.
- Heller, M. O., Taylor, W. R., Perka, C. and Duda, G. N. (2003). "The influence of alignment on the musculo-skeletal loading conditions at the knee." *Langenbecks Arch Surg* **388**(5): 291-297.
- Hofmann, S., Romero, J., Roth-Schiffel, E. and Albrecht, T. (2003). "[Rotational malalignment of the components may cause chronic pain or early failure in total knee arthroplasty]." *Orthopade* **32**(6): 469-476.
- Hollister, A. M., Jatana, S., Singh, A. K., Sullivan, W. W. and Lupichuk, A. G. (1993). "The axes of rotation of the knee." *Clin Orthop*(290): 259-268.
- Huberti, H. H. and Hayes, W. C. (1984). "Patellofemoral contact pressures. The influence of q-angle and tendofemoral contact." *J Bone Joint Surg Am* **66**(5): 715-724.
- Hungerford, D. S. and Barry, M. (1979). "Biomechanics of the patellofemoral joint." *Clin Orthop Relat Res* **144**: 9-15.

- Imran, A., Huss, R. A., Holstein, H. and O'Connor, J. J. (2000). "The variation in the orientations and moment arms of the knee extensor and flexor muscle tendons with increasing muscle force: a mathematical analysis." *Proc Inst Mech Eng [H]* **214**(3): 277-286.
- Insall, J. N., Binazzi, R., Soudry, M. and Mestriner, L. A. (1985). "Total knee arthroplasty." *Clin Orthop Relat Res*(192): 13-22.
- Insall, J. N., Scuderi, G. R., Komistek, R. D., Math, K., Dennis, D. A. and Anderson, D. T. (2002). "Correlation between condylar lift-off and femoral component alignment." *Clin Orthop Relat Res*(403): 143-152.
- Ishii, Y., Matsuda, Y., Sakata, S., Onda, N. and Omori, G. (2005). "Primary total knee arthroplasty using the Genesis I total knee prosthesis: a 5- to 10-year follow-up study." *Knee* **12**(5): 341-345.
- Jeffery, R. S., Morris, R. W. and Denham, R. A. (1991). "Coronal alignment after total knee replacement." *J Bone Joint Surg Br* **73**(5): 709-714.
- Jenny, J. Y. and Boeri, C. (2004). "Low reproducibility of the intra-operative measurement of the transepicondylar axis during total knee replacement." *Acta Orthop Scand* **75**(1): 74-77.
- Kansara, D. and Markel, D. C. (2006). "The effect of posterior tibial slope on range of motion after total knee arthroplasty." *J Arthroplasty* **21**(6): 809-813.
- Kassi, J. P., Heller, M. O., Stoeckle, U., Perka, C. and Duda, G. N. (2005). "Stair climbing is more critical than walking in pre-clinical assessment of primary stability in cementless THA in vitro." *J Biomech* **38**(5): 1143-1154.
- Katchburian, M. V., Bull, A. M., Shih, Y. F., Heatley, F. W. and Amis, A. A. (2003). "Measurement of patellar tracking: assessment and analysis of the literature." *Clin Orthop Relat Res* **412**: 241-259.
- Kaufer, H. (1971). "Mechanical function of the patella." *J Bone Joint Surg Am* **53**(8): 1551-1560.
- Kessler, O., Patil, S., Colwell, C. W., Jr. and D'Lima, D. D. (2008). "The effect of femoral component malrotation on patellar biomechanics." *J Biomech*.
- Kim, T. K., Chang, C. B., Kang, Y. G., Chung, B. J., Cho, H. J. and Seong, S. C. (2009). "Early clinical outcomes of floating platform mobile-bearing TKA: longitudinal comparison with fixed-bearing TKA." *Knee Surg Sports Traumatol Arthrosc*.
- Kim, Y. H., Kim, J. S. and Yoon, S. H. (2007). "Alignment and orientation of the components in total knee replacement with and without navigation support: a prospective, randomised study." *J Bone Joint Surg Br* **89**(4): 471-476.
- Koch, J. C. (1917). "The law of bone architecture." *Am J Anat* **21**: 177-298.
- Komistek, R. D., Dennis, D. A. and Mahfouz, M. (2003). "In vivo fluoroscopic analysis of the normal human knee." *Clin Orthop*(410): 69-81.
- König, C., Sharenkov, A., Matziolis, G., Taylor, W. R., Perka, C., Duda, G. N. and Heller, M. O. (2010). "Joint line elevation in revision TKA leads to increased patellofemoral contact forces." *J Orthop Res* **28**(1): 1-5.
- Krackow, K. A. and Mihalko, W. M. (1999). "The effect of medial release on flexion and extension gaps in cadaveric knees: implications for soft-tissue balancing in total knee arthroplasty." *Am J Knee Surg* **12**(4): 222-228.
- Kurtz, S., Ong, K., Lau, E., Mowat, F. and Halpern, M. (2007). "Projections of primary and revision hip and knee arthroplasty in the United States from 2005 to 2030." *J Bone Joint Surg Am* **89**(4): 780-785.
- Kutzner, I., Heinlein, B., Graichen, F., Bender, A., Rohlmann, A., Halder, A., Beier, A. and Bergmann, G. (2010). "Loading of the knee joint during activities of daily living measured in vivo in five subjects." *J Biomech* **43**(11): 2164-2173.
- Laskin, R. S. (1998). "Management of the patella during revision total knee replacement arthroplasty." *Orthop Clin North Am* **29**(2): 355-360.

- Laskin, R. S. (2002). "Joint line position restoration during revision total knee replacement." *Clin Orthop Relat Res*(404): 169-171.
- Lee, T. Q., Gerken, A. P., Glaser, F. E., Kim, W. C. and Anzel, S. H. (1997). "Patellofemoral joint kinematics and contact pressures in total knee arthroplasty." *Clin Orthop Relat Res* **340**: 257-266.
- Lewis, P., Rorabeck, C. H., Bourne, R. B. and Devane, P. (1994). "Posteromedial tibial polyethylene failure in total knee replacements." *Clin Orthop Relat Res*(299): 11-17.
- Li, G., DeFrate, L. E., Sun, H. and Gill, T. J. (2004). "In Vivo Elongation of the Anterior Cruciate Ligament and Posterior Cruciate Ligament During Knee Flexion." *Am J Sports Med* **32**(6): 1415-1420.
- Li, G., Rudy, T. W., Sakane, M., Kanamori, A., Ma, C. B. and Woo, S. L. (1999). "The importance of quadriceps and hamstring muscle loading on knee kinematics and in-situ forces in the ACL." *J Biomech* **32**(4): 395-400.
- Liau, J. J., Cheng, C. K., Huang, C. H. and Lo, W. H. (2002). "The effect of malalignment on stresses in polyethylene component of total knee prostheses--a finite element analysis." *Clin Biomech (Bristol, Avon)* **17**(2): 140-146.
- Lu, T. W. and O'Connor, J. J. (1996). "Fibre recruitment and shape changes of knee ligaments during motion: as revealed by a computer graphics-based model." *Proc Inst Mech Eng [H]* **210**(2): 71-79.
- Lutzner, J., Krummenauer, F., Wolf, C., Gunther, K. P. and Kirschner, S. (2008). "Computer-assisted and conventional total knee replacement: a comparative, prospective, randomised study with radiological and CT evaluation." *J Bone Joint Surg Br* **90**(8): 1039-1044.
- MacIntyre, N. J., Hill, N. A., Fellows, R. A., Ellis, R. E. and Wilson, D. R. (2006). "Patellofemoral joint kinematics in individuals with and without patellofemoral pain syndrome." *J Bone Joint Surg Am* **88**(12): 2596-2605.
- Mahoney, O. M. and Kinsey, T. L. (2006). "Modular femoral offset stems facilitate joint line restoration in revision knee arthroplasty." *Clin Orthop Relat Res* **446**: 93-98.
- Makris, C. A., Georgoulis, A. D., Papageorgiou, C. D., Moebius, U. G. and Soucacos, P. N. (2000). "Posterior cruciate ligament architecture: evaluation under microsurgical dissection." *Arthroscopy* **16**(6): 627-632.
- Mancuso, C. A., Ranawat, C. S., Esdaile, J. M., Johanson, N. A. and Charlson, M. E. (1996). "Indications for total hip and total knee arthroplasties. Results of orthopaedic surveys." *J Arthroplasty* **11**(1): 34-46.
- Mangaleshkar, S. R., Bajaj, S. K. and Thomas, A. P. (2002). "Denham total knee arthroplasty: a 10-year follow-up study." *J Arthroplasty* **17**(5): 550-555.
- Martin, J. W. and Whiteside, L. A. (1990). "The influence of joint line position on knee stability after condylar knee arthroplasty." *Clin Orthop Relat Res*(259): 146-156.
- Mason, J. J., Leszko, F., Johnson, T. and Komistek, R. D. (2008). "Patellofemoral joint forces." *J Biomech* **41**(11): 2337-2348.
- Mason, M., Belisle, A., Bonutti, P., Kolisek, F. R., Malkani, A. and Masini, M. (2006). "An accurate and reproducible method for locating the joint line during a revision total knee arthroplasty." *J Arthroplasty* **21**(8): 1147-1153.
- Matsumoto, H., Seedhom, B. B., Suda, Y., Otani, T. and Fujikawa, K. (2000). "Axis location of tibial rotation and its change with flexion angle." *Clin Orthop Relat Res*(371): 178-182.
- Matthews, L. S., Sonstegard, D. A. and Henke, J. A. (1977). "Load bearing characteristics of the patello-femoral joint." *Acta Orthop Scand* **48**(5): 511-516.
- Matziolis, G., Krockner, D., Tohtz, S., Weiss, U. and Perka, C. (2006). "[Accuracy of determination of the hip centre in navigated total knee arthroplasty]." *Z Orthop Ihre Grenzgeb* **144**(4): 362-366.

- Matziolis, G., Krockner, D., Weiss, U., Tohtz, S. and Perka, C. (2007). "A prospective, randomized study of computer-assisted and conventional total knee arthroplasty. Three-dimensional evaluation of implant alignment and rotation." *J Bone Joint Surg Am* **89**(2): 236-243.
- Mayman, D., Bourne, R. B., Rorabeck, C. H., Vaz, M. and Kramer, J. (2003). "Resurfacing versus not resurfacing the patella in total knee arthroplasty: 8- to 10-year results." *J Arthroplasty* **18**(5): 541-545.
- Menschik, A. (1974). "[Mechanics of the knee-joint. 1 (author's transl)]." *Z Orthop Ihre Grenzgeb* **112**(3): 481-495.
- Mesfar, W. and Shirazi-Adl, A. (2005). "Biomechanics of the knee joint in flexion under various quadriceps forces." *Knee* **12**(6): 424-434.
- Moewis, P. (2007). 3D Beschreibung der Muskeln zur Berechnung der muskuloskeletalen Belastungen in den unteren Extremitäten, Diplomarbeit. *Fachgebiet Biomedizinische Technik*. Berlin, TU - Berlin.
- Morlock, M., Schneider, E., Bluhm, A., Vollmer, M., Bergmann, G., Muller, V. and Honl, M. (2001). "Duration and frequency of every day activities in total hip patients." *J Biomech* **34**(7): 873-881.
- Muller, M. (1993). "The relationship between the rotation possibilities between femur and tibia and the lengths of the cruciate ligaments." *J Theor Biol* **161**(2): 199-220.
- Nagamine, R., Otani, T., White, S. E., McCarthy, D. S. and Whiteside, L. A. (1995a). "Patellar tracking measurement in the normal knee." *J Orthop Res* **13**(1): 115-122.
- Nagamine, R., White, S. E., McCarthy, D. S. and Whiteside, L. A. (1995b). "Effect of rotational malposition of the femoral component on knee stability kinematics after total knee arthroplasty." *J Arthroplasty* **10**(3): 265-270.
- Nakagawa, S., Johal, P., Pinskerova, V., Komatsu, T., Sosna, A., Williams, A. and Freeman, M. A. (2004). "The posterior cruciate ligament during flexion of the normal knee." *J Bone Joint Surg Br* **86**(3): 450-456.
- Nietert, M. (1977). "[The human knee-joint as a biomechanical problem (author's transl)]." *Biomed Tech (Berl)* **22**(1-2): 13-21.
- Nilsson, K. G., Karrholm, J. and Ekelund, L. (1990). "Knee motion in total knee arthroplasty. A roentgen stereophotogrammetric analysis of the kinematics of the Tricon-M knee prosthesis." *Clin Orthop Relat Res*(256): 147-161.
- Noble, P. C., Conditt, M. A., Cook, K. F. and Mathis, K. B. (2006). "The John Insall Award: Patient expectations affect satisfaction with total knee arthroplasty." *Clin Orthop Relat Res* **452**: 35-43.
- O'Connor, J. J., Shercliff, T. L., Biden, E. and Goodfellow, J. W. (1989). "The geometry of the knee in the sagittal plane." *Proc Inst Mech Eng [H]* **203**(4): 223-233.
- Ostermeier, S., Holst, M., Hurschler, C., Windhagen, H. and Stukenborg-Colsman, C. (2007). "Dynamic measurement of patellofemoral kinematics and contact pressure after lateral retinacular release: an in vitro study." *Knee Surg Sports Traumatol Arthrosc* **15**(5): 547-554.
- Otake, N., Chen, H., Yao, X. and Shoumura, S. (2007). "Morphologic study of the lateral and medial collateral ligaments of the human knee." *Okajimas Folia Anat Jpn* **83**(4): 115-122.
- P. Johal, A. Williams, P. Wragg, D. Hunt and Gedroyc, W. (2005). "Tibio-femoral movement in the living knee. A study of weight bearing and non-weight bearing knee kinematics using 'interventional' MRI." *Journal of Biomechanics* **38**: 269-276.
- Pape, D. and Kohn, D. (2007). "[Soft tissue balancing in valgus gonarthrosis]." *Orthopade* **36**(7): 657-658, 660-656.
- Park, S. E., DeFrate, L. E., Suggs, J. F., Gill, T. J., Rubash, H. E. and Li, G. (2005). "The change in length of the medial and lateral collateral ligaments during in vivo knee flexion." *Knee* **12**(5): 377-382.

- Parratte, S. and Pagnano, M. W. (2008). "Instability after total knee arthroplasty." *J Bone Joint Surg Am* **90**(1): 184-194.
- Partington, P. F., Sawhney, J., Rorabeck, C. H., Barrack, R. L. and Moore, J. (1999). "Joint line restoration after revision total knee arthroplasty." *Clin Orthop Relat Res*(367): 165-171.
- Patel, V. V., Hall, K., Ries, M., Lindsey, C., Ozhinsky, E., Lu, Y. and Majumdar, S. (2003). "Magnetic resonance imaging of patellofemoral kinematics with weight-bearing." *J Bone Joint Surg Am* **85-A**(12): 2419-2424.
- Patel, V. V., Hall, K., Ries, M., Lotz, J., Ozhinsky, E., Lindsey, C., Lu, Y. and Majumdar, S. (2004). "A three-dimensional MRI analysis of knee kinematics." *J Orthop Res* **22**(2): 283-292.
- Pauwels, F. (1951). "Über die Bedeutung der Bauprinzipien des Stütz- und Bewegungsapparates für die Beanspruchung des Röhrenknochens." *Acta Anat* **12**: 207-227.
- Pauwels, F. (1973). *Atlas zur Biomechanik der gesunden und kranken Hüfte*, Springer Verlag, Berlin.
- Peters, C. L. (2006). "Soft-tissue balancing in primary total knee arthroplasty." *Instr Course Lect* **55**: 413-417.
- Pierrynowski, M. R. (1982). *A physiological model for the solution of individual muscle forces during normal human walking*, Ph.D. thesis. Vancouver, Simon Fraser University.
- Pietsch, M. and Hofmann, S. (2007). "[From tibiofemoral instability to dislocation in total knee arthroplasty]." *Orthopade* **36**(10): 917-922, 924-917.
- Porteous, A. J., Hassaballa, M. A. and Newman, J. H. (2008). "Does the joint line matter in revision total knee replacement?" *J Bone Joint Surg Br* **90**(7): 879-884.
- Powers, C. M. (2000). "Patellar kinematics, part II: the influence of the depth of the trochlear groove in subjects with and without patellofemoral pain." *Phys Ther* **80**(10): 965-978.
- Powers, C. M., Lilley, J. C. and Lee, T. Q. (1998). "The effects of axial and multi-plane loading of the extensor mechanism on the patellofemoral joint." *Clin Biomech* **13**(8): 616-624.
- Putz, R., Muhlhofer, H. and Ercan, Y. (2007). "[Ligaments of the knee]." *Orthopade* **36**(7): 612, 614-619.
- Quapp, K. M. and Weiss, J. A. (1998). "Material characterization of human medial collateral ligament." *J Biomech Eng* **120**(6): 757-763.
- Quinet, R. J. and Winters, E. G. (1992). "Total joint replacement of the hip and knee." *Med Clin North Am* **76**(5): 1235-1251.
- Ramappa, A. J., Apreleva, M., Harrold, F. R., Fitzgibbons, P. G., Wilson, D. R. and Gill, T. J. (2006). "The effects of medialization and anteromedialization of the tibial tubercle on patellofemoral mechanics and kinematics." *Am J Sports Med* **34**(5): 749-756.
- Reinschmidt, C., van den Bogert, A. J., Nigg, B. M., Lundberg, A. and Murphy, N. (1997). "Effect of skin movement on the analysis of skeletal knee joint motion during running." *J Biomech* **30**(7): 729-732.
- Ritter, M. A., Montgomery, T. J., Zhou, H., Keating, M. E., Faris, P. M. and Meding, J. B. (1999). "The clinical significance of proximal tibial resection level in total knee arthroplasty." *Clin Orthop Relat Res*(360): 174-181.
- Robertsson, O. (2009). Swedish Knee Arthroplasty Register - Annual Report. Lund, Dept. of Orthopedics, Lund University Hospital.
- Robinson, J. R., Bull, A. M. and Amis, A. A. (2004a). "Structural properties of the medial collateral ligament complex of the human knee." *Journal of Biomechanics*.
- Robinson, J. R., Sanchez-Ballester, J., Bull, A. M., Thomas Rde, W. and Amis, A. A. (2004b). "The posteromedial corner revisited. An anatomical description of the passive restraining structures of the medial aspect of the human knee." *J Bone Joint Surg Br* **86**(5): 674-681.

- Rohen, J. W., Yokochi, C. and Lütjen-Drecoll, E. (2002). *Anatomie des Menschen*. Stuttgart-New York, Schattauer GmbH.
- Romero, J., Stahelin, T., Wyss, T. and Hofmann, S. (2003). "[Significance of axial rotation alignment of components of knee prostheses]." *Orthopade* **32**(6): 461-468.
- Rousseau, M. A., Lazennec, J. Y. and Catonne, Y. (2008). "Early mechanical failure in total knee arthroplasty." *Int Orthop* **32**(1): 53-56.
- Rouvillain, J. L., Pascal-Mousselard, H., Favuto, M., Kanor, M., Garron, E. and Catonne, Y. (2008). "The level of the joint line after cruciate-retaining total knee replacement: A new coordinate system." *Knee* **15**(1): 31-35.
- Rydell, N. W. (1966). "Forces acting in the femoral head-prosthesis." *Acta Orthop Scand* **37**, **Suppl 88**: 1-132.
- Sakai, N., Luo, Z.-P., Rand, J. A. and An, K. N. (1996). "Quadriceps forces and patellar motion in the anatomical model of the patellofemoral joint." *Knee* **3**(1): 1-7.
- Sakai, N., Luo, Z. P., Rand, J. A. and An, K. N. (2000). "The influence of weakness in the vastus medialis oblique muscle on the patellofemoral joint: an in vitro biomechanical study." *Clin Biomech* **15**(5): 335-339.
- Sakane, M., Livesay, G. A., Fox, R. J., Rudy, T. W., Runco, T. J. and Woo, S. L. (1999). "Relative contribution of the ACL, MCL, and bony contact to the anterior stability of the knee." *Knee Surg Sports Traumatol Arthrosc* **7**(2): 93-97.
- Salsich, G. B., Ward, S. R., Terk, M. R. and Powers, C. M. (2003). "In vivo assessment of patellofemoral joint contact area in individuals who are pain free." *Clin Orthop Relat Res* **417**: 277-284.
- Scheys, L., Jonkers, I., Loeckx, D., Maes, F., Spaepen, A. and Suetens, P. (2006). *Image Based Musculoskeletal Modeling Allows Personalized Biomechanical Analysis of Gait*. Berlin Heidelberg, Springer-Verlag.
- Schöttle, P., Goudakos, I., Rosenstiel, N., Hoffmann, J. E., Taylor, W. R., Duda, G. N. and Heller, M. O. (2009). "A comparison of techniques for fixation of the quadriceps muscle-tendon complex for in vitro biomechanical testing of the knee joint in sheep." *Med Eng Phys* **31**(1): 69-75.
- Scuderi, G. R. and Insall, J. N. (1992). "Total knee arthroplasty. Current clinical perspectives." *Clin Orthop Relat Res*(276): 26-32.
- Seebacher, J. R., Inglis, A. E., Marshall, J. L. and Warren, R. F. (1982). "The structure of the posterolateral aspect of the knee." *J Bone Joint Surg Am* **64**(4): 536-541.
- Seireg, A. and Arvikar, R. J. (1973). "A mathematical model for evaluation of forces in lower extremities of the musculo-skeletal system." *J Biomech* **6**(3): 313-326.
- Selvarajah, E. and Hooper, G. (2009). "Restoration of the Joint Line in Total Knee Arthroplasty." *J Arthroplasty* **24**(7): 1099-1102.
- Servant, C. T., Ramos, J. P. and Thomas, N. P. (2004). "The accuracy of magnetic resonance imaging in diagnosing chronic posterior cruciate ligament injury." *Knee* **11**(4): 265-270.
- Sharkey, P. F., Hozack, W. J., Rothman, R. H., Shastri, S. and Jacoby, S. M. (2002). "Insall Award paper. Why are total knee arthroplasties failing today?" *Clin Orthop Relat Res*(404): 7-13.
- Shaw, J. A. and Murray, D. G. (1974). "The longitudinal axis of the knee and the role of the cruciate ligaments in controlling transverse rotation." *J Bone Joint Surg Am* **56**(8): 1603-1609.
- Shelbourne, K. D., Patel, D. V. and Martini, D. J. (1996). "Classification and management of arthrofibrosis of the knee after anterior cruciate ligament reconstruction." *Am J Sports Med* **24**(6): 857-862.
- Skutek, M., van Griensven, M., Zeichen, J., Brauer, N. and Bosch, U. (2001). "Cyclic mechanical stretching enhances secretion of Interleukin 6 in human tendon fibroblasts." *Knee Surg Sports Traumatol Arthrosc* **9**(5): 322-326.

- Smith, P. N., Refshauge, K. M. and Scarvell, J. M. (2003). "Development of the concepts of knee kinematics." *Arch Phys Med Rehabil* **84**(12): 1895-1902.
- Spencer, J. M., Chauhan, S. K., Sloan, K., Taylor, A. and Beaver, R. J. (2007). "Computer navigation versus conventional total knee replacement: no difference in functional results at two years." *J Bone Joint Surg Br* **89**(4): 477-480.
- Spitzer, V., Ackerman, M. J., Scherzinger, A. L. and Whitlock, D. (1996). "The visible human male: a technical report." *J Am Med Inform Assoc* **3**(2): 118-130.
- Stagni, R., Fantozzi, S., Cappello, A. and Leardini, A. (2005). "Quantification of soft tissue artefact in motion analysis by combining 3D fluoroscopy and stereophotogrammetry: a study on two subjects." *Clin Biomech (Bristol, Avon)* **20**(3): 320-329.
- Strasser, H. (1917). *Lehrbuch der Muskel und Gelenkmechanik. Teil Untere Extremität*. Berlin, Springer Verlag. **3**: 335-338.
- Sutherland, D. H. (2001). "The evolution of clinical gait analysis part I: kinesiological EMG." *Gait Posture* **14**(1): 61-70.
- Takahashi, T., Wada, Y. and Yamamoto, H. (1997). "Soft-tissue balancing with pressure distribution during total knee arthroplasty." *J Bone Joint Surg Br* **79**(2): 235-239.
- Taylor, W. R., Ehrig, R. M., Duda, G. N., Schell, H., Seebeck, P. and Heller, M. O. (2005). "On the influence of soft tissue coverage in the determination of bone kinematics using skin markers." *J Orthop Res* **23**(4): 726-734.
- Taylor, W. R., Ehrig, R. M., Heller, M. O., Schell, H., Seebeck, P. and Duda, G. N. (2006). "Tibio-femoral joint contact forces in sheep." *J Biomech* **39**(5): 791-798.
- Taylor, W. R., Heller, M. O., Bergmann, G. and Duda, G. N. (2004). "Tibio-femoral loading during human gait and stair climbing." *J Orthop Res* **22**(3): 625-632.
- Thunnissen, J. G. M., Grootenboer, H. J., de Jongh, H. J. and Koopman, H. F. J. M. (1992). "Three-Dimensional Muscle Force Prediction During Gait." *VIII ESB*: 262.
- Toutoungi, D. E., Zavatsky, A. B. and O'Connor, J. J. (1997). "Parameter sensitivity of a mathematical model of the anterior cruciate ligament." *Proc Inst Mech Eng [H]* **211**(3): 235-246.
- Valstar, E. R., de Jong, F. W., Vrooman, H. A., Rozing, P. M. and Reiber, J. H. (2001). "Model-based Roentgen stereophotogrammetry of orthopaedic implants." *J Biomech* **34**(6): 715-722.
- Van de Velde, S. K., DeFrate, L. E., Gill, T. J., Moses, J. M., Papannagari, R. and Li, G. (2007). "The effect of anterior cruciate ligament deficiency on the in vivo elongation of the medial and lateral collateral ligaments." *Am J Sports Med* **35**(2): 294-300.
- van Kampen, A. and Huijskes, R. (1990). "The three-dimensional tracking pattern of the human patella." *J Orthop Res* **8**(3): 372-382.
- von Eisenhart-Rothe, R., Siebert, M., Bringmann, C., Vogl, T., Englmeier, K. H. and Graichen, H. (2004). "A new in vivo technique for determination of 3D kinematics and contact areas of the patello-femoral and tibio-femoral joint." *J Biomech* **37**(6): 927-934.
- von Eisenhart-Rothe, R., Vogl, T., Englmeier, K. H. and Dennis, D. A. (2007). "[TKA kinematics: In vivo techniques and results.]" *Orthopade* **36**(7): 620-627.
- Wallace, A. L., Harris, M. L., Walsh, W. R. and Bruce, W. J. (1998). "Intraoperative assessment of tibiofemoral contact stresses in total knee arthroplasty." *J Arthroplasty* **13**(8): 923-927.
- Wang, C. J. and Wang, H. E. (2000). "Early catastrophic failure of rotating hinge total knee prosthesis." *J Arthroplasty* **15**(3): 387-391.
- Wasielowski, R. C., Galante, J. O., Leighty, R. M., Natarajan, R. N. and Rosenberg, A. G. (1994). "Wear patterns on retrieved polyethylene tibial inserts and their relationship to technical considerations during total knee arthroplasty." *Clin Orthop Relat Res*(299): 31-43.

- Wasielowski, R. C., Galat, D. D. and Komistek, R. D. (2005). "Correlation of compartment pressure data from an intraoperative sensing device with postoperative fluoroscopic kinematic results in TKA patients." *J Biomech* **38**(2): 333-339.
- Weber, W. and Weber, E. (1836). *Mechanik der menschlichen Gehwerkzeuge*. Göttingen, Dieterichsche Buchhandlung.
- Whiteside, L. A. (2002). "Soft tissue balancing: the knee." *J Arthroplasty* **17**(4 Suppl 1): 23-27.
- Wilkins, K. J., Duong, L. V., McGarry, M. H., Kim, W. C. and Lee, T. Q. (2007). "Biomechanical effects of kneeling after total knee arthroplasty." *J Bone Joint Surg Am* **89**(12): 2745-2751.
- Wilson, D. R., Apreleva, M. V., Eichler, M. J. and Harrold, F. R. (2003). "Accuracy and repeatability of a pressure measurement system in the patellofemoral joint." *J Biomech* **36**(12): 1909-1915.
- Winter, D. A. (1991). *The biomechanics and motor control of human gait: Normal, elderly and pathological*, Univ. of Waterloo Press, Waterloo, Ontario, Canada.
- Wolff, J. (1892). *Das Gesetz der Transformation der Knochen*, A. Hirschwald, Berlin.
- Wu, G., Siegler, S., Allard, P., Kirtley, C., Leardini, A., Rosenbaum, D., Whittle, M., D'Lima, D. D., Cristofolini, L., Witte, H., Schmid, O. and Stokes, I. (2002). "ISB recommendation on definitions of joint coordinate system of various joints for the reporting of human joint motion--part I: ankle, hip, and spine. International Society of Biomechanics." *J Biomech* **35**(4): 543-548.
- Wu, J. Z., Herzog, W. and Epstein, M. (2000). "Joint contact mechanics in the early stages of osteoarthritis." *Med Eng Phys* **22**(1): 1-12.
- Wyss, T. F., Schuster, A. J., Munger, P., Pfluger, D. and Wehrli, U. (2006). "Does total knee joint replacement with the soft tissue balancing surgical technique maintain the natural joint line?" *Arch Orthop Trauma Surg* **126**(7): 480-486.
- Yau, W. P., Leung, A., Chiu, K. Y., Tang, W. M. and Ng, T. P. (2005). "Intraobserver errors in obtaining visually selected anatomic landmarks during registration process in nonimage-based navigation-assisted total knee arthroplasty: a cadaveric experiment." *J Arthroplasty* **20**(5): 591-601.
- Yercan, H. S., Ait Si Selmi, T., Sugun, T. S. and Neyret, P. (2005). "Tibiofemoral instability in primary total knee replacement: a review, Part 1: Basic principles and classification." *Knee* **12**(4): 257-266.
- Yoshino, N., Takai, S., Ohtsuki, Y. and Hirasawa, Y. (2001). "Computed tomography measurement of the surgical and clinical transepicondylar axis of the distal femur in osteoarthritic knees." *J Arthroplasty* **16**(4): 493-497.
- Zavatsky, A. B. and O'Connor, J. J. (1994). "Three-dimensional geometrical models of human knee ligaments." *Proc Inst Mech Eng [H]*(208): 229-240.
- Zavatsky, A. B., Oppold, P. T. and Price, A. J. (2004). "Simultaneous in vitro measurement of patellofemoral kinematics and forces." *J Biomech Eng* **126**(3): 351-356.
- Zhao, D., Banks, S. A., D'Lima, D. D., Colwell, C. W., Jr. and Fregly, B. J. (2007). "In vivo medial and lateral tibial loads during dynamic and high flexion activities." *J Orthop Res* **25**(5): 593-602.
- Zihlmann, M. S., Gerber, H., Stacoff, A., Burckhardt, K., Szekely, G. and Stussi, E. (2006). "Three-dimensional kinematics and kinetics of total knee arthroplasty during level walking using single plane video-fluoroscopy and force plates: A pilot study." *Gait Posture* **24**(4): 475-481.
- Zihlmann, M. S., Stacoff, A., Romero, J., Quervain, I. K. and Stussi, E. (2005). "Biomechanical background and clinical observations of rotational malalignment in TKA: literature review and consequences." *Clin Biomech (Bristol, Avon)* **20**(7): 661-668.

8 INDEX OF TABLES AND FIGURES

8.1 Index of Figures

Figure 1: Sketches of first ivory implants to replace the knee joint. Themistocles Gluck (1853 – 1942) was a pioneer of modern total knee replacement (image source: (Eynon-Lewis et al. 1992) & Wikipedia).

Figure 2: Posterior view of the knee showing the bony structures, the ligaments, menisci and the cartilages (Gray 1918).

Figure 3: The muscles of the knee from an anterior (left) and a posterior view (right) (Gray 1918).

Figure 4: Schematic representation of knee kinematics as a four-bar linkage system, displaying the posterior displacement of tibiofemoral contact (Dye 1987).

Figure 5: Anteromedial aspect of the knee with the patella, the patellar ligament and the tendon of the quadriceps muscle (Gray 1918).

Figure 6: Implants can offer different degrees of mechanical stabilization: non-constrained (left, Aesculap Columbus), posterior stabilized (middle, Smith&Nephew JOURNEY™ BCS) and constrained or hinged (right, Aesculap Blauth Total Hinge Knee).

Figure 7: anterior, lateral and posterior views (from left) of the musculoskeletal model developed by Heller and co-workers (Heller et al. 2001b).

Figure 8: Cross sectional colour image of the knee region taken from the Visible Human Project (Spitzer et al. 1996) (top). Coronal reconstruction of the whole colour image data set (right)

Figure 9: The soft tissue structures were segmented in the green channel, which was displayed as greyscale image, using a segmentation editor. The specific structures were marked and assigned to a material ID (left). Three-dimensional surface models were then reconstructed from this data (top).

Figure 10: Process of combining the bony structures used by Heller and co-workers in their musculoskeletal model (Heller et al. 2001b) with a 3D representation using the high-resolution colour images of the Visible Human dataset (Spitzer et al. 1996).

Figure 11: Three-dimensional representation of the muscles (including their tendons) that determine motion and stability in the knee joint (Moewis 2007). Muscles that are labelled in the anterior view (left image) are involved in joint extension, while muscles labelled in the posterior view (right image) mainly contribute to joint flexion.

Figure 12: The main passive joint stabilizers: collateral and cruciate ligaments, both menisci, as well as femur and tibia (König 2004). Not displayed are the tibial and femoral articular cartilage and the capsule.

Figure 13: Hausdorff Distance between the surface of the muscle and the surface of the bone projected as colour map onto the bone. The colour indicates the distance ranging from 0 mm (blue) to 2 mm and more (red).

Figure 14: Example of a larger muscle with changing direction (Gluteus Maximus) in which the planes for the surface intersection were defined orthogonal to the direction of the muscle fibres.

Figure 15: Musculoskeletal structures of the lower limb visualized as 3D surface models (left) and the muscular structures visualized as centroid lines (right).

Figure 16: The lever arm length of the Biceps Femoris in the axial plane for the straight line (left bar) and the centroid line (right bar) muscle representation.

Figure 17: Change in muscle lever arms in the axial plane of the knee. The change (%) in the lever arm derived from the centroid line is displayed relative to the straight line model.

Figure 18: Reconstructed bone surfaces and cruciate ligaments from MRI images at 0°, 30° and 90° knee flexion. Top: The movement of the femur relative to the tibia was analysed by registering the surface models of the tibiae at 30° and 90° knee flexion onto the tibia at 0° flexion. Bottom: Sagittal view of the tibia and the PCL as reconstructed from the MRI data. A shift from a lax concave shape at 0° to a taut ligament at 30° and 90° can be seen, posing the question as to whether a linear four-bar linkage model is capable of simulating the kinematics of the knee.

Figure 19: Definition of the femoral coordinate system. Left: A cylinder fitting technique was used to define the TE-axis. Right: A third proximal point was placed at the centre of the contour that was created by cutting the femoral surface orthogonal to the TE-axis through its centre.

Figure 20: Surface models of the cruciate ligaments were used to create proximity maps on the bony surface. Left: Elliptical attachment regions were defined by 37 landmarks, here demonstrated for the PCL's AM bundle. Right: Attachment regions (landmarks) for the ACL and PCL, shown as transparent structures, as reconstructed in one subject.

Figure 21: The four-bar linkage model (solid bars) for describing the movement of the femur relative to the tibia. Here, the reconstructed surface of the tibia is overlaid on the in vivo MR images at 0°, 30° and 90° flexion angle.

Figure 22: Effect of the considering internal / external rotation in the four-bar linkage model on the deviation between the predicted and the in vivo pose of the femur at 30° & 90° during passive (top) and active (bottom) knee flexion. The box plots show the median (bold line), the 25% quartiles (box dimensions) and the extreme (vertical lines) deviations of the predicted positions against the in vivo measured positions of the medial (grey) and the lateral (white) femoral reference TE-axis points.

Figure 23: Extension characteristics of the AM and PL bundles of the ACL (top) and AL and PM bundles of the PCL (bottom) under loaded (solid lines) and unloaded (broken lines) conditions throughout a full flexion cycle, as determined by the kinematic model. Standard deviations are indicated for the unloaded conditions.

Figure 24: Experimental set-up: a) at 12°, b) at 30° knee flexion in a CAD environment, and c) the cadaver knee with attached optical markers, pressure sensor and muscle loading devices.

Figure 25: Comparison of patellofemoral mean and peak pressures, contact area, joint force, medial-lateral position of the centre of force on the trochlea (CoF), patellar shift and tilt between a walking and a stair climbing load case at 12° knee flexion. Representative data of pressure distribution, contact area and medial-lateral CoF on the trochlea are presented graphically for each load case.

Figure 26: Comparison of patellofemoral mean and peak pressures, contact area, joint force, medial-lateral position of the centre of force on the trochlea (CoF), patellar shift and tilt between a walking and a stair climbing load case at 30° knee flexion. Representative data of pressure distribution, contact area and medial-lateral position CoF on the trochlea are presented graphically for each load case.

Figure 27: Collateral ligament function was derived using 3D models of the ligaments reconstructed from the Visible Human dataset (upper left). Landmarks were placed to define the proximal (blue) and distal (yellow) insertion sites of the lateral (upper middle) and the medial (upper right) collateral ligaments. Joint kinematics were obtained from MRI images at 0°, 30° and 90° knee flexion (bottom)

Figure 28: Average change in the distance between the ligament attachment sites (DA in %) of the LCL (black) and the MCL (green) relative to the straight-legged (0°) datum. Circles indicate the anterior portions of the ligament, triangles the posterior portions. Dashed lines represent the passive and solid the active knee flexion.

Figure 29: CAD model of the assembled ultra-congruent implant used in the study consisting of the femoral component, the tibial insert and the tibial component (Aesculap Columbus UC)

Figure 30: Virtual TKA surgery using 3D surface models of the tibia and the femur, as well as CAD models of the tibial and femoral components.

Figure 31: Cross-sectional view of a femoral component (Columbus UC, Aesculap AG, Tuttlingen, Germany). Centres of circles that were fitted to the articulating surfaces on the medial and lateral condyle defined the flexion axes of the femoral component.

Figure 32: The joint line level was simulated between a 5 mm distalization (left), the anatomical reconstruction (centre) and up to 15 mm elevation (right).

Figure 33: Joint contact forces after total knee arthroplasty were calculated using a validated musculoskeletal model for instances of stair climbing (displayed) and normal walking.

Figure 34: Exemplary patellofemoral joint contact force pattern during a cycle of normal walking, calculated for one patient (thick solid line). The contact forces were

recalculated after simulating joint line elevations of 10 and 15 mm (dashed lines) and a joint line distalization of 5 mm (thin solid line).

Figure 35: The average changes and the respective standard deviations in the patellofemoral and tibiofemoral contact forces of four subjects, caused by a distalization (green bars) or elevation (yellow and red bars) of the joint line, shown in multiples of body weight (BW) relative to the contact forces in the situation of an anatomically reconstructed joint line.

Figure 36: The medial and lateral collateral ligaments (here displayed together with the cruciate ligaments) were modelled using high-resolution cross-sectional images of the Visible Human dataset.

Figure 37: The medial and lateral collateral ligaments were each modelled as five portions to better characterize their functional behaviour throughout flexion. To this end, the femoral origin and tibial attachment sites of the medial (left) and the lateral (right) collateral ligaments were marked with landmarks. For the MCL, static wrapping points were introduced at the proximal tibia. The current study focussed on the analyses of the most anterior and posterior ligament regions (thick lines).

Figure 38: Length change patterns of the anterior (left) and posterior (right) regions of the medial (top) and lateral (bottom) collateral ligaments, as observed from extension to 90° of knee flexion. The dashed curve represents the anatomical reconstruction of the joint line, while the yellow and the red curve represent joint line elevations of 5 and 10 mm respectively.

Figure 39: Length change patterns of the collateral ligaments for the conditions of joint line elevation and no downsizing of the femoral component. The graphs show the length change patterns for the anterior (left) and posterior (right) regions of the medial (top) and lateral (bottom) collateral ligaments, as observed from extension to 90° flexion. The dashed curve represents the anatomical reconstruction of the joint line, while the solid curve represents a joint line elevation of 5 mm. The horizontal dotted line represents an average value for the maximum tensile strain of the collateral ligaments as reported in the literature.

Figure 40: Post-operative radiological assessment of femoral component placement showing an internal rotation of 6° relative to the transepicondylar axis (green

line). Internal rotations of more than 3° may lead to complications (Barrack et al. 2001; Berger et al. 1998; Hofmann et al. 2003).

Figure 41: Failed tibial polyethylene insert showing signs of intense mechanical destruction, indicative of an overloading condition in the knee.

Figure 42a: The variation of femoral component placement was simulated six degrees of freedom (DOF): 3 translational DOFs (green) and 3 rotational DOFs (blue).

Figure 42b: Exemplary visualization of a simulated femoral component malalignment. The rotation in the axial plane was varied between 5° external rotation (left), the anatomical reconstruction (centre) and up to 10° internal rotation (right).

Figure 43: The relative influence of individual malalignment parameters on patellofemoral contact forces (top). Histograms show the share of the specific levels of the individual malalignments in the total number of cases in which the contact forces increased 10% or more. Values are given for normal walking (left) and stair climbing (right).

Figure 44: The relative influence of individual malalignment parameters on tibiofemoral contact forces (top). Histograms show the share of the specific levels of the individual malalignments in the total number of cases in which the contact forces increased 10% or more. Values are given for normal walking (left) and stair climbing (right).

8.2 Index of Tables

Table 1: Deviation of the predicted and in vivo locations of the femoral reference points in the axial plane and in the coronal plane at both 30° and 90° . The deviation is shown for the model using the average i/e rotation of all subjects as an input. The deviations for passive and active knee motion are shown.

Table 2: Load profiles for each load case

Table 3: Results of patellofemoral contact mechanics and kinematics analysis: Median (Range)

Table 4: Simulated femoral component malalignment ranges and increments.

CURRICULUM VITAE

Christian König

Born in Berlin on June 17th, 1975

Education

- 1990 – 1996 *Abitur*, Alexander v. Humboldt Gymnasium, Berlin
- 1993 – 1994 *Diploma*, Park Center High School, Minneapolis, USA
- 1996 – 1997 *Civil Service*, Evangelische Kirchengemeinde Berlin-Köpenick, Berlin
- 1997 – 1999 *Physics*,
Brandenburgische Technische Universität Cottbus
- 1999 - 2000 *Vordiplom Mechanical Engineering*,
Brandenburgische Technische Universität Cottbus
- 2000 – 2004 *Diplom Mechanical Engineering / Biomedical Engineering*,
Technische Universität Berlin

Professional Experience

- 2004 – 2005 *Research Assistant*, Orthopaedic Research Laboratory,
Prince of Wales Hospital, Sydney, Australia
- 2005 – 2010 *Research Engineer*, Julius Wolff Institut / Centre for Musculoskeletal
Surgery, Charité Universitätsmedizin Berlin

Awards

- 2009 *3rd DGfB Young Investigator Award*, German Society for Biomechanics
- 2008 *3rd GOTS Young Investigator Award*,
Gesellschaft für Orthopädisch-Traumatologische Sportmedizin

Book Chapters

2011

GN Duda, MO Heller, T Pfitzner, WR Taylor, C König, G Bergmann, *Biomechanik des Kniegelenks* in: *AE-Manual der Endoprothetik, Knie*, DC Wirtz, Berlin, Springer, 2011, 1: 19-31

Publications

2011

C König, G Matziolis, A Sharenkov, C Perka, GN Duda, MO Heller, *Collateral ligament length change patterns after joint line elevation may not explain midflexion instability following TKA*, J Med Eng Phys, 2011, 33(10):1303-8.

GI Wassilew, MO Heller, O Hasart, C Perka, I Südhoff, V Janz, GN Duda, C König; *Ultrasound-based computer navigation of the acetabular component: a feasibility study.*, Arch Orthop Trauma Surg, 2011, (Epub ahead of print)

WR Taylor, BM Poeplau, C König, RM Ehrig, S Zachow, GN Duda, MO Heller, *The medial-lateral force distribution in the ovine stifle joint during walking* J Orthop Res, 2011, 29 (4):567-71

S Herrmann, C Koenig, M Heller, C Perka, S Greiner, *Reverse shoulder arthroplasty leads to significant biomechanical changes in the remaining rotator cuff*, J Orthop Surg Res, 2011, 16(6):42

GI Wassilew, C Perka, V Janz, C König, P Asbach, O Hasart, *Use of an Ultrasound-Based Navigation System for an Accurate Acetabular Positioning in Total Hip Arthroplasty A Prospective, Randomized, Controlled Study.* J Arthroplasty. 2011 (Epub ahead of print)

2010

C König, A Sharenkov, G Matziolis, WR Taylor, C Perka, GN Duda, MO Heller, *Joint line elevation in revision TKA leads to increased patellofemoral contact forces*, J Orthop Res, 2010, 28 (1):1-5

GI Wassilew, C Perka, V Janz, C König, P Asbach, O Hasart, *3D CT analysis of combined cup and stem anteversion in cases of cup navigation in hip arthroplasty*, Orthopedics, 2010, 33(10 Suppl):48-51

O Hasart, C Perka, C König, P Asbach, W Janz, G Wassilew, *Influence of body mass index and thickness of soft tissue on accuracy of ultrasound and pointer based registration in navigation of cup in hip arthroplasty.* Technol Health Care, 2010, 18(4-5):341-51.

IG Goudakos, C König, PB Schöttle, WR Taylor, JE Hoffmann, BM Pöpplau, NB Singh, GN Duda, MO Heller, *Regulation of the patellofemoral contact area: an essential mechanism in physiological patellofemoral joint mechanics?* J Biomech, 2010, 43(16):3237-9

2009

IG Goudakos, C König, PB Schöttle, WR Taylor, NB Singh, I Roberts, F Streitparth, GN Duda, MO Heller, *Stair climbing results in more challenging patellofemoral contact mechanics and kinematics than walking at early knee flexion under physiological-like quadriceps loading.* J Biomech, 2009, 42 (15):2590-2596.

WM Mihalko, KJ Saleh, MO Heller, B Mollard, C König, S Kammerzell, *Femoral neck cut level affects positioning of modular short-stem implant.* Orthopedics, 2009, 32 (10 Suppl):18-21.

2007

MO Heller, C König, H Graichen, S Hinterwimmer, RM Ehrig, GN Duda, WR Taylor, *A new model to predict in vivo human knee kinematics under physiological-like muscle activation.* J Biomech, 2007, 40 Suppl 1:S45-53.

MO Heller, G Matziolis, C König, WR Taylor, S Hinterwimmer, H Graichen, HC Hege, G Bergmann, C Perka, GN Duda, *[Musculoskeletal biomechanics of the knee joint : Principles of preoperative planning for osteotomy and joint replacement.]*, Orthopade. 2007 Jul;36(7):628-34

Oral Presentations

2010

C König, I Südhoff, B Mollard, A Sharenkov, O Hasart, GN Duda, MO Heller, *Navigated ultrasound enables accurate cup positioning in total hip arthroplasty*, 10th Annual Meeting of the International Society for Computer Assisted Surgery, Paris, France

2006

WR Taylor, C König, AD Speirs, RM Ehrig, GN Duda, MO Heller, *Die medio-laterale Kraftverteilung im Schafsknee*, Deutscher Kongress für Orthopädie und Unfallchirurgie, Berlin

Poster Presentations

2010

C König, G Matziolis, A Sharenkov, WR Taylor, GN Duda, C Perka, MO Heller, *Can midflexion instability after TKA be a consequence of joint line elevation?*, Annual Meeting of Orthopaedic Research Society, 2010, New Orleans, USA

I Goudakos, PB Schöttle, C König, WR Taylor, GN Duda, MO Heller, *The Significance of Graft Tension in Medial Patellofemoral Ligament (MPFL) reconstruction for Patellofemoral Biomechanics*, Annual Meeting of Orthopaedic Research Society, 2010, New Orleans, USA

WM Mihalko, KJ Saleh, B Mollard, C König, MO Heller, S Kammerzell, *Computer assisted validation of femoral neck resection level for a modular metaphyseal short stem*, Annual Meeting of Orthopaedic Research Society, 2010, New Orleans, USA

C König, I Südhoff, B Mollard, A Sharenkov, O Hasart, MO Heller, *Navigated Ultrasound Enables Accurate Cup Positioning in Total Hip Arthroplasty*, 17th Congress of the European Society of Biomechanics, Edinburgh, UK

C König, G Matziolis, A Sharenkov, GN Duda, C Perka, MO Heller, *Can midflexion instability after TKA be a consequence of joint line elevation?*, 17th Congress of the European Society of Biomechanics, Edinburgh, UK

2009

I Südhoff, C König; B Mollard; A Sharenkov, O Hasart, MO Heller, *Navigated Ultrasound in Total Hip Arthroplasty*, World Congress of Biomechanics, 2009, Munich, Germany

2008

C König, G Matziolis, A Sharenkov, WR Taylor, C Perka, GN Duda, MO Heller, *How important is joint line reconstruction in TKA? – A biomechanical investigation*, Annual Meeting of Orthopaedic Research Society, 2008, San Francisco, USA

I Goudakos, C König, PB Schöttle, I Roberts, N Rosenstiel, WR Taylor, MO Heller, *Muscle Activity Impact on Patellofemoral Contact Mechanics and Kinematics*, Annual Meeting of Orthopaedic Research Society, San Francisco, USA, 2008

AS Trepczynski, WR Taylor, C König, G Matziolis, RL Adamson, GN Duda, C Perka, MO Heller, *A New Geometrical Model to Predict the Patellar Tendon Angle at*

High Degrees of Knee Flexion, Annual Meeting of Orthopaedic Research Society, 2008, San Francisco, USA

2007

C König, G Matziolis, W R Taylor, A Sharenkov, H Graichen, S Hinterwimmer, GN Duda, MO Heller, *The collateral ligaments during active and passive knee flexion: an in vivo study*, Jahrestagung der Deutschen Gesellschaft für Biomechanik, 2007, Köln

C König, A Sharenkov, G Matziolis, WR Taylor, C Perka, GN Duda, MO Heller, *The Importance of Joint Line Reconstruction in TKA – A Biomechanical Investigation*, 16th Congress, European Society of Biomechanics, 2007, Lucerne, Switzerland

MO Heller, C König, A Sharenkov, G Matziolis, WR Taylor, C Perka, GN Duda, *Wie zwingend ist die Rekonstruktion der Gelenklinie nach Knie-TEP aus biomechanischer Sicht?*, Deutscher Kongress für Orthopädie und Unfallchirurgie, 2007, Berlin

I Goudakos, C König, P Schöttle, W Taylor, G Duda, M Heller, *Impact of muscle load level on patello-femoral contact mechanics and kinematics*. 16th Congress, European Society of Biomechanics, 2007, Lucerne, Switzerland

2006

WR Taylor, C König, AD Speirs, RM Ehrig, GN Duda and MO Heller, *The medio-lateral force distribution in the sheep knee during walking*, 5th World Congress of Biomechanics, 2006, Munich, Germany

2005

MO Heller, GN Duda, C König, WR Taylor, R Ehrig, S Hinterwimmer, H Graichen, *Validation of a new model of human knee kinematics against in vivo data under physiologic neuromuscular activation patterns*. Annual Meeting of Orthopaedic Research Society, Washington, D.C, USA, 2005

Meinen Schwestern und Eltern,
meinen wunderbaren Freunden und all den Kollegen,
die mich so ausdauernd unterstützt und ermutigt haben
meinen tiefen und ehrlichen Dank.

EIDESSTATTLICHE ERKLÄRUNG

Hiermit erkläre ich, Christian König, an Eides statt, dass ich die vorgelegte Dissertation selbst verfasst habe und keine anderen als die angegebenen Quellen und Hilfsmittel verwendet habe. Außerdem erkläre ich, dass ich an keiner anderen Stelle ein Promotionsverfahren beantragt habe.

Berlin, den _____

Christian König